REPORT NO.
UC-SESM 74-1

STRUCTURES AND MATERIALS RESEARCH
DEPARTMENT OF CIVIL ENGINEERING

FULL-SCALE STUDIES ON THE STRUCTURAL BEHAVIOR OF LARGE DIAMETER PIPES UNDER COMBINED LOADING

by
J. G. BOUWKAMP
R. M. STEPHEN

Report to the Sponsor:
ALYESKA PIPELINE SERVICE CO.

JANUARY 1974

STRUCTURAL ENGINEERING LABORATORY
UNIVERSITY OF CALIFORNIA
BERKELEY CALIFORNIA

Structures and Materials Research
Department of Civil Engineering
Division of Structural Engineering
and Structural Mechanics

FULL-SCALE STUDIES ON THE STRUCTURAL BEHAVIOR OF LARGE DIAMETER PIPES UNDER COMBINED LOADING

A Report of an Investigation

by

J. G. Bouwkamp
Professor of Civil Engineering

and

R. M. Stephen
Principal Development Engineer

to

Alyeska Pipeline Services Company
Houston, Texas

College of Engineering
Office of Research Services
University of California

January 1974

TABLE OF CONTENTS

LIST OF TABLES

LIST OF FIGURES

I. INTRODUCTION

I.1 General

Structural design in general is affected by a set of behavior criteria and specific analytical procedures which permit the evaluation of the structural response to any given set of loads, whatever their origin might be. A design will be considered safe when the analytically derived values do not surpass the limits set by the behavior criteria. The factor of safety, to be reflected in the behavior criteria, depends on reliability of material properties, knowledge of design loadings, accuracy of the analytical procedures used to evaluate the structural response, serviceability, maintenance, repair and replacements costs, etc. The factor of safety can be reduced when engineering aspects as material properties, and analytical procedures are highly reliable and where design loads are well defined. On the other hand economic factors associated with serviceability, maintenance, repair and replacement might well require an increase of the factor of safety.

The foregoing considerations are specifically important if the structural design deals with a system which is uncommon or even unique, or which has an economic and environmental impact far greater than normally considered in structural design. The proposed Trans-Alaska pipeline is a typical example of a structural system which is highly complex both from an engineering and economic point of view.

To resolve the structural engineering aspects of the pipe behavior, full scale studies are desirable, particularly when experience with similar systems is limited or non-existent. Such studies permit establishing pipe deformation criteria which are considered permissible without seriously affecting the efficient operation of the line. Similarly, deformation criteria derived from these tests can impose an adequate factor of safety

against rupture. The results from experimental studies, important as they may be, are of limited value unless the response can be fully predicted theoretically. This is particularly significant if one considers the cost of full-scale studies and the complexity and the variation of the load conditions for which the pipe has to be designed. Thus, to assure the structural safety of the Trans-Alaska pipeline, extensive studies on the material aspects, the gross structural response and the development of accurate analytical procedures for predicting the structural response of the aboveground and buried pipeline are appropriate for a project of this scope.

Construction of the pipeline in an arctic region may require placement of the 48 in. diameter steel sections at sub-freezing temperatures. However, under operation, the temperature of the oil in the pressurized line will elevate the temperature of the pipe and will tend to expand the line both radially and longitudinally. While the radial expansion of the pipe cross section is basically unrestrained, the longitudinal expansion for a buried line will be restricted by longitudinal friction between the exterior pipe surface and surrounding soil, or other causes preventing the line from expanding longitudinally. Therefore, a compressive axial force will be introduced. For any given temperature, this load will be maximum when the longitudinal expansion is fully restricted.

In addition to the forementioned internal pressure and the temperature induced axial forces, the possible settlement of a non-insulated or hot line, which tends to melt the frozen soil surrounding it, causes a bending of the line and must be considered in a full-scale experimental study.

I.2 Objective and Scope

In order to determine the structural behavior of the 48 in. diameter pipeline, a total of eight full-scale studies on seven test specimens have

been carried out at the University of California, Berkeley[1,2]. In these studies the actual load conditions were simulated by introducing in the pipe section a constant internal pressure and a constant axial load reflecting the full longitudinal restraint of the pipeline. Furthermore, in order to simulate the behavior of the pipeline due to potential settlements, lateral loads were applied to introduce a pure moment along the test section.

The behavior of this test section was monitored in detail by extensive instrumentation. Tests were carried out for different operational temperatures and internal pressures. Each specimen was studied under step-wise increased lateral loads until a wrinkling of the pipe wall developed. Subsequently the test was continued until finally a rupture of the pipe wall occurred. The resulting displacements and curvatures are significant in establishing both operational limits as affected by the local wrinkling or buckling of the pipe wall, and safety limits necessary to prevent a rupture of the line. Equally important, these results also permit an evaluation of the accuracy of refined methods of analysis developed to predict the pipe behavior under any given load condition. The latter aspect is particularly signifant since the pipe response is basically non-linear. A correlation between the experimental data and the analytical results, using advanced analytical methods, would illustrate the accuracy of these methods and would permit, with confidence, the prediction of the line behavior under any given load condition. This report covers the results of the experimental research program. The development of computer programs to analyze the non-linear behavior of the pipeline was carried out separate from this contract. However, a comparative study using both analytical and experimental results is presented. The results show typically and excellent agreement between the two sets of data.

I.3 Acknowledgement

The work reported herein was conducted in the Structural Research Laboratory, Division of Structural Engineering and Structural Mechanics, Department of Civil Engineering, University of California, Berkeley. The program was carried out under a research contract between the Regents of the University of California and the Alyeska Pipeline Service Company.

The authors are indebted to Professor E. P. Popov for his invaluable cooperation in the preparation phase of the program as well as for his continued interest and advise during the later stages of this study. The authors further wish to express their appreciation to Professor G. H. Powell for his consultation. Also, the laboratory staff for their valuable advice and assistance during the performance of this test program is gratefully acknowledged.

II. TEST DESIGN

The design of an experimental program generally involves the establishment of the minimum specimen size necessary to yield reliable data, the selection of the equipment, the method and sequence of loading, the development of the instrumentation, and finally the selection of the data acquisition and data reduction procedures. Since the experimental research program was to yield data which would be applicable directly to the proposed 48 in. diameter Trans-Alaska pipeline, it was decided to study the affect of the combined load conditions on prototype pipe sections. Thus, possible variations of the material properties of model and prototype are eliminated. Furthermore, the prototype test selection guarantees that the buckling behavior of the test specimen will be fully representative of the actual behavior of the pipeline under similar load conditions.

II.1 Test Specimen

In order to permit the development of a representative state of stress, due to both axial load and bending moment, the length of the actual test section was selected as approximately three times the pipe diameter or 11 feet, as shown in Fig. 1. To obtain a uniform compressive stress in this section, due to axial loads P_A, an additional length of at least 4 feet, equal to the pipe O.D., on either end was considered necessary. Because the test section was to be subjected to a pure bending moment introduced by a set of lateral loads (P_L) applied symmetrically to the pipe specimen outside the center test section, as shown in Fig. 1, the associated shear force in the end sections could conceivably cause a premature buckling of the tube wall in the end sections. Therefore, the shearing stresses in those sections should be kept low. This was done by increasing the distance between the test

section and the reaction points to about 2.5 times the pipe O.D. or 10 ft. - 3 in. and by increasing the nominal wall thickness of the end sections. To permit a uniform stress distribution under axial load and pressurization of the pipe specimens, the ends were capped with stiffened plates to assure a uniform axial load distribution in the test section. These end caps were fabricated with a two-inch radius slot to fit the four-inch diameter pin on the top and bottom swivel plate assembly. The end caps were oriented on the specimens so that the slot was perpendicular to the plane of laterial loading. Considering the foregoing dimensional requirements as well as the size limitations imposed by the test arrangement, the total length of the standard specimen was selected as 31.5 feet.

Since the pipeline has both longitudinal and circumferential full-penetration welds, it was considered necessary to test these welds under the most severe load conditions. Thus, it was decided to have a circumferential weld at the center of the test section and longitudinal welds in the extreme fiber regions. The latter welds were placed in the compression zone for one half of the test section and in the tensile zone for the other half. The same consideration led to the design of the spiral welded pipe specimen with welds in the upper and lower portion of the test section starting in the central, extreme-fiber regions of the compression and tensile zones respectively.

II.2 Test Equipment

Because of the compressive force capability of the 4,000,000 lb. Southwark-Emery Universal testing machine at the Structural Research Laboratory, Richmond Field Station, U. C. Berkeley, the basic pipe specimen was designed for this machine. Hence, the specimen was placed in a vertical position. To limit the unlikely occurrence of shear buckling, the 10 ft. - 3 in. long end sections were fabricated from X65 pipe with a nominal wall thickness of 0.562 in.

The lateral loads were applied to the 0.562 in sections in two pairs to allow a load distribution which would provide nominal bearing pressures approximately equal to the maximum anticipated internal pressure.

Since the universal testing machine does not permit horizontal forces acting at the top loading head, the reactive forces of the lateral loads applied to the specimen had to be fully reacted by a self contained loading frame as shown in Fig. 3. The principal elements of the frame are four coupled W36 x 230 beam sections - Fig. 4 - and two reaction fixtures between the beams and the pins of the top and bottom load plates. The lateral load was introduced by eight 200 kip double acting load cylinders, arranged in pairs at four different levels. The stroke capacity was 36 in. The cylinder loads were transmitted in pairs to the specimen through 1-5/8 in. diameter steel cables and distributed by means of steel curved loading yokes as shown in Fig. 5 A 10 in. wide, 1/2 in. thick neoprene pad was placed between the pipe wall and each yoke. To prevent horizontal secondary loads being introduced on the testing machine through restraint of the W36 x 230 beam sections during testing, the bottom support of the four diagonal bracing members was designed to slide freely while performing the test. Furthermore, to prevent any external restraint due to a binding between the end capping plates of the specimen and the top and bottom loading plates under inplane bending of the specimen, the load plates were tapered to permit free end rotation of the pipe specimen.

II. 3 Loading

Each specimen was subjected to a series of loadings which simulated in the center 11 ft. test section of the pipe the stresses and deformations which might be encountered in the field. These loadings included internal pressurization, axial load, and lateral load.

Each specimen was initially subjected to an internal pressurization causing a 95% yield stress of the pipe material in the test section. Using the actual yield stress (f_y) of the particular pipe material as determined from a longitudinal wall test coupon, and the measured wall thickness (t) of the test section, the "95%" pressurization was calculated as:

$$p_{95} = 0.95\ (f_y \cdot t)/r_i$$

where r_i is the inside radius. This pressurization (p_{95}) was maintained for at least 8 hours after which it was dropped to the working or test pressure. This pressurization (p_{95}) was also applied to the specimen for a minimum of 8 hours following the initial buckling phase of the test.

Axial loads were applied to the specimens through the pins on the top and bottom load plates. The magnitude of the total axial load, P_A, was the sum of the axial load required to simulate the temperature restraint condition, the axial load required to compensate for the reactions on the top and bottom plates due to the internal pressurization and the longitudinal restaint of the actual line under pressure; i.e.

$$P_A = \alpha \Delta T E A_m + \pi \frac{D_i^2}{4} \cdot p_i - \mu \frac{p_i D_i}{2t} \cdot A_m ,$$

in which α = coefficient of linear expansion of material; μ = Poisson's ratio; ΔT = temperature differential between installation and operation of the line; E = modulus of elasticity of material; A_m = cross-sectional area of pipe; D_i = inside diameter of pipe; t = thickness of pipe; and p_i = internal pressure.

The lateral loads, P_L, acting around the compression face side of the specimen were applied through loading yokes and cables which in turn were attached to eight 8-in. bore, 36-in.-travel hydraulic cylinders. The reactions from these lateral loads were through the pins on either end of the specimen as shown in Fig. 2.

The resulting moment in the center 11-ft. test section ($52.5 \times P_L$) was primarily due to the lateral loading; however, as soon as the specimen deflected laterally, an additional moment due to the axial load and center deflection ($P_A \times \Delta_{av}$) was imposed to make up the total moment at the center section.

II·4 Instrumentation

Each specimen was instrumented with electrical resistance strain gages, potentiometers for measuring deformations, pressure transducers for measuring applied loads, and curvature gages for determining the overall bending of the specimen.

The strain gages used were 2 or 3 element post-yield gages with a gage length of 10 mm. With the type of adhesive used, the gages were capable of recording strains of more than 10%. The strain gages were almost exclusively located in the center 11 ft. test section. Specimens 1,2,3,6 and 7 were instrumented with gages both on the inside and outside of the pipe wall. These gages were typically placed opposite to one another in order to determine any local bending of the pipe wall prior to buckling.

Potentiometers were used to measure the radial deformation as well as the bending deformation of the pipe wall. To determine the pipe wall bending, potentiometers were located on both the tension and compression face of the pipe at some seven locations on each face.

The curvature gages (or clip gages) were attached to steel tubular rings which in turn were held in contact with the pipe wall by means of spring loaded pins at 3 locations. The potentiometers which made up this curvature gage covered the test section and had a gage length L of basically 10 ft. The "fiber" distance between the tension and compression face was either 74 or 85 in. (see Fig. 10). Under the assumption that plain sections remain plain under bending, which was substantiated in these tests, the overall radius of curvature R in feet of this 10 ft. pipe test section was determined as:

$$R(ft) = L(ft) \times \frac{\text{Distance between Potentiometers (in.)}}{\left| \sum \text{Potentiometer readings (in.)} \right|}$$

The above instrumentation which amounted to about 300 channels was read on a Low Speed Scanner data acquisition system developed at the University of California. A X-Y recorder was used during the lateral loading test sequence to monitor the center displacement.

III. TEST PROGRAM

In order to study the potential behavior of the pipeline the specimens were to be subjected to a number of different load conditions. The basic parameters in these studies were the internal pressure, p_i, and the temperature differential, ΔT, between the tie-in or installation temperature and the temperature under operation. At the outset of these studies, one could expect that high internal pressures would delay the buckling of the pipe wall. Also the resulting radial stresses and strains due to a high pressurization would potentially "soften" the pipeline bending stiffness. Furthermore, a large temperature differential would produce effectively a larger axial force in the line and cause a reduction of the over-load or bending capacity of the pipe section. To evaluate these phenomena under increasing lateral loads, a total of seven specimens under different simulated pressure and temperature conditions have been investigated. These tests were carried out until a buckling of the pipe wall occurred. In the case of five specimens, the tests were continued until under excessive deformations a rupture of the pipe wall occurred. Furthermore, one of the test specimens was used to study the affect of a pressure drop on the stability of the pipe wall. It should be noted specifically that the tests were carried out at room temperature (approximately $70^{o}F$). Although this condition does not reflect the actual hot line service temperatures, it is most unlikely that the difference between the actual test and service temperatures would have affected the material properties and structural response of the test specimens.

III.1 Test Specimen and Load Selection

Seven specimens were fabricated from nominal 48 inch diameter longitudinally welded pipe. With the exception of Specimen No. 6, the 48 inch diam-

eter test section was fabricated from X60 pipe, with a nominal wall thickness of 0.462 in. and a minimum yield stress of 60 ksi. In the care of specimen No. 6 the pipe material for the entire length was X65 with a minimum yield stress of 65 ksi and a nominal wall thickness of 0.562 in. The arrangement of the circumferential weld at the center of the test section and the 180 degree offset of the longitudinal welds for all specimens, except Specimens No. 6 and No. 7, is shown in Figure 2a. Specimen No. 6 had a single longitudinal weld in the tension side at 45 degrees to the axes of loading and Specimen No. 7 had a spiral weld arrangement as shown in Fig. 2b. Each specimen was approximately 31 ft.- 4 1/2 in. in length and was made up of an eleven foot center test section, a 7 ft. - 8 in. loading section on each end of the test section, and the thirty inch end caps at each end of the specimen. A typical test specimen is shown in Figure 6. All pipe welds were specified as full penetration single bevel welds. Table I lists some of the characteristics of the pipe used in the test specimens. The wall thickness of the test section for all specimens except No. 4 and No. 5 was measured at a number of points and the average wall thickness was determined. In the case of Specimens No. 4 and No. 5 the pipe wall thickness was determined by the overall length and weight. Typical stress-strain curves of the pipe material are shown in Figure 7. The basic load characteristics for each of the seven specimens tested are presented in Table II.

The minimum wall thickness, together with the actual yield stress (f_y), was used to determine the pre-pressurization pressure to produce a circumferential pipe stress of 0.95 f_y. The test working pressure was subsequently reduced to an internal pressure of about 900-950 psi producing a 0.72 f_y circumferential stress in the pipe test section (Specimens Nos. 1, 2, 4, and 5A). Since the working pressure under operation could well drop below this level,

TABLE I - CHARACTERISTICS OF PIPE USED IN TEST SPECIMENS

SPECIMEN No.	TEST SECTION				LOADING SECTION			
	Pipe No.	Nominal Thickness	Avg. Measured Thickness*	Min. Measured Thickness	Pipe No.	Nominal Thickness	Avg. Measured Thickness*	Min. Measured Thickness
		in.	in.	in.		in.	in.	in.
1	1007	0.462	0.495	0.485	3643 3487	0.562	0.587	0.581
2	1007	0.462	0.485	0.472	3643 3487	0.562	0.586	0.570
3	1007	0.462	0.490	0.480	3487 3643	0.562	0.587	0.577
4	1021	0.462	0.487**	———	3418	0.562	——***	——***
5	1021	0.462	0.487**	———	3418	0.562	——***	——***
6	3743	0.562	0.585	0.579	3743	0.562	0.585	0.579
7	K1212	0.462	0.467	0.458	3643 3487	0.562	0.587	0.580

* Measured at a number of points and the average thickness determined.

** Pipe wall thickness determined by overall length and weight.

*** No measurements taken on this pipe.

TABLE II - LOAD DATA OF PIPE TEST SPECIMENS

SPECIMEN	TEST SECTION		LOADING		
	Nominal Thickness	Avg. Measured Thickness	Internal Pressure	ΔT	P_A Axial Load
	in.	in.	psi	°F	kip
1	0.462	0.495	942	135	2580
2	0.462	0.485	917	135	2520
3	0.462	0.490	25	135	1920
4	0.462	0.487	950	90	1920
5 5A	0.462	0.487	150 950	90 90	1373 1920
6	0.562	0.585	150	90	1630
7	0.462	0.467	150	90	1322

lower pressure levels were introduced as well (Specimen 3 at 25 psi; Specimens Nos. 5, 6 and 7 at 150 psi). In these tests water was used instead of oil.

In order to study the influence of the temperature differential, ΔT, on the pipeline behavior, two basic temperatures of 135°F and 90°F have been considered (Specimens Nos. 1, 2, 3 at 135°F and Specimens Nos. 4 through 7 at 90°F). The combined effects of p_i and ΔT are reflected in the axial load, P_A, as noted earlier and as listed in Table II.

The selection of the internal pressure, p_i, and the temperature differential, ΔT, after Test No. 1 was based on the preceding test results and was guided by the analytical studies which paralleled this experimental program. By applying effectively extreme combinations of ΔT and p_i, the applicability

of the theoretical methods developed could be established. Also, the actual wall buckling phenomenon could be determined accurately to allow establishing appropriate margins of operational safety for design purposes.

III.2 Loading Program

Normally, the load sequence was pressurization, axial loading, and lateral loading. However, the fifth specimen was subjected to two different load sequences. First, in Test No. 5, the specimen was subjected to the basic load sequence. However, during the later phase of the test, the internal pressure of 150 psi was dropped to 0 psi--such as would occur during a temporary line shutdown. The same experiment was repeated in Test No. 5A, with the pipe specimen rotated 180^{o} around on its axis and subjected to a reversed bending as compared to the lateral load application in Test No. 5. In this case, the pressure was dropped from 950 psi to 0 psi. The purpose of these two tests was to determine the behavior of the line under a precurved condition and an imposed pressure drop. The results clearly supported the analytical predictions that the pipe wall would not buckle at this lowered pressure, even though the curvature at that instance was larger than that at which wall buckling had occurred for a low-pressure specimen subjected to typically increasing lateral loads.

With the exception of test No. 5A, all specimens were loaded until wrinkling of the wall occurred. Following this loading phase, Specimens 2, 3, 4, 6 and 7 were subjected to post-buckling tests until failure of the wall occurred. To perform these tests in the cases of Specimens 2, 3 and 4, the pipe was first deformed far enough so that the moment produced by the eccentricity of the axial load in the buckled cross section alone was large enough to bend the pipe specimen further. Subsequently the specimen was rotated 180^{o} around the center axis so that the eight load cylinders would again have to

pull in order to control the increasing deformation of the pipe--away from the lateral loading frame--as a result of the axial load. In the cases of Specimens 6 and 7, the buckle was extended immediately after the initial buckle developed and without rotating the specimen.

IV. TEST RESULTS

IV.1 SPECIMEN NO. 1

1.1 Description of Specimen and Instrumentation

The test section of specimen No. 1 was fabricated from pipe number 1007 and had an average measured wall thickness of 0.495 in. The mechanical properties of this material as determined from longitudinal test specimens tested in accordance to API Std and ASTM A370 gave a yield stress of 63,500 psi at 0.5 percent strain, a modulus of elasticity of 29.8×10^6 psi, and an ultimate tensile strength of 81,500 psi (see Fig. 7).

In order to evaluate the basic response of the specimen to the applied loadings, a number of strain gages were placed both in the inside and outside of the specimen wall. However, in order to assess the pipe behavior, only a limited number of longitudinal strain gages on the tension and compression face of the specimen are presented. The location of these gages is shown in Fig. 8. The location of clip-gage potentiometers (Nos. 34 and 35) and displacement gages, evenly spaced along crown lines on the compression and tension face, are shown in Fig. 10. The overall gage length of the clip-gage potentiometers was 10 ft. The distance between these gages was 74 inches. The average center displacement Δ_{av}, to determine the eccentricity moment P_A. Δ_{av}, was calculated as $(\Delta_8 + \Delta_{18})$ (0.5).

1.2 Test Objective

As noted previously, the test objective for specimen No. 1 was to impose a loading condition which would simulate a high internal pressure (p_{72}= 942 psi); a high temperature differential (Δ_T = 135°F); and a lateral load which would simulate a settlement of the pipeline.

1.3 Load Sequence

The specimen was initially pressurized to 1244 psi, after this pressure was maintained for 8 hours the pressure was dropped to the working pressure of 942 psi. Subsequently, the axial load was applied to a maximum of 2,580 kips. Of this total axial load, 650 kips counteracted the effect of internal pressure and 1,930 kips was due to the load caused by simulating the 135°F temperature differential

The total nominal lateral load P_L was applied in 50 kip increments up to 400 kips. After reaching the 400 kip load level an attempt was made to increase the load with an increment of 100 kips. However, prior to reaching the 500 kip loading, a buckling of the specimen took place at a load of 497 kip. The specimen was subsequently subjected to an internal pressure of 1244 psi which was maintained for about 12 hours.

1.4 Test Results

The results for specimen No. 1 are presented as the bending moments at the pipe mid-section (Table III); the radius of curvature and gross strain data (Table IV); and the pertinent strain gage data along compression and tension crown lines (Table V). The maximum total lateral load applied to the specimen when buckling occurred was 497 kip. As it was not possible to take a set of displacement and strain data at the instance of buckling, pertinent data for this load level were either derived from the displacement data recorded at the last pre-buckling load of 401 kip, or from the post-buckling strain data taken at loads of 440 kip and 78 kip. The continuous XY record at the mid-span section indicated that the displacement had doubled while increasing the load from 401 kip to 497 kip. The strain data were derived through extrapolation as described in Fig. 9. This method is based on the observed linear reduction of the pipe displacements following buckling and has been applied to gages which were not immediately affected by the local buckling.

The total bending moment at the pipe mid-section when buckling occurred was 30873 kip-inches and the radius was 627 feet.

In comparing the gross strains from the clip gages (Table IV) with the average strains as measured by the strain gages along the crown lines (Table V), it was observed that the gross tension strains are maximum 20 percent higher than the average measured tension strains. The gross compression strains for higher loads are only 5 percent lower than the average measured compression strains.

As shown in Table IV, the total average measured strain at buckling was +795 micro in/in on the tension face and -5735 micro in/in on the compression face.

Buckling of the specimen occurred in the 0.462 in. wall pipe about 8 in. below the upper circumferential weld. The buckle developed as a typical bulging of the pipe wall. Figures 11 and 12 show the buckle after the specimen had been deflected to about 9 in. at the center or about 5 times the deflection at the start of the buckle.

The post-pressurization of the specimen to p_{95} = 1244 psi showed no leaks or other detrimental effects to the specimen.

IV.2 SPECIMEN NO. 2

2.1 Description of Specimen and Instrumentation

The test section of this specimen was fabricated from the same pipe number (1007) as specimen No. 1 and in this case had an average measured wall thickness of 0.485 in. The mechanical properties were the same as the first specimen.

The instrumentation on this specimen was identical to specimen No. 1.

2.2 Test Objective

Specimen No. 2 was studied to check the total test reliability. Hence, the same load conditions as for specimen No. 1 were introduced, namely: high internal pressure condition (p_{72}= 917 psi), a high temperature differential condition

(ΔT = 135°F) and a lateral loading which would simulate a settlement of the pipeline.

After having observed the location of the buckle in specimen No. 1, some 8 inches below the upper circumferential weld and about 10 inches below the bottom of the upper loading yoke, the possibility that the near presence of the loading yokes may have contributed to the buckle at the aforementioned location was considered in depth. To reduce any possible influence of the loading yokes, a set of girdles were placed around the test section immediately adjacent to each set of yokes. Each girdle was made up of a 1/2 inch thick neoprene pad 24 inches wide wrapped completely around the pipe. Over this were placed nine rows of double stainless steel bands 1-1/4 in. wide and 0.040 in. thick. The neoprene pad and bands extended 2 inches beyond the weld on the loading section of the specimen. The bands on each girdle extended some 16 inches over the test section of the specimen, as shown in Fig. 19.

2.3 Load Sequence

The specimen was initially pressurized to 1210 psi and the pressure was maintained for a minimum of 8 hours after which it was dropped to the working pressure of 917 psi. Axial load was applied to a maximum of 2520 kips. Of this total axial load, 620 kips was to counteract the internal pressure effect and 1900 kips was due to the load caused by simulating the 135°F temperature differential.

The total nominal lateral load P_L was applied in 100 kip increments up to 300 kips. Following the application of single 50 kip increments (to 350 kips) 25 kip increments were applied until a load of 425 kip had been reached. Subsequently, the lateral load was increased step-wise in 12.5 kip increments until buckling of the specimen took place at a load of 460 kips.

Following the initial buckling, the internal pressure was increased again to 1210 psi. This pressure was sustained for 8 hours.

Although the initial objective of this test was to establish buckling under an increasing lateral load, the results clearly showed that the operational integrity of the line would not be impaired by a buckling development. In order to assess the actual strength of the pipe, an additional post-buckling test was undertaken. For that purpose the specimen was rotated 180 degrees around its vertical axis, so that the buckle would face the loading frame. The specimen was again pressurized to 917 psi. While the axial load of 2520 kips was applied a lateral load was introduced simultaneously in an attempt to maintain the same buckled configuration of the specimen as at the end of the initial buckling test. Subsequently, the specimen was further deformed, through the action of the axial load and the resulting eccentricity moment, until rupture occurred.

2.4 Initial Buckling Test Results

The results for Specimen No. 2 are presented as the bending moments at the pipe mid-section (Table VI); the radius of curvature and gross strain data (Table VII); and the pertinent strain gage data along compression and tension crown lines (Table VIII). Becuase it was impossible to take a set of data at the instance of buckling, the pertinent data shown in the forementioned tables are evaluated using the X-Y recorded center displacement values at loads or 460 kip (buckling) and 453 kip (pre-buckling). The center displacement at buckling was 1.13 times the value recorded at the 453 kip loading. The same factor has been applied to all pertinent strain data.

The total bending moment at the pipe mid-section when buckling occurred was 28239 kip-in. and the radius was 608 ft. The maximum total lateral load applied to the specimen when buckling occurred was 460 kip.

In comparing the gross strains from the clip gages (Table VII) with the average strains as measured by the strain gages along the crown lines (Table VIII), it was observed that the gross strains on the tension and compression face at the higher loads are respectively about 20 and 10 percent higher than the average measured strains along these crown lines. As shown in Table VIII the total average measured strain at buckling was +796 micro in./in. on the tension face and -4726 micro in./in. on the compression face.

Buckling of the specimen occurred in the 0.462 in. wall pipe about 24 in. above the lower circumferential weld. The buckle formed in a typical bulging of the pipe wall similar to that shown in Figures 11 and 12 for Specimen No. 1. At buckling the center displacement was about 1.6 inches. This displacement was increased until at the end of this initial buckling phase the center displacement of the specimen was about 5.5 inches. The post-pressurization of the specimen to 1210 psi showed no leaks or other detrimental effects to the specimen.

2.5 Post-Buckling Test

In order to undertake the post-buckling test the specimen was rotated in the testing apparatus so that the buckle would face the loading frame after the loading yokes and instrumentation were again connected. The specimen was again pressurized to 917 psi. Next, the axial and lateral loads were applied simultaneously to the specimen in an attempt to maintain the same buckled configuration of the specimen as at the end of the initial buckling test program. Despite the greatest care exercised during this loading sequence the specimen deflected an additional 8 in. The total lateral load required to maintain the required 2520 kip axial load under this additional deformation was 800 kip. At this point all strains, pressure gages and potentiometers were recorded. Subsequently, under the influence of the axial load and an initial and temporary release of the lateral load, the specimen was allowed to deflect in 2 inch increments.

Readings were taken at each of these displacement steps. At a total lateral load of 1140 kip a second buckle began to develop some 6 in. below the upper weld. Failure in the original buckle finally occurred after the total center displacement had reached 24.9 in. The total displacement measured at the location of the buckle was 30.5 in. The maximum total lateral load at that instance was 1200 kip. Fig. 13 shows the overall specimen after completion of the post-buckling test and Fig. 14 shows the configuration of the pipe centerline and angular rotation of the pipe at the end of the initial and post-buckling tests.

Failure of the specimen was in the pipe wall and was basically a combined shear and tearing failure of the wall. As the specimens was deflected from its initially buckled condition, the buckle began to fold back as shown in Figures 15 and 16 and failure occurred under the fold on the compression face in the location indicated on the figures. This failure of the pipe wall was some 6 to 8 in. in length and approximately 1/2 to 3/4 in. in width and was observed just after the lateral load had reached the maximum of 1200 kips.

IV.3 SPECIMEN NO. 3

3.1 Description of Specimen and Instrumentation

The test section of this specimen which was fabricated from the same pipe number (1007) as Specimen No. 1 and No. 2 had an average measured wall thickness of 0.490 inches. The mechanical properties were the same as Specimen No. 1.

Although a considerable number of strain gages were recorded, only the results of a limited number of longitudinal strain gages on the tension and compression face were analyzed to evaluate the total response of this specimen to the applied loadings. The location of these gages is shown in Fig. 17.

The location of the clip gage potentiometers Nos. 26 and 27 with an overall gage length of 10 ft. and a distance between the poteniometers of 86.125 in.

is shown in Fig. 18. The same figure also shows the location of the other potentiometers and the basic data reduction criteria for the evaluation of the radius of curvature and gross-strains.

3.2 Test Objective

In contrast with the test objectives of the first two specimens, the objective of the test program on Specimen No. 3 was to develop a loading condition which would simulate a low internal pressure (p_i = 25 psi), a high temperature differential (ΔT = 135°F), and a lateral load which would simulate settlement of the pipeline.

3.3 Load Sequence

The specimen was initially pressurized to 1230 psi. After this pressure had been maintained for 8 hours the pressure was reduced to the test pressure condition of 25 psi and an axial load of 1920 kip was applied. Of this total axial load only 20 kip was to counteract the internal pressure effect and 1900 kip was due to the load caused by simulating the 135°F temperature differential.

The total nominal lateral load was applied in 100 kip increments up to 500 kips and then in 50 kip increments to 650 kips. Finally load increments of 25 kip were applied until buckling occurred. After the initial buckling the specimen was again pressurized to 1230 psi and maintained in that condition for at least 8 hours.

Following this initial buckling phase the specimen was subjected to the post-buckling test. The specimen was rotated in a manner similar to Specimen No. 2. Subsequently, after the internal pressure and axial load had been applied again the specimen was permitted to deform until rupture occurred.

3.4 Initial Buckling Test Results

The results for specimen No. 3 are tabulated with the bending moments at the pipe mid-section presented in Table IX and the radius of curvature and gross-

strain data in Table X. The pertinent strain gage data along the compression and tension crown lines are recorded in Table XI.

The total bending moment at the pipe mid-section when buckling occurred was 42,158 kip-in. as shown in Table IX. The radius of curvature at that instance was 779 ft. Buckling of the specimen occurred under a lateral load of 751 kip while recording the data at this load level.

In comparing the gross strains from the clip gages (Table X) with the average strains measured by the strain gages along the crown lines, (Table XI) it is observed that at the higher lateral load levels the gross strains for the tension and the compression face are respectively 20 and 30 percent higher than the average measured strains along these crown lines. This trend is similar in principle to that observed in the previous specimens.

The total average measured strain at 724 kip lateral load was +796 micro in./in. on the tension face and -2694 micro in./in. on the compression face. Strain data at 751 kip are not very reliable since buckling was imminent.

Buckling of the specimen occurred in the 0.462 inch wall pipe approximately 6 to 8 inches below the center circumferential weld. The buckle in this low-pressure test was a typical diamond shaped, inward-outward, buckle as shown in Fig. 19. The average center displacement at buckling was about 1.4 in. This displacement was intentionally increased until it had reached a value of about 5 3/4 inches.

The post-pressurization of this specimen to 1230 psi showed no leaks or other detrimental effects to the specimen.

3.5 Post-Buckling Test Results

The specimen was rotated in the test frame 180 degrees prior to undertaking the post-buckling test. The loading yokes and instrument were reconnected and the specimen was pressurized to 25 psi. After gradually increasing both the

axial load and the lateral holding force, maximum load values of 1920 kip and 540 kip respectively were required to maintain the same buckled configuration as at the end of the initial buckling test program. Initial instrumentation readings were taken at this point and the specimen was allowed to deflect 2 in. by reducing the lateral load. As the specimen was approaching this 2 in. deflection and the lateral load was being increased to 500 kip to stabalize this deformation pattern, a second buckle started to form on the "tension" face of the specimen. At that time both the axial and lateral loads were decreased to zero.

As the specimen would not take any further lateral loading under the 25 psi condition, it was decided to continue the post-buckling test after increasing the internal pressure to 932 psi and the axial load accordingly to 2550 kip. In order to maintain the original 5 3/4 in. deflection both the pressure and the axial and lateral loads were introduced gradually. The associated lateral load was 290 kip. The specimen was now allowed to deflect in 2 inch increments by reducing the lateral loads somewhat to allow the specimen to deflect. However, this load was then increased to maintain the new deflected shape. At a maximum total lateral load of 1450 kips a second buckle developed immediately below the upper circumferential weld line. The pipe center displacement at this instance was 31.0 in. The specimen continued to deflect to about 33.0 in. At this point both the axial and lateral loads had to be reduced in order to control the displacement. At a load of 100 kip lateral, 500 kip axial and an internal pressure of 500 psi, the specimen failed. The overall configuration of the specimen after failure is shown in Fig. 20.

Failure of the specimen was in the pipe wall and was basically a shear failure of the wall similar to that noted in specimen No. 2. As the specimen deflected following initial buckling, the buckle began to fold both downward and inward.

The configuration at failure is shown in Fig. 21 and 22 with the local rupture located under the fold as indicated by the arrow in both figures. This shear-tearing failure caused a crack of about 4 to 5 inches in length and approximately 1/2 inch in width.

IV. 4 SPECIMEN NO. 4

4. 1 Description of Specimen and Instrumentation

The test section of this specimen was fabricated from pipe number 1021 and had an average wall thickness, determined from overall weight and length of pipe, of 0.487 inches. The mechanical properties of this material were the same as that from pipe number 1007.

The strain gage data obtained in the tests on the first three specimens indicated clearly that the longitudinal bending of the tube wall was insignificant. Therefore, it was decided to delete the interior gages. This decision also permitted delivery to the laboratory of the complete specimen. In the earlier tests the specimen was first delivered without the end caps in order to allow installation of the interior gages. Before testing, the specimen was transported back to the fabrication yard to weld on the end caps.

Based on the above consideration only strain gages on the outside of the specimen were applied in this study. In order to evaluate the response of the specimen to the applied loadings the gages along the compression and tension-phase crown lines have been analyzed. The location of those gages is shown in Fig. 2

The clip gage potentiometers were located as shown in Fig. 24. Gages No. 26 and 27 with total gage length of 10 ft. and a distance between potentiometers of 85.250 in. permit the evaluation of the gross-curvature of the entire test section. In order to correlate the possible development of buckling in either the upper or lower half of the test section with an increase of the

curvature in that portion of the test section, additional clip gages were installed in this study. The upper section clip gage, with potentiometers Nos. 28 and 30, had a gage length of 5 ft. and a distance of 68.25 in. The lower section clip gage with potentiometers Nos. 29 and 31, as shown in Fig. 24, had a gage length of 5 ft. and a horizontal distance normal to the plane of bending of 69.625 in.

The typical location of the equally spaced displacement potentiometers along the compression and tension face of the pipe are also shown in Fig. 24. The center displacement of the specimen used in the determination of the total moments is the average displacement as measured by potentiometers Nos. 8 and 18 on the compression and tension faces, respectively. The basic data reduction criteria to evaluate the radius of curvature and the gross strains are also shown in Fig. 24.

4.2 Test Objective

The objective of the test program on specimen No. 4 was to develop a loading condition which would simulate a high internal pressure condition, producing a hoop stress in the pipe wall of 0.72 f_y, and a moderately high temperature differential condition (T = 90°F). Under those conditions, the effective axial load in the pipe specimen would be less than in the first three specimens tested. Thus, a delay of the buckling of the pipe wall under an increasing lateral load which simulates a settlement of the pipeline could be expected.

4. 3 Load Sequence

The specimen was initially pressurized to 1255 psi and this pressure was maintained for a minimum of 8 hours. After the pressure was dropped to the testing pressure of 950 psi an axial load P_A of 1920 kip was applied. Of this total axial load 650 kip counteracted the effect of the internal pressure and 1270 kip was due to the load caused by simulating the 90°F temperature differential.

The total nominal lateral load was applied in 100 kip increments up to 400 kip and then in 50 kip increments to 500 kip. After reaching this load the incremental

loads were reduced to 25 kip until a load of 600 kip had been attained. Following this load the load was increased in 10 kip increments until buckling occurred at a load of 647 kip. After the specimen had been further deformed (center displacement 8 1/2 in.) the internal pressure was raised again to 1255 psi to introduce a hoop stress in the test wall of 0.95 fy. This pressure was maintained for more than 8 hours.

Following this initial buckling phase the specimen was subjected to a post-buckling test. The specimen was rotated 180 degrees in a manner similar to specimen No. 2. Subsequently, after the internal pressure and axial load had been applied again, the specimen was deformed until rupture occurred.

4. 4 Initial Buckling Test Results

The results for specimen No. 4 are tabulated with the bending moments at the pipe mid-section presented in Table XII, and the radius of curvature and gross-strain data for the total test section presented in Table XIII. As it was not possible to record the strain just prior to buckling the strain data at buckling are presented as approximate values. These values are based on the strains recorded under a lateral load of 640 kip times a factor of 1.18 being the ratio between the center displacements at buckling and at the preceding load of 640 kip. A comparison of the radii of curvature of the total test section as well as both the upper and lower half sections, as based on clip-gage data, are presented in Table XIV.

The total bending moment at the pipe mid-section when buckling occurred was 38,733 kip-in. while the radius of curvature of the total section was 436 ft. The maximum total lateral load applied to the specimen when buckling was 647 kip.

In comparing the gross strains from the clip gages (Table XIII) with the average strains as measured by the strain gages along the crown lines, (Table XV), it was observed that the tension strains at loads above 502 kip are initially

the same in both cases. The gross compression strains are about 10 percent smaller than the average measured compression strains. The total average strain at buckling as shown in Table XV was calculated as +1816 micro in/in. on the tension face and -8196 micro in./in. on the compression face.

Buckling of the specimen occurred in the 0.462 inch wall pipe about 36 inches below the center circumferential weld. The buckle formed as a typical bulging of the pipe wall. Fig. 25 shows the buckled specimen after the center of the specimen had been deflected to about 8-1/2 in. or some 3.5 times the deflection just prior to buckling. A close-up of the buckle under the imposed deformation of 8-1/2 in. is shown in Fig. 26. The post-pressurization of the specimen showed no leaks or other detrimental effects to the specimen.

4.5 Post Buckling Test Results

The specimen was rotated in the test fixtures 180 degrees prior to starting the post-buckling tests. The pipe deformation and rotation prior to the post-buckling test is shown in Fig. 27. The loading yokes and instrumentation were reconnected and the specimen was pressurized to 950 psi. While the axial load was gradually introduced, the lateral loads were applied simultaneously in order to maintain the same deformed shape of the specimen as was observed at the end of the initial buckling test. The axial and lateral loads in this balanced condition were 1920 kips and 300 kips, respectively. After initial readings were taken at this point the specimen was allowed to deflect in 1 in. increments. Later on these increments were increased to 2 in. To allow these deflections to develop the lateral load had to be reduced first. However, when the deflection approached the 1 or 2 inch incremental distance, the lateral load as again increased to maintain the incremental deflection. The maximum lateral load required just prior to failure was 1078 kips. While the next

incremental deflection was introduced the specimen failed. The lateral load at that instant was 980 kips and the center displacement was 34.5 in. The post-buckling displacements, moments and rotations are tabulated in Table XVI. An overall view of the specimen after the post-buckling test is shown in Fig. 28. The displacement of the specimen at the location of the buckle was 41.0 in. while the angle of rotation between the upper and lower portions of the pipe specimen amounted to about 25 degrees.

Failure of the specimen occurred in the pipe wall and was a shear-tearing type failure. As the specimen deflected, the wall of the pipe folded back as shown in Fig. 29 and 30 and the failure occurred in the fold as the upper portion of the specimen was being pushed down and the lower portion was pushed upward. The failure was approximately 12 in. in length and about 1/2 in. in width.

IV.5 SPECIMEN NO. 5

5.1 Description of Specimen and Instrumentation

The test section of this specimen was fabricated from pipe number 1021, the same as specimen No. 4. When this specimen was first brought into the laboratory, it was found that the two sections of the pipe which make up the test section were misaligned at the center circumferential weld by about 3/16 inch. The specimen was sent back to the fabricator for realignment and welding. When the specimen was returned, the alignment had been improved. However, the two test sections still showed a maximum misalignment of 1/8 in. at the center circumferential weld.

This specimen was instrumented according to a strain gage layout similar to specimen No. 4. For the purposes of evaluating the basic response of the specimen to the applied loadings, the results of a number of pertinent longitudinal strain gages on the tension and compression face have been considered.

The location of these gages is shown in Fig. 31.

The clip gage potentiometers Nos. 26 and 27, as shown in Fig. 32, are to determine the curvature and gross strains over the entire test section. The total typical gage length is 10 ft. and the distance between the potentiometers is 86.5 in. In addition to the curvature data for the entire test section, potentiometers Nos. 28 and 30 in the upper and Nos. 29 and 31 in the lower half of the section will permit an evaluation of the curvature in those portions of the test section. The gage lengths for both clip gage arrangements is 5 ft. and the distance 68.625 in. The potentiometers measuring the pipe displacement along the tension and compression crown lines are also shown in Fig. 32. The pipe center displacement is again taken as the average of the potentiometer readings Nos. 8 and 18. The basic reduction procedures for evaluating the radii of curvature and the gross strains are presented in Fig. 32.

5.2 Test Objective

Following the results of the previous tests the question was raised if the pipe section of a pressurized line would remain stable under a pressure drop, even in case of imminent buckling of the pressurized pipe due to the induced lateral displacements (reflecting a large overburden pressure). Therefore, specimen No. 5 was studied under a moderately high internal pressure condition of p_i = 150 psi and a simulated high temperature differential of $\Delta T = 90°F$. Upon reaching a high lateral load level, the pressure was dropped. After raising the pressure again to 150 psi the test was continued by increasing the lateral load.

5.3 Load Sequence

The specimen was initially pressurized to 1255 psi. After this pressure had been maintained for 8 hours the pressure was dropped to the testing pressure of 150 psi. Subsequently, an axial load of 1373 kips was applied.

Of this total axial load, 103 kips counteracted the internal pressure effect and 1270 kips was required to simulate the effect of a 90°F temperature differential.

The nominal lateral load was applied in 100 kip increments up to 700 kips and then in 50 kip increments to 800 kips. At 800 kips the internal pressure was dropped to 0 psi. Because of the pressure drop the axial load was reduced to 1270 kips while the lateral load remained unchanged. The specimen was subsequently repressurized to 150 psi and the lateral load increased again. Prior to reaching the next 50 kip increment of loading, the buckling occurred. After buckling, the pressure was raised again to 1255 psi and maintained for at least 8 hours.

5. 4 Buckling Test Results

The results for specimen No. 5 are tabulated with the bending moments at the pipe mid-section presented in Table XVII and the total section radius of curvature and the gross-strain data in Table XVIII. The radii of curvature for the total test section as well as for the upper and lower halves of this section are shown in Table XIX. The pertinent strain data are presented in Table XX . As it was impossible to take a set of readings at the buckling load, the pertinent potentiometer data shown are based on the X-Y recorder displacements where it was found that the displacement at the buckling load was the same as the displacement recorded after buckling at a lateral load of 722 kips. The strain data at buckling can be extrapolated as 1.08 times the strain values recorded at the last 801 kip loading.

The test indicated that the specimen successfully withstood the depressuration and repressurization sequence. This procedure was carried out after a lateral load of 801 kips and a center displacement of 1.23 in. had been introduced.

While increasing the lateral load on the repressurized specimen failure due to buckling occurred under a load of 843 kips, as indicated in Table XVII. The corresponding moment was 46233 kip-in. and the radius of curvature for the total test section was 900 ft. Buckling was exhibited by the initial formation of a very small buckle in the lower half of the test section about 4 inches below the center circumferential weld as shown in Fig. 33. At this point the test was immediately stopped.

In comparing the gross strains from the clip gages (Table XVIII) with the averaged measured strains along the crown lines (Table XX) at the last 800 kip loading, it was observed that the gross strains on the compression and tension face were respectively 5 and 7 percent larger than the measured strains.

The 8-hour post pressurization test of the specimen at a pressure of 1255 psi showed no leaks or other detrimental effects.

IV. 6 SPECIMEN NO. 5A

6. 1 Description of Specimen and Instrumentation

The buckling deformation of specimen No. 5 was arrested almost immediately when observed (see Fig. 33). Therefore, the pipe was only locally overstrained. Since the residual strains, particularly on the tension face of the pipe wall were relatively small, it was decided to use the same specimen again to assess the buckling resistance of the pipe section as influenced by a pressure drop from a relatively high internal pressure level. For that purpose specimen No. 5 was rotated 180 degrees around the vertical axis, so that under renewed lateral loading the previous tension face would be subjected to compressive stresses.

The existing strain gage layout of specimen No. 5 was supplemented for specimen 5A so that the resulting instrumentation, in reference to the compressive and tensile stress regions of the test section, was similar to the gaging of specimens

Nos. 4 and 5. The strain-gage instrumentation, pertinent for evaluating the basic response of the specimen, is presented in Fig. 34.

The location of the clip gage Nos. 26 and 27 measuring the curvature over the entire test-section, as well as the clip gage potentiometers Nos. 28 and 30, and Nos. 29 and 31, to evaluate the curvature of the upper and lower test halves, are shown in Fig. 35. The same figure also presents the procedures to evaluate both the gross strains in the test section and the several radii of curvature indicated above. The gage length of the overall-curvature clip gages amounts to 10 ft, with the lateral distance between the two gages being 86.625 in. The clip gage arrangements for the upper and lower test sections have a gage length of 5 ft. and a distance across the section of 68.625 in. The potentiometers measuring the pipe displacement along the tension and compression crown lines are also shown in Fig. 35. The pipe center displacement is again taken as the average of the mid-span potentiometer readings Nos. 8 and 18.

6. 2 Test Objective

The test objective for specimen No. 5A, was the same as for specimen No. 5; namely to assess the stability of the pipe wall under an internal pressure drop while the wall was already carrying large compressive stresses due to the deformations caused by the simulated overburden pressure. While the studies of specimen No. 5 dealt with a pressure drop from a moderate level(p_i = 150 psi) the studies on specimen No. 5A concerned the behavior of the pipe under a pressure drop of 950 psi. In both instances the attained gross deformation pattern was to remain unaltered during the depressurization procedure.

6. 3 Load Sequence

After the specimen was pressurized to 950 psi an axial load of 1920 kips was applied. Of this total load, 650 kips was required to counteract the internal pressure effect and 1270 kips to simulate the 90°F temperature differential.

The total nominal lateral load was applied in 100 kip increments up to 400 kips and then in 50 kip increments to 600 kips. At the 600 kip load level the pressure was dropped from 950 psi to 0 psi. Simultaneously the axial load P_A was reduced to 1270 kips, reflecting only the temperature differnetial $T = 90°F$. Because of the satisfactory performance of the specimen under this condition, it was decided to pressurize the pipe again and to terminate the test at that stage. Hence, after pressurizing the pipe specimen to 950 psi and increasing the axial load again to 1920 kips all loads were removed.

6. 4 Test Results

The results for specimen No. 5A are tabulated with the bending moments at the pipe mid-section presented in Table XXI, and the total section radius of curvature and the gross strain data in Table XXII. The radii of curvature for the total section as well as for the upper and lower halves of the section are shown in Table XXIII. The pertinent strain data are presented in Table XXIV.

After the lateral load had been increased step-wise to a maximum value of 600 kips the specimen was depressurized.

The specimen withstood the depressurization successfully as the lateral load could be maintained. The radius of curvature over the total test section decreased only slightly from 780 feet at 600 kips and 950 psi to 742 feet at 589 kips and 0 psi. Upon repressurization the radius was 746 feet at 598 kip and 950 psi.

In comparing the gross strains from the clip gages (Table XXII) with the average measured strains along the crown lines (Table XXIV) at the last 600 kip loading, it was observed that the gross strains on the compression face were about 5 percent larger than the measured strains. For the tension face the gross strains were 2 percent smaller.

IV. 7 SPECIMEN NO. 6

7. 1 Description of Specimen and Instrumentation

Specimen No. 6 was entirely fabricated from pipe number 3743, with a nominal wall thickness of 0.562 in. The stress -strain relationship for this pipe material is shown in Fig. 7 and clearly indicates that it meets the X65 minimum yield requirement of 65 ksi.

This specimen was instrumented with both interior and exterior gages. Typically, interior gages were placed in the laboratory prior to the return of the specimen to the fabricator for welding of the end caps. Upon return to the laboratory the exterior gages were installed. For the purposes of evaluating the basic response of the specimen to the applied loadings, the results of a number of pertinent gages on the tension and compression face have been considered. The location of these gages is shown in Fig. 36.

The clip gage instrumentation as shown in Fig. 37 is basically similar to that used in previous studies. Again, potentiomenters Nos. 26 and 27 permitted evaluating the curvature and gross-strains in the overall section. The gage length and the lateral distance of these gages is 10 ft. and 86.625 in., respectively. The potentiometers Nos. 28 and 30, and Nos. 29 and 31 allowed the evaluation of the curvature in the upper and lower halves of the test section respectively. The gage length of these units if 5 ft. and the lateral distance 68.625 in. The potentiometers to measure lateral pipe displacements along both the tension and compression crown lines are also presented in Fig. 37.

7.2 Test Objectives

The purpose of this study was to evaluate the response of a thick-walled pipe under an increasing simulated settlement of the pipeline while being subjected to a moderately low internal pressure of p_i = 150 psi, and a simulated differential temperature condition of $\Delta T = 90°F$. The test results were to provide not

only information about the initial buckling behavior but also about the post-buckling response of this pipe.

7. 3 Load Sequence

The specimen was pressurized initially up to a pressure p_i = 1680 psi. This pressure, which was maintained for 8 hours, was introduced to create typically a hoop-stress in the pipe wall of 0.95 f_y. The yield stress f_y was the actual yield stress (f_y = 72 ksi) as determined from the standard coupon test.

Following the pressure test, the internal water pressure was reduced to 150 psi and an axial load of 1630 kips was introduced. Of this total load, 101 kips reflected the internal pressure condition and 1529 kips the effect of the 90°F temerature differential.

The lateral load was applied initially in increments of nominally 100 kips until a load of 800 kips had been reached. Subsequently the increments were reduced to 50 kips. While in the process of recording the strain and potentiometer data at a load of 1352 kips, the specimen buckled. Following buckling the specimen was immediately subjected to a post-buckling test.

7. 4 Initial Buckling Test Results

The results of specimen No. 6 are tabulated with the bending moments at the pipe mid-span section presented in Table XXV and the total section radius of curvature and the gross-strain data shown in Table XXVI. The radii of curvature for the total test section as well as for the upper and lower halves of this section are shown in Table XXVII. Finally, the pertinent strain data from both interior and exterior gages are presented in Table XXVIII. As it was not possible to take a set of strain data at the instance of buckling (1352 kips) the strains indicated at that level were extrapolated by applying a factor of 1.12 to the data recorded at a lateral load of 1304 kips. This factor reflects the ratio of the continuously recorded center deflection of the pipe wall (tension

face) under the lateral loads of 1352 and 1305 kips. The total bending moment at which buckling occurred was 75,536 kip-in. The radius of curvature over the entire section at that instance was 486 ft. Under buckling the specimen exhibited a typical outward bulging of the pipe wall at the center of the specimen. Following buckling the specimen was immediately subjected to a post-buckling test.

An observation of the strain data presented in Table XXVIII shows in general a very uniform strain level at each load level. While the tensile strains were initially larger than the compressive values, at higher lateral loads (above 702 kips) the tensile strains were increasingly smaller than the compressive strains. Comparing the gross-strain data (Table XXVI) with the average measured strains (Table XXVIII) shows in general a very close agreement.

7. 5 Post-Buckling Test Results

In order to carry out the typical post-buckling test the specimen was left in the test machine without being rotated 180 degrees around its center line.

After the lateral load was first removed, the specimen was only subjected to the operating pressure of 150 psi and the basic axial load of 1630 kips. While reapplying the lateral load the pipe center displacement increased to 5 in. At that stage the buckle developed an outward-inward pattern. This shape prevailed throughout the post-buckling test. During this procedure the axial load was gradually reduced. Namely, under an axial load of 1005 kips and a lateral load of 350 kips the center displacement reached 11 in. With an axial load decreased to 500 kips and a lateral load of 440 kips, the center displacement was 14 in. This procedure was continued until a center displacement of 48 in. had been reached. At that stage no further displacements could be introduced becuase of limitations induced by the test setup. Rupture did not occur. A detailed and general view of the buckled specimen is shown in Fig. 38 and 39 respectively.

IV. 8 SPECIMEN NO. 7

8.1 Description of Specimen and Instrumentation

The test section of Specimen No. 7 was taken from pipe K1212, a spiral weld X60 pipe with a nominal wall thickness of 0.462 in. The spiral weld made a 360 degree revolution over a 5 ft length of pipe. At midspan where the two 5 ft-6 in test sections meet, the spiral weld started in the compression face of the upper half and the tension face of the lower half. (see also Fig. 2). The stress-strain relationship for this pipe material is shown in Fig. 7. With a yield stress of 68 ksi (at 0.5% strain) the material clearly surpasses the minimum nominal yield stress of 60 ksi, required for X60 pipe.

This specimen was instrumented with both interior and exterior gages. The location of a number of gages, used to evaluate the basic behavior of the pipe is shown in Fig. 40.

The clip gage instrumentation is shown in Fig. 41 and is basically the same as the one used in specimen No. 6. While the gage lengths of 10 ft. (for gages Nos. 26 and 27) and 5 ft. (for gages Nos. 28 and 30 and Nos. 29 and 31) are unchanged, the lateral distances between the corresponding gages are 85.688 in. and 69.750 in., respectively. Fig. 41 also shows the location of the potentiometers along the compression and tension crown lines, as well as the basic procedures to determine the radii of curvature and gross-strain values.

8.2 Test Objective

The primary objective of this study was to evaluate the behavior of a spiral welded pipe under an increasing simulated settlement of the pipeline while being subjected to an internal pressure of p_i = 150 psi and an axial load simulating a temperature differential (between the installation and operating temperatures) of $\Delta T = 90°F$. Following the initial buckling study under the above conditions, the specimen was to be subjected to excessive deformations in order to establish the rupture deformation.

8. 3 Load Sequence

The water filled specimen was pressurized initially to a pre-test pressure of 1244 psi reflecting a circumferential stress of 0.95 f_y. After this pressure had been maintained for 8 hours without showing any leakage, the pressure was reduced to the test pressure of 150 psi. Subsequently an axial load of 1322 kips was introduced. Of this total load 103 kips was needed to counteract the internal pressure effects. The remaining 1219 kips simulated the effect of the temperature differential of 90°F.

The lateral load was applied first in increments of nominally 100 kips. After reaching a 600 kip load, load intervals were reduced to 50 kips. Following buckling at a load of 865 kips the specimen was immediately subjected to a post-buckling test (without rotating the specimen 180 degrees around its center axis).

8. 4 Initial Buckling Test Results

The bending-moments for specimen No. 7 due to the different lateral load levels are presented in Table XXIX. The corresponding radii of curvature and gross tensile and compressive strains are presented in Table XXX. For comparative purposes the radii of curvature for the gross test section as well as for the upper and lower test halves are presented in Table XXXI. Finally, the strain data for the pertinent strain gages shown in Fig. 40 are presented in Table XXII. Because it was impossible to take strain readings at the buckling load of 865 kips, the tabulated data at that load level is obtained by applying a factor of 1.05 to the data recorded at a load of 850 kips. The factor 1.05, reflects the ratio between the center-span deflection at the 865 and 850 kip load levels, as recorded by the X-Y recorder, which monitored continuously the center displacement versus the lateral load.

The total moment at the instance of buckling was 47,297 kip-in. The radius of curavature of the entire test section at that instance was 920 ft.

Buckling occurred by the formation of a typical outward bulging of the pipe wall about 8 in. below the center circumferential weld. Following the initial buckling, the specimen was subjected to the post-buckling test.

The strain data presented in Table XXXII show in general a good agreement at each load level. The gross strain values are in general larger than the measured strains--a fact which has been observed almost consistently in the earlier tests.

8. 5 Post Buckling Test Results

The post buckling test was performed immediately following the development of an initial buckling after a center displacement of about 1.60 in. as recorded by the X-Y recorder. In extending the buckle, the lateral load dropped off to 500 kips. At that instance the displacement had increased to 3.25 in. and the buckle developed an inward-outward pattern. Under a continuously increasing center displacement the lateral load reduced to zero, and the axial load to about 875 kips. The corresponding center displacement was 8.0 in. While the pipe further deflected the axial load resistance reduced rapidly. At a displacement of 33 in. the axial load had fallen to approximately 400 kips. Rupture of the pipe wall in the folded region of the buckle finally occurred under a center displacement of 43 in. and an axial load of 380 kips. A side view of the highly deformed specimen is shown in Fig. 42. An overall view of the compression side of the pipe following failure under a 43 in. center displacement is shown in Fig. 43.

V. SUPPLEMENTAL OBSERVATIONS

During the test program a number of specific studies were performed to assess in detail the behavior of the pipe section under the combined load conditions. The results were necessary to establish the appropriateness of certain assumptions made in the analytical program and to allow a better interpretation of the previously discussed overall pipe behavior. Furthermore, in order to study the effect of cracks under high stress levels, three specimens with intentionally induced flawes (through-thickness saw cuts) in both the longitudinal welds and in the adjacent heat-affected zone of the pipe wall were investigated.

V.1 LONGITUDINAL STRAINS

The actual distribution of the longitudinal strains in a typical transverse cross-section of the pipe is important for the analytical procedures which were developed in a separate study. In these studies it was assumed that, even under post-yield strain conditions, plane section of the entire pipe cross-section would remain plane. In order to assess this hypothesis a number of cross-sections were instrumented with longitudinal strain gages.

In the first two specimens gages were placed on the inside and outside face of the pipe wall at both the compression and tensile crown lines and at angular intervals of 22.5° and 45° from these lines. The strain data for the two sections located in the upper and lower test sections, 24 in. from the center weld, will be reviewed. The results for Specimen No. 1 are presented in Figures 44 and 45. Buckling in this case occurred in a region about 36 in. above the upper instrumented section at a total lateral load of 497 kips. Observing the strain data one may conclude that, despite the lack of strain information in the neutral strain regions, the results

clearly imply a linear strain distribution across the observed pipe section. The same conclusion can be drawn from the data presented for Specimen No. 2 as shown in Figures 46 and 47. In that case buckling under a total lateral load of 460 kips occurred in a region about 18 in. below the lower instrumented section. In observing the strain data for a lateral load of 453 kips it is important to note that the strain distribution remains linear even when the lateral load approaches buckling.

In order to futher substantiate the above noted phenomenon for thick-walled and spiral-welded pipes, pertinent test data for Specimens No. 6 and 7 are presented. Longitudinal strain gage data for the thick-walled (0.562 in. nominal) Specimen No. 6 are shown in Figures 49, 50 and 51. The cross-sections J as shown in Fig. 52 are located at distances of 42 in. above and below the center section G. In this study strain gages were also placed at the "neutral axis" of the pipe section. Up to a nominal lateral load of 1100k the strain across the section is truly linear. Subsequently, particular in the center section (G), (See Figure 51) strains in the extreme compressive region tend to depart from the linear strain distribution. This phenomenon is not surprising if one considers the extremely high local strain level and the fact that buckling occurred at that location under a total lateral load of 1352k. An observation of the strain data presented in Figure 50 indicates a basic strain linearity up to a lateral load of 1200k. However, at 1300k. a non-linear cross-section strain development seems to occur, similar to that noted for section G (Fig. 51). Even though at incipient buckling there is a departure from linearity at these high strain values (5000 - 6000 μ in./in), the overall response of the specimen supports the assumption that plane section remain plane. Therefore, the hypothesis of this phenomenon on which the analysis has been based is completely valid in predicting the gross pipe column-bending behavior.

The previous conclusion is also supported by the strain results obtained from the spiral welded Specimen No. 7. The strain data presented in Figures 53 and 54, for two sections (E) located in 24 in. above and below the center weld, show again a linear strain distribution across the section. This basic linear behavior of the pipe cross-section can be observed even at loads (851 kips) close to the lateral buckling load of 865 kips. Hence, one may conclude in general that the hypothesis of plane sections remain plane under bending is correct.

In addition to the above evidence in support of the hypothesis of "plane sections remain plane", two additional observations are significant.

Firstly, the strain distribution due to bending only, as shown in the previous four figures, clearly shows that the neutral axis (zero-strain) under increasing lateral loads gradually moves from the centroidal position to a location significantly closer to the tension face of the pipe section. This shift together with the pre-compressive strain condition due to the axial load P_A causes the introduction of compressive strains in about 75 to 85% of the pipe cross-section. Figure 48 shows such combined overall gross strain distributions, as obtained from the clip gage data. These results indicate that 25% of the pipe cross-section, near the compression crown line, is subjected to relatively uniform compressive strains. Over this 90° - arc region with a circumferential length of about 38 in. the strains vary between about 85% and 100% of maximum. Actually, in the central 45° - arc region of the compression zone the extreme strains vary no more than 4 - 5% from the average strain value. These observations are particularly important since the theoretical buckling studies of circular pipes carried out separately assume a uniform compressive strain. Thus, the observed near uniformity of the compressive strain implies that the specific theory may well be used to predict the buckling behavior of the

pipe line. Actually, the generally observed occurence of buckling over a significant circumferential section of the pipe wall seems to support the validity of the assumed uniform compressive strains.

A second observation important for both the beam-column analysis of the pipe line as well as the experimental studies, concerns the virtual equality of the strains measured at the same location on the inner and outer faces of the pipe wall. Reviewing the data presented in Figures 44 thru 47 shows that, almost invariably, comparative results agree very well. Based on these results, it was decided, for future specimens, the placement of interior gages should be omitted.

V.2 CIRCUMFERENTIAL STRAINS AND CROSS-SECTIONAL DEFORMATIONS

In order to evaluate the behavior of the circular cross-section under the effect of lateral loads a detailed study of the circumferential strains has been carried out. This investigation was performed for the heavily instrumented sections J and G of Specimen No. 6. The exact location of these sections is shown in Figure 52. In interpreting the results it should be noted that buckling under a load of 1352 kips occurred at the center section (G).

The strain gage data for gages placed at intervals of 22.5° and 45° on both the inside and outer face of the pipe wall are presented in Figures 55, 56 and 57. Also shown are the average circumferential, or hoop strains for each of the three sections at different load levels. Comparing the absolute values of the average circumferential strains along the compression crown line at a load of 1352 kips with the corresponding longitudinal strains as shown in Figs. 49, 50 and 51, we note that the hoop strains are between 0.4 and 0.5 of the longitudinal strain values. In the tension zone this ratio is closer to 0.3.

The difference of the inner and outer surface hoop strains in comparison with the average hoop strain clearly indicates a transverse bending of the circular cross-section of the pipe wall. The strain data invariably indicate independent of load magnitude or section that in the compression zone of the pipe wall the transverse tensile hoop strains are larger on the inside surface than on the outside. The transverse strain data on the tension zone show that the transverse compressive strains are larger on the outside than on the inside of the pipe wall. Thus, in both the extreme compression and tensile regions the pipe wall tends to bend inward. As expected a completely opposite trend is evident in the regions located 90° away from the tensile and compressive crown lines. In those regions the outer face of the pipe wall is invariable strained in hoop-tension, while the inner face is subjected to a lower tension or even compression hoop strain. This basic strain condition is shown in Figure 58. The same figure shows a number of cross sectional deformation patterns which totally underscore the above strain observations. However, it should be noted that these deformations are not more than 0.031 in. or less than 0.05% of the pipe diameter.

V.3 CURVATURE DATA

The curvature data presented in this report have been derived from the clip gage deflectometer, measuring the longitudinal deformations over the length of both the entire test section as well as over the upper and lower test halves.

Calculating the curvatures from the measured strain data along the compression and tensile crown lines showed in general a good to excellent agreement with the clip gage curvature values. This result is not surprising if one considers the good agreement between the gross-strain data using the

basic clip gage data and the acutally measured strains.

However, using the data from the deflectometers spaced along the tensile and compression crown lines of the test section, the curvature values are invariably larger than the curvature values derived from the clip gage data. This discrepancy has been the subject of extensive studies. In these studies calculations were carried out to achieve an optimum fit of both circular and parabolic curves through the recorded displacement data along the crown lines. However, invariably the radii of curvature were smaller than those calculated form the clip-gage data. Detailed studies of the circumferential bending strains as observed in the previous section and shown in Figure 58, indicate that this phenomenon is less pronounced near the lateral loading points (yokes) than in the actual test section. Actually, the inward bending of the pipe along the compression and tensile crown lines is significantly larger (3 to 4 times) in the center portion of the test section than near the loading points. This phenomenon thus affects the potentiometer readings along the tensile and compression crown lines, in an uneven manner. Therefore, the deflectometer readings on the compression side near the center section show a larger added displacement than those located in the upper and lower test halves. In principle this development explains in part the larger curvature values derived from the displacement readings on the compression side as compared to the values derived from the clip gage data.

It has been impossible to explain these discrepencies completely. In general there is no doubt that the clip gage data provide the most reliable and realistic information from which to determine the curvature values for the total pipe section. After all, the crown displacement data provide only data on the relative motion of the wall rather than the entire section. Also since the clip gage data resulted in more conservative curvature values, the

radii of curvature presented in the earlier tables should be used in assessing appropriate design criteria.

V.4 INFLUENCE OF WELD DEFECTS

In order to investigate the effect of material defects on the behavior of the pipe under actual load conditions three specimens were tested with both through - thickness cuts and weld defects.

Specimens No. 2 and 3 have been tested with intentially introduced defects at the junctions of the center circumferential weld and the longitudinal welds on both the compression and tension face of the specimen. The defects were oriented parallel to the longitudinal weld and introduced as through-thickness cuts in both the center of this weld and in the immediately adjacent heat-affected zone, as shown in Fig. 59. These cracks were sealed from the inside to prevent leakage under pressure.

In addition to these through cuts the circumferential welds at both the center of the test section (MK B) and at the junction between the test and loading sections (MK A) were affected intentionally by inappropriate weld procedures to achieve hairline surface cracks. Despite these multiple defects neither the through-cuts nor the surface cracks affected the response of the specimens in any detrimental manner. Even during the post-buckling test, up to failure, these defects did not trigger any crack propagation or caused ultimate failure. The same conclusion can be drawn from the test observations of the spiral weld specimen No. 7 which was likewise defected by through-thickness cuts in the spiral weld as shown in Fig. 61.

In general one can observe that the pipe material is highly ductile and will only fail under unusual and extreme deformations.

VI TEST COMPILATION AND CONCLUSIONS

VI.1 COMPILATION

The basic test data and the radii of curvature at the end of the initial buckling test phase are tabulated in Table XXXIII. Furthermore, the moment-curvature relationship for each test with the curvature values based on the overall section clip-gage data, are presented in Fig. 62. The moment versus compressive gross-strain values due to bending only are shown in Fig. 63.

Following the initial buckling phase, five specimens (Nos. 2, 3, 4, 6 and 7) were also subjected to so-called post-buckling tests until failure of the pipe wall occurred. The total angular changes over the buckled region at the point of failure for all but specimen No. 6 are presented in Table XXXIV. Although specimen No. 6 did not fail because of test displacement limitations the final angular deformation is nevertheless included in the latter table.

VI.2 CONCLUSION

The results of this study clearly indicate that the pipe behavior can be divided into two functionally different phases. Namely, an initial pre-buckling phase followed by a post-buckling phase. Failure which occurred only at the end of the post-buckling phase resulted from excessive local deformations and a tearing of the pipe wall. Actually, after buckling of the pipe wall at relatively low curvature values occurs, the cross-sectional changes are small enough not to affect the through-flow capacity of the pipe appreciably. Following buckling the pipe is capable of undergoing further deformations which are twenty to thirty times those observed initially.

In general highly pressurized pipes (p_i = 900 psi) have effectively a lower bending stiffness - and moment capacity - than pipes with a lower internal pressure (P_i = 150 psi). Consequently buckling of these high pressurized sections will occur at smaller radii of curvature. Studies further indicated that the pipe wall remained stable when the pipe was subjected to a complete depressurization and repressurization procedure. This aspect was investigated after the compressive strains in the pipe had already reached near-buckling strain levels under the initial pressure condition.

Buckling occurred in two basic forms. For the higher pressurized pipes (p_i = 150 - 950 psi) initial buckling develops as an outward buckling of the pipe wall over a substantial portion (up to 75%) of the pipe circumference. For sections with a low internal pressure (p_i = 25 psi), the buckled wall takes on a diamond like in-and-outward type of deformation pattern. The low-pressure buckling pattern was clearly evident in specimen test No. 3. However, in the post-buckling phase specimen pressurized at 150 psi could not maintain this outward buckling phenomena and exhibited the typical low pressure in-and-outward type final deformation pattern. This is evident in specimens No. 6 and 7 as shown in Figs. 38, 38 and 42, 43.

An observation of the longitudinal strains in transverse sections indicate a uniform strain distribution across the section even up to loads nearing the buckling load level. This phenomenon supports the hypothesis used in analytical studies, that plane sections remain plane. Only in a couple of cases where such sections were located in the immediate vicinity of a buckling zone, did the extreme compressive strains depart locally from the generally observed planar strain pattern. However, these deviations do not warrant a modification of the basic hypothesis in any way. The

longitudinal strain data further show that the neutral axis (zero strain) for the combined case of axial loads and bending moments, moves distinctly towards the tension face of the pipe wall (see Fig. 48). As a result about 75 to 85% of the pipe wall may be subjected to compressive strains. This development further produces a relatively uniform state of strain in a region on the compression face near the crown line of the pipe. Fortunately, this development agrees closely with the analytical assumption of a uniform state of stress in predicting theoretically the strain level at which buckling of the wall may occur. The noted compressive strain distribution is undoubtedly related to the observed bulging of the pipe wall over a significant portion of the pipe circumference particularly for the highly pressurized pipe specimens. (Figs. 11, 12, 13, 25 and 26).

Transverse, or hoop, strain data and deformation measurements of the pipe cross section indicate that the pipe wall in the maximum strained compression and tension zones tends to move inward. In between those regions the pipe wall moves outward. Thus, the pipe cross section deforms into an ellipse with the shorter axis oriented in the plane of loading. These secondard out-of-roundness displacements are very small and less than 0.05% of the pipe outer diameter.

Studies as to the affect of weld defects in the form of through-thickness saw cuts in the welds and in the adjacent heat-affected zone as well as hair cracks induced intentionally due to inappropriate welding, proved to be most encouraging. Despite the high strains in these regions the tests were carried out without noting any affect of these defects. Actually, failure occurred elsewhere and only after excessive local deformations in the post-buckled zone. Even then failure was of a total ductile nature.

There is every indication that the experimental study has yielded invaluable information necessary for an appropriate determination of the operational margins of safety and the subsequent safety against rupture. Such a study is particularly important if the results can be used to determine the applicability and accuracy of analytical methods to be used in predicting the pipeline behavior under load conditions different from those included in the test program. In this connection Fig. 64 illustrates the close agreement between the actual test results and predicted values obtained from an analytical study developed independently from this experimental program. There is every indication that such a combined experimental and theoretical approach will result in an optimum design of the Trans-Alaska Pipeline.

VII. REFERENCES

1. Bouwkamp, J. G., "Structural Behavior of a Large Diameter Pipeline Under Combined Loading," Proceedings 23rd Annual Pipeline Conference, API, Division of Transportation, pp 118-155, April 1972.

2. Bouwkamp, J. G., Stephen, R. M., "Large Diameter Pipe Under Combined Loading," Journal of the Transportation Division, Proceedings of the American Society of Civil Engineers, Vol. 99, Note 3, pp. 521-536, August 1973.

TABLE III - SPECIMEN NO. 1 - BENDING MOMENT AT PIPE MID-SECTION

Internal pressure: p_i = 942 psi

Axial load: P_A = 2580 kip; (ΔT = 135°F)

Lateral Load	CENTER DEFLECTION			MOMENT		
	Δ_8	Δ_{18}	Δ_{av}	$P_A \cdot \Delta_{av}$	M_{lat}	M_{total}
kip	in.	in.	in.	k-in.	k-in.	k-in.
0	.002	.000	.001	3	0	3
48	.072	-.076	.074	191	2507	2698
100	.172	-.175	.173	447	5270	5717
149	.276	-.274	.275	710	7805	8515
202	.350	-.354	.352	909	10597	11506
254	.458	-.457	.457	1180	13346	14526
302	.601	-.583	.592	1527	15881	17408
350	.766	-.744	.755	1948	18388	20336
401	.937	-.914	.926	2388	21051	23439
497	1.874*	-1.828*	1.851	4780	26093	30873

*Based on continuous X-Y recorder data; displacement taken as twice displacement at 401 kip.

TABLE IV - SPECIMEN NO. 1 - CLIPGAGE DATA (RADIUS OF CURVATURE AND GROSS STRAINS)

Internal pressure: p_i = 942 psi

Axial load: P_A = 2580 kip; (ΔT = 135°F)

Lateral Load	Moment	Radius of Curvature	Curvature	Gross Strains From Clipgage	
				Tension Face	Compression Face
kip	k-in	Ft.	Ft^{-1}	micro in/in	micro in/in
0	0	∞	0.	0	0
48	2698	23270	$.4297 \times 10^{-4}$	84	-88
100	5717	10238	$.9768 \times 10^{-4}$	179	-211
149	8515	15129	$.1950 \times 10^{-3}$	314	-466
202	11506	4239	$.2359 \times 10^{-3}$	404	-539
254	14526	3135	$.3190 \times 10^{-3}$	542	-734
302	17408	2213	$.4519 \times 10^{-3}$	705	-1103
350	20336	1625	$.6153 \times 10^{-3}$	876	-1586
401	23439	1254	$.7977 \times 10^{-3}$	1080	-2110
497	30873	627*	$.1590 \times 10^{-2}$	2160	-4220

* Based on X-Y recorder data; data at 497 kip obtained from extrapolation that overall displacement of pipe at 497 kip equals twice the overall displacement at 401 kip.

TABLE V. SPECIMEN NO. 1 - PERTINENT STRAIN DATA ALONG COMPRESSION AND TENSION CROWN LINES (MICRO IN/IN)

Gage No.	Int. press. p_i=942 psi	Axial Load P_A=2580 kip	Lateral load $P_{lateral}$ (kips)				
			48	100	149	202	254
UPPER HALF OF TEST SECTION							
914	+400	-1090	+ 80	+190	+290	+390	+470
622	+390	-1130	- 90	-230	-480	-590	-830
624	+370	-1150	-110	-270	-540	-660	-890
626	+350	-1140	-110	-260	-510	-630	-840
628	+390	-1150	-110	-260	-480	-600	-800
222	+360	- 880	(+ 50)	(+110)			
224	+350	- 810	(+ 70)	(+140)			
226	+420	-1000	(+ 80)	(+180)	[1]		
228	+460	- 990	(+ 75)	(+160)			
LOWER HALF OF TEST SECTION							
1014	+380	-1130	+ 80	+190	+300	+410	+500
828	+370	-1150	-100	-260	-490	-610	-810
826	+330	-1130	-100	-250	-470	-580	-790
824	+340	-1160	-100	-270	-620	-730	-1040
822	+390	-1160	- 90	-230	-470	-580	-820
428	+320	-1040	- 70	-210	-430	-510	-710
426	+420	-1030	- 90	-220	-440	-540	-700
424	+320	-1070	- 90	-240	-590	-690	-960
422	+290	-1040	- 80	-190	-370	-460	-630
Average strain upper-half of test section (compression side)							
-	+390	-1030	(-110)[2]	(-260)	(-500)	(-620)	(-840)
Average strain lower half of test section (compression side)							
-	+350	-1100	- 90	-230	-490	-590	-810

[1] Inside strain results doubtful, hence omitted.
[2] Based on external strains only

TABLE V (CONTINUED): SPECIMEN NO. 1 - PERTINENT STRAIN DATA ALONG COMPRESSION AND TENSION CROWN LINES (MICRO IN/IN)

Gage No.	Lateral Load $P_{lateral}$ (kips)			
	302	350	401	497[3]
UPPER HALF OF TEST SECTION				
914	+ 590	+ 730	+ 870	+1500
622	-1220	-1800	-2620	-7870
624	-1270	-1780	-2410	-4730
626	-1160	-1570	-2080	-4200
628	-1080	-1410	-1820	-3840
222				
224				
226	[1]			
228				
LOWER HALF OF TEST SECTION				
1014	+ 630	+ 770	+ 920	+1530
828	-1090	-1390	-1720	-3010
826	-1070	-1410	-1800	-3170
824	-1580	-2270	-3110	-6750
822	-1200	-1740	-2500	-6510
428	- 970	-1410	-1690	-2930
426	- 930	-1190	-1470	-2280
424	-1510	-2290	-3190	-8350
422	- 960	-1440	-2140	-6350

Total average strain at buckling

Average strain upper half of test section (compression side)					Tension	Compression
-	(-1180)[2]	(-1640)	(-2230)	(-5160)	+810	-5800
Average strain lower half of test section (compression side)						
-	-1160	-1640	-2200	-4920	+780	-5670

[1] Inside strain results doubtful, hence omitted

[2] Based on external strains only

[3] Strains obtained from graphical extrapolation. See Fig. 9.

TABLE VI - SPECIMEN NO. 2 - BENDING MOMENT AT PIPE MID-SECTION

Internal pressure: p_i = 917 psi

Axial load: P_A = 2580 kip; (ΔT = 135°F)

Lateral Load	CENTER DEFLECTION			MOMENT		
	Δ_8	Δ_{18}	Δ_{av}	$P_A \cdot \Delta_{av}$	M_{lat}	M_{total}
kip	in.	in.	in.	k-in.	k-in.	k-in.
0	.002	0.	.001	2	0	2
101	.123	-.151	.137	344	5308	5652
198	.334	-.356	.345	870	10413	11283
299	.595	-.590	.593	1493	15706	17199
357	.738	-.711	.724	1825	18764	20589
376	.838	-.800	.819	2063	19716	21779
401	.920	-.869	.894	2253	21029	23282
425	1.151	-1.075	1.113	2805	22312	25117
435	1.285	-1.202	1.244	3134	22837	25971
453	1.485	-1.387	1.436	3619	23769	27388
460	1.678*	-1.567*	1.623	4089	24150	28239

*Based on X-Y recorder data; displacement taken as 1.13 times the displacement at 453 kip.

TABLE VII - SPECIMEN NO. 2 - CLIPGAGE DATA (RADIUS OF CURVATURE AND GROSS STRAINS)

Internal pressure: p_i = 917 psi

Axial load: P_A = 2580 kip; (ΔT = 135°F)

Lateral Load	Moment	Radius of Curvature	Curvature	Gross Strains From Clipgage	
				Tension Face	Compression Face
kip	k-in	Ft.	Ft^{-1}	micro in/in	micro in/in
0	2	∞	0.	0	0
101	5652	9714	$.1029 \times 10^{-3}$	178	-233
198	11283	3796	$.2635 \times 10^{-3}$	424	-629
299	17199	2046	$.4888 \times 10^{-3}$	720	-1235
357	20589	1649	$.6064 \times 10^{-3}$	875	-1550
376	21779	1400	$.7142 \times 10^{-3}$	978	-1878
401	23282	1220	$.8200 \times 10^{-3}$	1091	-2188
425	25117	936	$.1068 \times 10^{-2}$	1322	-2951
435	25971	816	$.1225 \times 10^{-2}$	1454	-3444
453	27388	687	$.1455 \times 10^{-2}$	1640	-4177
460	28239	608*	$.1644 \times 10^{-2}$	1854	-4721

* Based on X-Y recorder data; data at 460 kip obtained from extrapolation that overall displacement of pipe at 460 kip equals 1.13 times the overall displacement at 453 kip.

TABLE VIII - SPECIMEN NO. 2 - PERTINENT STRAIN DATA ALONG COMPRESSION AND TENSION CROWN LINES (MICRO IN/IN)

Gage No.	Int. press. p_i=917 psi	Axial Load P_A=2520 kip	Lateral load $P_{lateral}$ (kips)				
			101	198	299	357	375
UPPER HALF OF TEST SECTION							
914	+342	-1059	+198	+430	+ 675	+ 815	+ 868
622	+315	-1053	-181	-437	-	-	-
624	+249	-1028	-199	-559	-1155	-1509	-1830
626	+314	-1128	-221	-593	-1153	-1477	-1749
628	+332	-1096	-211	-536	- 899	-1091	-1218
222	+646	- 967	-163	-384	- 640	- 765	- 844
224	+465	- 951	-182	-504	-1017	-1379	-1642
226	+754	- 925	-178	-479	- 954	-1204	-1452
228	+992	- 879	-164	-403	- 673	- 815	- 829
LOWER HALF OF TEST SECTION							
1014	+ 318	-1033	+201	+431	+ 686	+ 834	+ 886
828	+ 334	-1104	-220	-650	-1315	-1673	-1953
826	+ 309	-1051	-196	-502	- 872	-1073	-1217
824	+ 279	-1057	-237	-820	-1967	-2643	-3232
822	+ 354	-1100	-178	-442	- 780	- 981	-1125
428	+1083	- 966	-168	-492	-1086	-1405	-1700
426	-	-	-	-	-	-	-
424	+ 414	-1112	-235	-811	-1929	-1509	-3107
422	+ 829	-1027	-146	-317	- 425	- 486	- 489
Average strain upper half of test section (compression side)							
-	+ 508	-1003	-187	-487	- 975	-1246	-1453
Average strain lower half of test section (compression side)							
-	+ 549	-1061	-197	-598	-1250	-1450	-1934

TABLE VIII (CONTINUED): SPECIMEN NO. 2 - PERTINENT STRAIN DATA ALONG COMPRESSION AND TENSION CROWN LINES (MICRO IN/IN)

Gage No.	Lateral load $P_{lateral}$ (kips)				
	400	425	435	453	460[1]
UPPER HALF OF TEST SECTION					
914	+ 964	+1110	+1191	+1308	+1478
622	-	-	-	-	-
624	-2196	-3108	-3690	-4416	-4991
626	-2042	-2730	-3166	-3658	-4134
628	-1337	-1572	-1737	-1909	-2157
222	- 899	- 978	-1006	-1029	-1163
224	-1958	-2785	-3275	-3929	-4439
226	-1696	-2296	-2618	-3019	-3411
228	-1032	-1275	-1436	-1643	-1856
LOWER HALF OF TEST SECTION					
1014	+ 981	+1130	+1223	+1368	+1546
828	-2266	-3057	-3590	-4301	-4861
826	-1349	-1562	-1679	-1751	-1979
824	-3935	-5676	-6873	-8976	-10143
822	-1265	-1527	-1681	-1819	-2055
428	-2018	-2852	-3372	-4068	-4597
426	-	-	-	-	-
424	-3727	-5171	-5975	-6910	-7808
422	- 473	- 383	- 312	- 193	- 218

Average strain upper half of test section (compression side)					
-	-1710	-2294	-2654	-3096	-3498
Average strain lower half of test section (compression side					
-	-2231	-3111	-3632	-4378	-4947

Total average strain at buckle	
Tension	Compression
+761	-3993
+831	-5459

[1]Based on X-Y recorder data; strains obtained from extrapolation that overall strain at 460 kip equals 1.13 times strain at 453 kip.

TABLE IX - SPECIMEN NO. 3 - BENDING MOMENT AT PIPE MID-SECTION

Internal pressure: p_i = 25 psi

Axial load: P_A = 1920 kip; (ΔT = 135°F)

Lateral Load	CENTER DEFLECTION			MOMENT		
	Δ_8	Δ_{18}	Δ_{av}	$P_A \cdot \Delta$	M_{lat}	M_{total}
kip	in.	in.	in.	k-in.	k-in.	k-in.
0	.002	0.	.001	1	29	30
103	.113	0.	.057	108	5409	5517
200	.275	-.132	.204	390	10486	10876
301	.449	-.277	.363	697	15822	16519
400	.621	-.419	.520	998	21000	21998
498	.830	-.558	.694	1331	26135	27466
549	.936	-.633	.784	1505	28803	30308
599	1.067	-.717	.892	1713	31456	33169
649	1.221	-.809	1.015	1948	34096	36044
676	1.336	-.873	1.104	2120	35466	37586
698	1.433	-.920	1.176	2258	36620	38878
724	1.546	-.959	1.253	2405	38033	40438
751	1.813	-1.042	1.427	2740	39418	42158

TABLE X - SPECIMEN NO. 3 - CLIPGAGE DATA (RADIUS OF CURVATURE AND GROSS STRAINS)

Internal pressure: p_i = 25 psi

Axial load: P_A = 1920 kip; (ΔT = 135°F)

Lateral Load	Moment	Radius of Curvature	Curvature	Gross Strains From Clipgage	
				Tension Face	Compression Face
kip	k-in	Ft.	Ft^{-1}	micro in/in	micro in/in
0	0	∞	0.	0	0
103	5517	13358	$.7486 \times 10^{-4}$	121	-179
200	10876	5439	$.1839 \times 10^{-3}$	333	-403
301	16519	3248	$.3078 \times 10^{-3}$	566	-666
400	21998	2323	$.4304 \times 10^{-3}$	791	-931
498	27466	1742	$.5739 \times 10^{-3}$	1041	-1256
549	30308	1559	$.6415 \times 10^{-3}$	1158	-1408
599	33169	1365	$.7327 \times 10^{-3}$	1328	-1603
649	36044	1046	$.9556 \times 10^{-3}$	1667	-2156
676	37586	1008	$.9918 \times 10^{-3}$	1716	-2251
698	38878	949	$.1054 \times 10^{-2}$	1798	-2418
724	40438	878	$.1139 \times 10^{-2}$	1905	-2652
751	42158	779	$.1284 \times 10^{-2}$	2082	-3057

TABLE XI - SPECIMEN NO. 3 - PERTINENT STRAIN DATA ALONG COMPRESSION AND TENSION CROWN LINES (MICRO IN/IN)

Gage No.	Int. press. p_i=25 psi	Axial Load P_A=1290 kip	Lateral load $P_{lateral}$ (kips)				
			103	200	301	400	498
UPPER HALF OF TEST SECTION							
914	14.	-809	195	405	596	791	1021
622	12	-791	-175	-356	-575	-787	-1030
616	11	-744	-165	-339	-561	-768	-1018
624	10	-790	-179	-364	-595	-811	-1063
626	15	-818	-185	-378	-620	-856	-1146
222	87	-641	-123	-247	-408	-574	- 772
224	-	-	-	-	-	-	-
226	124	-673	-140	-281	-463	-647	- 872
228	-	-	-	-	-	-	-
LOWER HALF OF TEST SECTION							
1014	12	-820	195	412	610	803	1030
826	-	-	-	-	-	-	-
824	9	-751	-160	-322	-559	-788	-1096
816	12	-810	-168	-341	-596	-834	-1153
822	9	-753	-155	-318	-556	-774	-1045
428	68	-667	-151	-308	-510	-721	-1016
426	104	-654	-143	-292	-491	-691	- 994
424	25	-819	-180	-367	-606	-843	-1171
422	133	-702	-141	-291	-486	-674	- 919
Average strain upper half of test section (compression side)							
-	39	-755	-161	-328	-537	-740	- 985
Average strain lower half of test section (compression side)							
-	47	-747	-157	-320	-545	-762	-1055

TABLE XI (CONTINUED): SPECIMEN NO. 3 - PERTINENT STRAIN DATA ALONG COMPRESSION AND TENSION CROWN LINES (MICRO IN/IN)

Gage No.	Lateral load $P_{lateral}$ (kips)						
	549	599	649	676	698	724	751*
UPPER HALF OF TEST SECTION							
914	1128	1228	1349	1420	1483	1555	1698
622	-1152	-1303	-1457	-1554	-1629	-1708	-1456
616	-1134	-1288	-1449	-1550	-1624	-1711	- 560
624	-1191	-1350	-1515	-1617	-1694	-1783	- 424
626	-1296	-1483	-1690	-1822	-1926	-2041	- 245
222	- 855	- 986	-1116	-1187	-1254	-1329	-1339
224	-	-	-	-	-	-	-
226	- 968	-1112	-1254	-1339	-1407	-1471	-1436
228	-	-	-	-	-	-	-
LOWER HALF OF TEST SECTION							
1014	1105	1240	1364	1437	1504	1640	1778
826	-	-	-	-	-	-	-
824	-1245	-1517	-1825	-2051	-2247	-2510	-1851
816	-1302	-1580	-1885	-2106	-2297	-2549	-1737
822	-1160	-1392	-1619	-1780	-1911	-2076	-1264
428	-1173	-1389	-1635	-1762	-1829	-1764	- 633
426	-1159	-1413	-1779	-2047	-2334	-2751	-2799
424	-1355	-1609	-1941	-2187	-2410	-2719	-2704
422	-1036	-1192	-1368	-1473	-1567	-1666	-1618
Average strain upper half of test section (compression side)							
-	-1097	-1252	-1411	-1511	-1588	-1675	- 911
Average strain lower half of test section (compression side)							
-	-1203	-1435	-1721	-1918	-2082	-2297	-2058

Total average strain at 724 kip	
Tension	Compression
760	-2391
832	-2997

*Buckling occurred during the recording of this load; hence, results questionable.

TABLE XII - SPECIMEN NO. 4 - BENDING MOMENT AT PIPE MID-SECTION

Internal pressure: p_i = 950 psi

Axial load: P_A = 1920 kip (ΔT = 90°F)

Lateral Load	CENTER DEFLECTION			MOMENT		
	Δ_8	Δ_{18}	Δ_{av}	$P_A \cdot \Delta_{av}$	M_{lat}	M_{total}
kip	in.	in.	in.	k-in.	k-in.	k-in.
4	-.010	.006	-.008	-14	230	215
102	.134	-.131	.133	254	5380	5634
199	.267	-.267	.267	512	10456	10968
301	.423	-.422	.422	811	15778	16589
400	.605	-.575	.590	1133	20999	22132
450	.762	-.708	.735	1411	23610	25021
502	.947	-.879	.927	1778	26337	28115
525	1.079	-.971	1.025	1967	27577	29544
551	1.203	-1.071	1.137	2183	28918	31101
576	1.410	-1.244	1.327	2547	30230	32777
601	1.623	-1.428	1.526	2929	31557	34486
612	1.736	-1.528	1.632	3133	32120	35253
621	1.847	-1.624	1.736	3333	32610	35943
629	2.016	-1.770	1.893	3634	33042	36677
640	2.251	-1.982	2.116	4063	33577	37640
647*	2.611*	-2.299*	2.455	4713	34020	38733

*Displacement data extrapolated from the X-Y recorder data, where the center displacement Δ_c at buckling = 1.18 Δ_c at 640 kip.

TABLE XIII - SPECIMEN NO. 4 - CLIPGAGE DATA (RADIUS OF CURVATURE AND GROSS STRAINS)

Internal pressure: p_i = 950 psi

Axial load: P_A = 1920 kip (ΔT = 90°F)

Lateral Load	Moment	Radius of Curvature	Curvature	Gross Strains From Clipgage	
				Tension Face	Compression Face
kip	k-in	Ft.	Ft^{-1}	micro in/in	micro in/in
0.	215	∞	0.	0	0
102	5634	12804	$.7810 \times 10^{-4}$	106	-206
199.	10969	5777	$.1731 \times 10^{-3}$	286	-406
301	16589	3527	$.2836 \times 10^{-3}$	500	-635
400	22132	2270	$.4405 \times 10^{-3}$	753	-1008
450	25022	1807	$.5534 \times 10^{-3}$	895	-1318
502	28115	1393	$.7176 \times 10^{-3}$	1070	-1800
525	29544	1243	$.8043 \times 10^{-3}$	1163	-2053
551	31101	1079	$.9264 \times 10^{-3}$	1274	-2431
576	32778	897	$.1115 \times 10^{-2}$	1416	-3043
601	34486	761	$.1313 \times 10^{-2}$	1575	-3677
612	35253	697	$.1435 \times 10^{-2}$	1646	-4093
621	35943	646	$.1548 \times 10^{-2}$	1728	-4465
629	36678	579	$.1727 \times 10^{-2}$	1841	-5065
640	37640	505	$.1979 \times 10^{-2}$	1983	-5933
647	38733	436	$.2296 \times 10^{-2}$	2301*	-6882*

* Strains determined as 1.18 times strains at 640 kip

TABLE XIV - SPECIMEN NO. 4 - RADIUS OF CURVATURE FOR TOTAL TEST SECTION, AND UPPER AND LOWER HALVES (CLIPGAGE DATA)

Lateral Load	Moment	Radius of Curvature		
		Total Section	Upper half	Lower half
kip	k-in	Ft.	Ft.	Ft.
4	215	∞	∞	∞
102	5634	12804	11320	11320
199	10968	5777	5715	5245
301	16589	3527	3505	3295
400	22132	2270	2250	2125
450	25021	1807	1805	1670
502	28115	1393	1415	1275
525	29544	1243	1270	1145
551	31101	1079	1105	990
576	32777	897	910	835
601	34486	761	770	715
612	35253	697	705	660
621	35943	646	655	615
629	36677	579	585	550
640	37640	505	515	470
647	38733	436	445	406

TABLE XV - SPECIMEN NO. 4 - PERTINENT STRAIN DATA ALONG COMPRESSION AND TENSION CROWN LINES (MICRO IN/IN)

Gage No.	Int. press. p_i=950 psi	Axial load P_A=1920 kip	Lateral load $P_{lateral}$ (kips)				
			102	199	301	400	450
UPPER HALF OF TEST SECTION							
914	320	-812	196	371	612	830	968
622	351	-838	-167	-353	-542	-871	-1123
616	361	-834	-166	-353	-540	-887	-1157
624	345	-841	-170	-359	-552	-913	-1194
626	336	-821	-168	-356	-543	-848	-1055
LOWER HALF OF TEST SECTION							
1014	314	-818	192	370	597	819	955
826	334	-833	-176	-375	-576	-1213	-1827
824	315	-835	-171	-365	-567	-1217	-1805
816	313	-832	-168	-360	-552	-1101	-1580
822	304	-830	-167	-363	-545	-1003	-1372
Average strain upper half of test section (compression side)							
-	348	-834	-168	-355	-545	1800	-1132
Average strain lower half of test section (compression side)							
-	316	-833	-170	-366	-560	-1134	-1646

TABLE XV (CONTINUED): SPECIMEN NO. 4 - PERTINENT STRAIN DATA ALONG COMPRESSION AND TENSION CROWN LINES (MICRO IN/IN)

Gage No.	Lateral load $P_{lateral}$ (kips)									
	502	525	551	576	601	612	621	629	640	647*
UPPER HALF OF TEST SECTION										
914	1139	1213	1316	1452	1591	1691	1734	1857	2007	2328
622	-1505	-1736	-2097	-2690	-3306	-3668	-4028	-4522	-5158	-5983
616	-1575	-1834	-2256	-2954	-3718	-4162	-4603	-5208	-5981	-6938
624	-1641	-1923	-2393	-3175	-4009	-4487	-4949	-5572	-6336	-7350
626	-1328	-1474	-1695	-1939	-2186	-2303	-2440	-2588	-2757	-3190
LOWER HALF OF TEST SECTION										
1014	1126	1201	1311	1439	1576	1669	1724	1834	1983	2301
826	-2706	-3164	-3777	-4550	-5178	-5470	-5743	-6025	-6313	-7323
824	-2722	-3220	-3974	-5117	-6352	-7091	-7863	-9068	-11179	-12968
816	-2303	-2702	-3303	-4224	-5239	-5850	-6505	-7529	-9344	-10839
822	-1905	-2191	-2617	-3240	-3888	-4245	-4627	-5162	-5993	-6952
Average strain upper half of test section (compression side)										
-	-1513	-1742	-2105	-2689	-3305	-3655	-4005	-4472	-5058	-5868
Average strain lower half of test section (compression side)										
-	-2409	-2819	-3418	-4283	-5164	-5664	-6184	-6946	-8208	-9521

	Tension	Compression
	1836	-6354
	1797	-10038

*Based on X-Y recorder data; strains obtained from extrapolation that overall strain at 647 kip equals 1.16 times strain at 640 kip.

TABLE XVI - SPECIMEN NO. 4 - POST-BUCKLING DISPLACEMENT, MOMENT AND ROTATION

Internal pressure: p_i = 950 psi

Axial load: P_A = 1920 kip; (ΔT = 90°F)

Displacement		Lateral	Moment			Rotation
Δ_c	Δ_{buckle}	Load	M_{axial}	M_{lat}	M_{total}	
in.	in.	kip	kip-in	k-in	k-in	degrees
8.5	10.1	300	+19400	-15750	3650	6°20'
9.5	11.3	185	21700	9700	12000	7° 0'
10.5	12.5	183	24000	9600	14400	7°38'
12.5	14.85	230	28500	12070	16430	9°11'
14.5	17.25	410	33100	21500	11000	10°47'
16.5	19.00	470	37000	24700	12900	12°14'
18.5	22.00	539	42200	28300	13900	13°15'
20.5	24.35	650	46700	34100	12600	15°04'
22.25	26.40	585	50700	30700	20000	16°14'
24.00	28.50	788	54700	41300	13400	17°39'
26.00	30.90	911	59300	47800	11500	19°12'
28.00	33.30	865	64000	45400	18800	20°20'
30.00	35.60	915	68500	48000	20500	21°42'
31.00	36.80	1078	70600	56500	13500	22°56'
34.5*	41.0	980	78600	51500	27100	24°44'

*Failure Displacement

TABLE XVII - SPECIMEN NO. 5 - BENDING MOMENT AT PIPE MID-SECTION

Internal pressure: p_i = 150 psi

Axial load: P_A = 1373 kip; (ΔT = 90°F)

Lateral Load	CENTER DEFLECTION			MOMENT		
	Δ_8	Δ_{18}	Δ_{av}	$P_A \cdot \Delta$	M_{lat}	M_{total}
kip	in.	in.	in.	k-in.	k-in.	k-in.
		0.	0.	0	0	0
205	.259	-.204	.232	318	10745	11063
400	.543	-.456	.499	685	21014	21699
499	.697	-.587	.642	881	26178	27059
601	.874	-.721	.797	1094	31557	32651
701	1.113	-.910	1.012	1389	36793	38182
751	1.234	-.999	1.112	1527	39432	40959
801	1.374	-1.084	1.229	1687	42028	43715
at p_i = 0 psi						
801	1.530	-1.056	1.293	1641*	42028	43669
p_i = 150 psi						
801	1.539	-1.148	1.344	1846	42028	43874
843	1.656	-1.220	1.438	1975	44258	46233

Note: at 843 kip a small buckle started to form in the lower test half; test immediately stopped.

*P_A = 1270 kip for p_i = 0 psi

TABLE XVIII - SPECIMEN NO. 5 - CLIPGAGE DATA (RADIUS OF CURVATURE AND GROSS STRAINS)

Internal pressure: p_i = 150 psi

Axial load: P_A = 1373 kip; ($\Delta T = 90°F$)

Lateral Load	Moment	Radius of Curvature	Curvature	Gross Strains From Clipgage	
				Tension Face	Compression Face
kip	k-in	Ft.	Ft^{-1}	micro in/in	micro in/in
0	0	∞	0.	0.	0
205	11063	5862	$.1706 \times 10^{-3}$	317.	-362
400	21699	2698	$.3707 \times 10^{-3}$	726.	-749
499	27059	2082	$.4802 \times 10^{-3}$	927	-985'
601	32651	1641	$.6092 \times 10^{-3}$	1167	-1259
701	38182	1314	$.7608 \times 10^{-3}$	1412	-1617
751	40959	1185	$.8436 \times 10^{-3}$	1541	-1818
801	43715	1061	$.9425 \times 10^{-3}$	1677	-2077
at p_i = 0 psi					
801	43669*	1035	$.9662 \times 10^{-3}$	1672	-2189
p_i = 150 psi					
801	43715	1004	$.9960 \times 10^{-3}$	1754	-2228
843	46233	900	$.1111 \times 10^{-2}$	1786	-2665

* P_A = 1270 kip for p_i = 0 psi

TABLE XIX - SPECIMEN NO. 5 - RADIUS OF CURVATURE FOR TOTAL TEST SECTION, AND UPPER AND LOWER HALVES (CLIPGAGE DATA)

Lateral Load	Moment	Radius of Curvature		
		Total Section	Upper half	Lower half
kip	k-in	Ft.	Ft.	Ft.
0	0	∞	∞	∞
205	11063	5862	5501	5528
400	21699	2698	2571	2515
499	27059	2082	1976	1946
601	32651	1641	1544	1596
701	38182	1314	1181	1326
751	40959	1185	1053	1218
801	43715	1061	946	1097
801*	43806	1035	932	1050
801	43874	1004	1020	890
843	46233	900	840	885

* with p_i = 0 psi, P_A = 1270 kips.

TABLE XX - SPECIMEN NO. 5 - PERTINENT STRAIN DATA ALONG COMPRESSION AND TENSION CROWN LINES (MICRO IN/IN)

Gage No.	Int. press. p_i=150 psi	Axial load P_A=1373 kip	Lateral load $P_{lateral}$ (kips)				
			205	400	499	601	701
UPPER HALF OF TEST SECTION							
914	58	-543	382	778	976	1199	1442
622	63	-510	-357	-733	-947	-1204	-1503
616	59	-469	-337	-691	-897	-1143	-1441
624	64	-508	-362	-750	-976	-1246	-1576
626	59	-520	-381	-788	-1025	-1308	-1641
LOWER HALF OF TEST SECTION							
1014	37	-467	344	703	887	1085	1301
826	41	-526	-369	-785	-1040	-1369	-1832
824	41	-521	-367	-767	-1010	-1320	-1751
816	45	-525	-366	-762	-998	-1299	-1714
822	47	-529	-369	-768	-1000	-1296	-1693
Average strain upper half of test section (compression side)							
-	61	-510	-359	-740	-961	-1250	-1540
Average strain lower half of test section (compression side)							
-	42	-513	-368	-770	-1012	-1321	-1747

TABLE XX (CONTINUED): SPECIMEN NO. 5 - PERTINENT STRAIN DATA ALONG COMPRESSION AND TENSION CROWN LINES (MICRO IN/IN

Gage No.	Lateral load $P_{lateral}$ (kips)			
	751	801	801/0 psi	801/150 psi
UPPER HALF OF TEST SECTION				
914	1565	1682	1685	1717
622	-1659	-1826	-1885	-1888
616	-1595	-1757	-1811	-1826
624	-1747	-1915	-1986	-1986
626	-1808	-1953	-2031	-2000
LOWER HALF OF TEST SECTION				
1014	1413	1521	1524	1541
826	-2078	-2342	-2437	-2424
824	-1984	-2254	-2354	-2367
816	-1937	-2194	-2286	-2303
822	-1903	-2140	-2225	-2249
Average strain upper half of test section				
-	-1702	-1863	-1928	-1925
Average strain lower half of test section				
-	-1976	-2232	-2326	-2336

Total average strain at final reading 801 kip (150 psi)

Tension	Compression
1232	-2374
1111	-2807

TABLE XXI. SPECIMEN NO. 5A - BENDING MOMENT AT PIPE MID-SECTION

Internal pressure: p_i = 950 psi

Axial load: P_A = 1920 kip; (ΔT = 90°F)

Lateral Load	CENTER DEFLECTION			MOMENT		
	Δ_8	Δ_{18}	Δ_{av}	$P_A \cdot \Delta$	M_{lat}	M_{total}
kip	in	in	in	k-in	k-in	k-in
96	.126	-.140	.133	256	5048	5304
194	.274	-.271	.272	523	10197	10720
301	.415	-.415	.415	796	15993	16589
400	.566	-.554	.560	1075	20985	22060
450	.679	-.648	.664	1274	23610	24884
501	.818	-.776	.797	1530	26293	27823
550	.967	-.896	.932	1789	28889	30678
600	1.264	-1.158	1.211	2325	31500	33825
600*	1.347	-1.234	1.291	2479	31485	33964
at p_i = 0 psi						
587	1.615	-.945	1.280	2457	30837	33294
at p_i = 950 psi						
598	1.505	-1.360	1.432	2750	31370	34120

*Reading just prior to pressure drop.

TABLE XXII - SPECIMEN NO. 5A - CLIPGAGE DATA (RADIUS OF CURVATURE AND GROSS STRAINS)

Internal pressure: p_i = 950 psi

Axial load: P_A = 1920 kip; ($\Delta T = 90°F$)

Lateral Load	Moment	Radius of Curvature	Curvature	Gross Strains From Clipgage	
				Tension Face	Compression Face
kip	k-in	Ft.	Ft^{-1}	micro in/in	micro in/in
0.	0	∞	0.	0.	0
96	5304	14663	$.6820 \times 10^{-4}$	122	-150
194	10720	6321	$.1582 \times 10^{-3}$	315	-318
301	16589	3488	$.2867 \times 10^{-3}$	478	-668
400	22060	2534	$.3947 \times 10^{-3}$	755	-825
450	24884	2162	$.4626 \times 10^{-3}$	910	-940
501	27823	1818	$.5502 \times 10^{-3}$	1107	-1094
550	30678	1373	$.7285 \times 10^{-3}$	1282	-1632
600	33825	914	$.1094 \times 10^{-2}$	1479	-2898
600*	33964	780	$.1282 \times 10^{-2}$	1570	-3650
587**	33294	742	$.1349 \times 10^{-2}$	1490	-3810
598	34120	746	$.1340 \times 10^{-2}$	1570	-3780

* Reading just prior to pressure drop.

** With p_i = 0 psi, P_A = 1270 psi

TABLE XXIII - SPECIMEN NO. 5A - RADIUS OF CURVATURE FOR TOTAL TEST SECTION, AND UPPER AND LOWER HALVES (CLIPGAGE DATA)

Lateral Load	Moment	Radius of Curvature		
		Total Section	Upper half	Lower half
kip	k-in	Ft.	Ft.	Ft.
0	0	∞	∞	∞
96	5304	14663	11000	12000
194	10720	6321	5320	5460
301	16589	3488	3280	3380
400	22060	2534	2190	2360
450	24884	2162	1805	1975
501	27823	1818	1425	1700
550	30678	1373	1100	1420
600	33825	914	765	1095
600*	33964	780	664	1000
587**	33294	742	585	1040
598	34120	746	578	1020

* Reading just prior to pressure drop

** With p_i = 0 psi, P_A = 1270 kips

TABLE XXIV - SPECIMEN NO. 5A - PERTINENT STRAIN DATA ALONG COMPRESSION AND TENSION CROWN LINES (MICRO IN/IN)

Gage No.	Int. press. p_i=950 psi	Axial Load P_A=1920 kip	Lateral load $P_{lateral}$ (kips)				
			96	194	301	400	450
UPPER HALF OF TEST SECTION							
626	377	-836	179	371	569	794	912
608	328	-	-	-	-	-	-
914	317	-829	-206	-427	-667	-1017	-1276
902	319	-826	-208	-431	-694	-1114	-1462
LOWER HALF OF TEST SECTION							
826	328	-802	165	350	548	764	874
1002	306	-793	-192	-387	-611	-856	-1001
1014	256	-747	-180	-370	-579	-841	-997
808	299	-786	-186	-377	-606	-876	-1048
Average strain upper half of test section (compression face)							
-	321	-827	-207	-429	-680	-1065	-1369
Average strain lower half of test section (compression face)							
-	284	-775	-186	-378	-599	-857	-1015

TABLE XXIV (CONTINUED): SPECIMEN NO. 5A - PERTINENT STRAIN DATA ALONG COMPRESSION AND TENSION CROWN LINES (MICRO IN/IN)

Gage No.	Lateral load $P_{lateral}$ 501	550	600	600*	587/0 psi	598/950 psi
UPPER HALF OF TEST SECTION						
626	1050	1209	1426	1469	1294	1609
608	-	-	-	-	-	-
914	-1660	-2254	-3322	-3700	-4046	-4103
902	-1993	-2831	-4410	-4983	-5496	-5626
LOWER HALF OF TEST SECTION						
826	1012	1168	1382	1423	1321	1596
1002	-1148	-1298	-1478	-1531	-1762	-1706
1014	-1195	-1451	-1884	-2030	-2154	-2251
808	-1280	-1620	-2352	-2649	-2793	-2984
Average strain upper half of test section (compression face)						
-	-1826	-2543	-3866	-4341	-4771	-4865
Average strain lower half of test section (compression face)						
-	-1208	-1456	-1905	-2070	-2236	-2313

Total average strain at final reading 598 kip (950 psi)

Tension	Compression
1150	-5371
1122	-2804

*Reading just prior to pressure drop

TABLE XXV - SPECIMEN NO. 6 - BENDING MOMENT AT PIPE MID-SECTION

Internal pressure: p_i = 150 psi

Axial load: P_A = 1630 kip; (ΔT = 90°F)

Lateral Load	CENTER DEFLECTION			MOMENT		
	Δ_8	Δ_{18}	Δ_{av}	$P_A \cdot \Delta_{av}$	M_{lat}	M_{total}
kip	in.	in.	in.	k-in.	k-in.	k-in.
0	0.	0.	0.	0	0	0
202	.239	-.225	.232	379	10629	11008
301	.364	-.352	.358	583	15793	16376
403	.485	-.456	.471	767	21172	21939
500	.625	-.574	.599	978	26249	27226
599	.779	-.709	.744	1212	31427	32639
702	.934	-.841	.888	1446	36836	38283
801	1.098	-.961	1.030	1678	42043	43721
899	1.306	-1.136	1.221	1991	47206	49197
950	1.410	-1.204	1.307	2130	49860	51990
1002	1.536	-1.298	1.417	2309	52600	54910
1049	1.664	-1.393	1.528	2491	55096	57587
1098	1.820	-1.501	1.661	2706	57634	60341
1149	2.011	-1.612	1.811	2958	60302	63255
1201	2.198	-1.753	1.975	3219	63043	66262
1201	2.284	-1.806	2.045	3333	63043	66376
1249	2.456	-1.924	2.190	3570	65581	69151
1304	2.816	-2.175	2.496	4068	68466	72534
1352	3.154*	-2.437*	2.795	4556	70980	75536

*Based on X-Y recorder data; displacement taken as 1.12 times the displacement at 1304 kip.

TABLE XXVI - SPECIMEN NO. 6 - CLIPGAGE DATA (RADIUS OF CURVATURE AND GROSS STRAINS)

Internal pressure: p_i = 150 psi

Axial load: P_A = 1630 kip; (ΔT = 90°F)

Lateral Load	Moment	Radius of Curvature	Curvature	Gross Strains From Clipgage	
				Tension Face	Compression Face
kip	k-in	Ft.	Ft^{-1}	micro in/in	micro in/in
0	0	∞	0.	0	0
202	11008	6734	$.1485 \times 10^{-3}$	271	-336
301	16376	4274	$.2340 \times 10^{-3}$	443	-513
403	21939	3130	$.31941 \times 10^{-3}$	610	-695
500	27226	2426	$.4123 \times 10^{-3}$	808	-876
590	32639	1979	$.5054 \times 10^{-3}$	996	-1068
702	38283	1672	$.5979 \times 10^{-3}$	1177	-1265
801	43721	1408	$.7100 \times 10^{-3}$	1408	-1491
899	49197	1200	$.8336 \times 10^{-3}$	1637	-1767
950	51990	1109	$.9020 \times 10^{-3}$	1756	-1928
1002	54910	1019	$.98181 \times 10^{-3}$	1896	-2114
1049	57587	940	$.1064 \times 10^{-2}$	2031	-2314
1998	60341	870	$.1150 \times 10^{-2}$	2178	-2518
1149	63255	783	$.1277 \times 10^{-2}$	2363	-2853
1201	66263	701	$.1427 \times 10^{-2}$	2567	-3260
1201	66376	676	$.1480 \times 10^{-2}$	2633	-3413
1249	69151	630	$.1587 \times 10^{-2}$	2775	-3707
1304	72534	544	$.1838 \times 10^{-2}$	3098	-4409
1352	75536	486*	$.2058 \times 10^{-2*}$	3468*	-4938*

* Based on X-Y recorder data; data at 1352 kip obtained from extrapolation that overall displacement of pipe at 1352 kip equals 1.12 times the overall displacement at 1304 kip.

TABLE XXVII - SPECIMEN NO. 6 - RADIUS OF CURVATURE FOR TOTAL TEST SECTION, AND UPPER AND LOWER SECTIONS (CLIPGAGE DATA)

Lateral Load	Moment	Radius of Curvature		
		Total Section	Upper half	Lower half
kip	k-in	Ft.	Ft.	Ft.
0	0	∞	∞	∞
202	11008	6734	7020	5929
301	16376	4274	4237	3959
403	21939	3130	3043	3011
500	27226	2426	2354	2374
599	32639	1979	1920	1962
702	38283	1672	1642	1656
800	43721	1408	1352	1434
899	49197	1200	1118	1240
950	51990	1109	1026	1159
1001	54910	1019	932	1068
1049	57587	940	858	989
1098	60341	870	783	920
1158	63255	783	744	787
1200	66262	701	678	690
1200	66376	676	648	671
1249	69151	630	598	630
1304	72534	544	522	540
1352	75536	486	466	483

TABLE XXVIII - SPECIMEN NO. 6 - PERTINENT STRAIN DATA ALONG COMPRESSION AND TENSION CROWN LINES (MICRO IN/IN)

Gage No.	Int. press. p_i=150 psi	Axial Load P_A=1630 kip	Lateral load $P_{lateral}$ (kips)					
			202	301	403	500	599	702
UPPER HALF OF TEST SECTION								
914	73	-531	320	469	709	861	1050	1232
426	88	-492	320	478	676	830	1021	1210
622	71	-544	-333	-495	-627	-822	-998	-1202
626	73	-550	-340	-505	-636	-839	-1017	-1224
624	72	-550	-345	-514	-642	-846	-1027	-1240
222	145	-471	-266	-422	-536	-718	-889	-1088
CENTER OF TEST SECTION								
526	78	-548	345	507	717	898	1042	1239
126	81	-528	262	385	575	695	852	1000
632	77	-559	-362	-535	-675	-891	-1088	-1314
232	554	-421	-359	-505	-618	-814	-999	-1223
LOWER HALF OF TEST SECTION								
1014	80	-545	313	460	671	831	1017	1206
326	110	-588	318	472	660	839	1003	1191
824	72	-513	-326	-483	-589	-782	-945	-1132
826	77	-542	-337	-500	-614	-816	-985	-1189
822	75	-552	-339	-502	-619	-828	-1002	-1208
432	124	-474	-325	-480	-611	-799	-979	-1192
Average strain upper half of test section (compression side)								
-	90	-529	-321	-486	-610	-806	-983	-1189
Average strain lower half of test section (compression side)								
-	87	-521	-332	-493	-608	-807	-978	-1178

TABLE XXVIII (CONTINUED): SPECIMEN NO. 6 - PERTINENT STRAIN DATA ALONG COMPRESSION AND TENSION CROWN LINES (MICRO IN/IN)

Gage No.	Lateral load $P_{lateral}$ (kips)								
	801	899	950	1002	1049	1098	1149	1201	1201
UPPER HALF OF TEST SECTION									
914	1434	1647	1738	1857	1960	2029	2170	2316	2362
426	1402	1610	1714	1839	1947	2070	2222	2380	2428
622	-1443	-1735	-1902	-2085	-2278	-2548	-2855	-3186	-3318
626	-1466	-1761	-1933	-2119	-2319	-2597	-2924	-3270	-3413
624	-1490	-1795	-1973	-2168	-2374	-2664	-3006	-3372	-3521
222	-1323	-1620	-1788	-1982	-2191	-2475	-2844	-3233	-3422
CENTER OF TEST SECTION									
526	1441	1653	1753	1874	1982	2056	2202	2356	2404
126	1160	1317	1384	1473	1535	1564	1664	1774	1792
632	-1592	-1951	-2165	-2415	-2684	-3046	-3539	-4051	-4264
232	-1491	-1861	-2087	-2377	-2689	-3097	-3745	-4454	-4821
LOWER HALF OF TEST SECTION									
1014	1398	1600	1692	1814	1921	1991	2136	2292	2340
326	1380	1590	1690	1813	1919	2034	2185	2344	2392
824	-1360	-1636	-1799	-1980	-2186	-2456	-2828	-3239	-3403
826	-1417	-1702	-1876	-2064	-2277	-2577	-2953	-3374	-3543
822	-1452	-1753	-1937	-2135	-2358	-2672	-3064	-3503	-3684
432	-1434	-1746	-1923	-2138	-2374	-2657	-3123	-3648	-3895
Average strain upper half of test section (compression side)									
-	-1431	-1728	-1899	-2089	-2291	-2571	-2907	-3265	-3419
Average strain lower half of test section (compression side)									
-	-1416	-1709	-1884	-2079	-2299	-2591	-2992	-3441	-3631

TABLE XXVIII (CONTINUED): SPECIMEN NO. 6 - PERTINENT STRAIN DATA ALONG COMPRESSION AND TENSION CROWN LINES (MICRO IN/IN)

Gage No.	Lateral load $P_{lateral}$ (kips)		
	1249	1304	1352[1]
UPPER HALF OF TEST SECTION			
914	2496	2768	3100
426	2568	2840	3181
622	-3589	-4158	-4657
626	-3700	-4298	-4814
624	-3820	-4455	-4990
222	-3758	-4587	-5136
CENTER OF TEST SECTION			
526	2549	2811	3148
126	1891	2095	2347
632	-4732	-5845	-6546
232	-5568	-8531	-9555
LOWER HALF OF TEST SECTION			
1014	2507	2757	3088
326	2533	2810	3147
824	-3793	-4611	-5165
826	-3950	-4776	-5350
822	-4104	-4479	-5577
432	-4383	-5769	-6461
Average strain upper half of test section (compression side)			
-	-3717	-4375	-4899
Average strain lower half of test section (compression side)			
-	-4058	-5034	-5638

	Tension	Compression
	2710	-5338
	2646	-6072

[1] Based on X-Y recorder data; strains obtained from extrapolation that overall strain at 1352 kip equals 1.12 times strain at 1304 kip.

TABLE XXIX - SPECIMEN NO. 7 - BENDING MOMENT AT PIPE MID-SECTION

Internal pressure: p_i = 150 psi

Axial Load: P_A = 1322 kip; ($\Delta T = 90°F$)

Lateral Load	CENTER DEFLECTION			MOMENT		
	Δ_8	Δ_{18}	Δ_{av}	$P_A \cdot \Delta_{av}$	M_{lat}	M_{total}
kip	in.	in.	in.	k-in.	k-in.	k-in.
0	0.	0.	0.	0	0	0
100	.146	-.093	.120	158	5249	5407
199	.297	-.225	.261	345	10456	10801
300	.438	-.353	.395	523	15735	16258
401	.575	-.474	.525	694	21028	21722
451	.651	-.538	.595	786	23697	24483
499	.721	-.599	.660	872	26178	27050
550	.795	-.660	.728	962	28889	29851
599	.892	-.742	.817	1080	31456	32536
650	.982	-.809	.895	1184	34110	35294
699	1.089	-.890	.989	1308	36721	38029
752	1.188	-.955	1.072	1417	39461	40878
799	1.330	-1.052	1.191	1574	41971	43545
851	1.557	-1.158	1.358	1795	44668	46463
865	1.635*	-1.216*	1.426	1885	45412	47297

*Based on X-Y recorder data; displacement taken as 1.05 times the displacement at 851 kip.

TABLE XXX - SPECIMEN NO. 7 - CLIPGAGE DATA (RADIUS OF CURVATURE AND GROSS STRAINS)

Internal pressure: p_i = 150 psi

Axial load: P_A = 1322 kip; ($\Delta T = 90°F$)

Lateral Load	Moment	Radius of Curvature	Curvature	Gross Strains From Clipgage	
				Tension Face	Compression Face
kip	k-in	Ft.	Ft^{-1}	micro in/in	micro in/in
0	0		0.	0	0
100	5408	11955	$.08365 \times 10^{-3}$	127	-215
199	10801	5262	$.1901 \times 10^{-3}$	332	-444
300	16258	3405	$.2937 \times 10^{-3}$	540	-658
401	21722	2459	$.4067 \times 10^{-3}$	785	-875
451	24483	2199	$.4547 \times 10^{-3}$	890	-967
499	27050	1944	$.5145 \times 10^{-3}$	1013	-1088
550	29851	1750	$.5716 \times 10^{-3}$	1121	-1213
599	32536	1578	$.6339 \times 10^{-3}$	1243	-1346
650	35294	1432	$.6983 \times 10^{-3}$	1380	-1472
699	38029	1315	$.7606 \times 10^{-3}$	1494	-1612
752	40878	1197	$.8352 \times 10^{-3}$	1621	-1790
799	43546	1096	$.9125 \times 10^{-3}$	1750	-1977
851	46463	966	$.1035 \times 10^{-2}$	1904	-2324
865	47297	920*	$.1087 \times 10^{-2*}$	2000*	-2440*

* Based on X-Y recorder data; data at 865 kip obtained from extrapolation that overall displacement of pipe at 865 kip equals 1.05 times the overall displacement at 851 kip.

TABLE XXXI - SPECIMEN NO. 7 - RADIUS OF CURVATURE FOR TOTAL TEST SECTION, AND UPPER AND LOWER SECTIONS (CLIPGAGE DATA)

Lateral Load	Moment	Radius of Curvature		
		Total Section	Upper half	Lower half
kip	k-in	Ft.	Ft.	Ft.
0	0	∞	∞	∞
100	5407	11955	12926	10115
199	10801	5262	6057	4560
300	16258	3405	3578	3052
401	21722	2459	2469	2303
451	24483	2199	2190	2088
499	27050	1944	1891	1866
550	29851	1750	1690	1710
599	32536	1578	1500	1555
650	35294	1432	1376	1425
699	38029	1315	1264	1311
752	40878	1197	1151	1202
799	43545	1096	1050	1104
851	46463	966	920	989
865	47297	920	876	942

TABLE XXXII - SPECIMEN NO. 7 - PERTINENT STRAIN DATA ALONG COMPRESSION AND TENSION CROWN LINES (MICRO IN/IN)

Gage No.	Int. press. p_i=150 psi	Axial Load P_A=1322 kip	Lateral load $P_{lateral}$ (kips) 100	199	300	401	451	499	550	599	650
UPPER HALF OF TEST SECTION											
608	+ 71	-510	+177	+379	+580	+780	+858	+ 954	+1072	+1184	+1280
914	+ 69	-526	+186	+407	+618	+834	+912	+1013	+1150	+1270	+1369
622	+ 61	-533	+178	-357	-544	-748	-857	- 969	-1050	-1155	-1277
616	+ 60	-531	-182	-361	-552	-762	-871	- 987	-1068	-1178	-1304
624	+ 59	-545	-188	-376	-574	-795	-911	-1035	-1126	-1247	-1387
626	+ 60	-539	-193	-384	-585	-810	-926	-1051	-1145	-1268	-1410
222	+312	-435	-156	-311	-478	-677	-776	- 889	- 969	-1088	-1238
224	+254	-395	-157	-309	-471	-655	-745	- 842	- 900	- 991	-1099
226	+174	-440	-169	-334	-508	-708	-809	- 917	- 988	-1090	-1210
228	+190	-451	-173	-340	-516	-714	-811	- 917	- 984	-1084	-1199
LOWER HALF OF TEST SECTION											
1014	+ 59	-513	+175	+383	+591	+799	+882	+ 981	+1101	+1213	+1316
808	+ 62	-519	+165	+367	+570	+773	+849	+ 943	+1066	+1177	+1276
826	+ 58	-504	-185	-359	-542	-746	-858	- 978	-1065	-1188	-1340
824	+ 69	-527	-210	-384	-568	-768	-878	- 991	-1068	-1178	-1306
816	+ 69	-523	-210	-379	-562	-764	-875	- 990	-1071	-1187	-1325
822	+ 57	-544	-226	-403	-589	-800	-913	-1030	-1112	-1229	-1370
428	+204	-530	-184	-369	-561	-771	-871	- 984	-1077	-1197	-1328
426	+ 75	-536	-189	-376	-564	-766	-861	- 964	-1049	-1159	-1297
424	+ 88	-521	-185	-359	-537	-734	-828	- 930	-1016	-1119	-1228
422	+ 97	-553	-197	-339	-492	-651	-734	- 818	- 884	- 969	-1062
Average strain upper half of test section (compression side)											
-	146	-484	-175	-347	-529	-734	-838	- 951	-1029	-1138	-1266
Average strain lower half of test section (compression side)											
-	90	-530	-198	-371	-552	-750	-852	- 961	-1043	-1153	-1282

TABLE XXXII (CONTINUED): SPECIMEN NO. 7 - PERTINENT STRAIN DATA ALONG COMPRESSION AND TENSION CROWN LINES (MICRO IN/IN)

Gage No.	Lateral load $P_{lateral}$ (kips)				
	699	752	799	851	865[1]
UPPER HALF OF TEST SECTION					
608	+1382	+1507	+1615	+1745	1832
914	+1480	+1615	+1729	+1866	1960
622	-1399	-1524	-1655	-1757	-1844
616	-1429	-1556	-1706	-1859	-1952
624	-1527	-1677	-1850	-2008	-2108
626	-1555	-1720	-1387	-1998	-2098
222	-1391	-1577	-1749	-1916	-2011
224	-1201	-1304	-1440	-1582	-1661
226	-1327	-1443	-1559	-1600	-1680
228	-1310	-1422	-1539	-1424	-1495
LOWER HALF OF TEST SECTION					
1014	+1424	+1548	+1659	+1798	1888
808	+1378	+1506	+1617	+1760	1849
826	-1498	-1706	-1957	-2108	-2213
824	-1439	-1607	-1891	-2618	-2749
816	-1474	-1692	-2007	-2520	-2646
822	-1516	-1701	-1986	-2632	-2763
428	-1454	-1566	-1640	-1178	-1237
426	-1424	-1573	-1750	-1858	-1951
424	-1335	-1439	-1474	-1272	-1335
422	-1154	-1238	-1313	-1292	-1357
Average strain upper half of test section (compression side)					
-	-1392	-1528	-1674	-1768	-1856
Average strain lower half of test section (compression side)					
-	-1412	-1565	-1752	-1935	-2031

Total average strain at buckle	
Tension	Compression
1449	-2194
1413	-2471

[1]Based on X-Y recorder data; strains obtained from extrapolation that overall strain at 865 kip equals 1.05 times strain at 851 kip.

TABLE XXXIII - BASIC TEST DATA AT END OF INITIAL BUCKLING TEST PHASE

Specimen No.	Internal Pressure (psi)	Axial Load (kip)	Lateral Load (kip)	Moment (k-in)	Radius of Curvature (Ft)
1	942	2580	497	30873	627
2	917	2580	460	28239	608
3	25	1920	751	42158	779
4	950	1920	647	38733	436
5	150	1373	843	46233	900
5A	950	1920	600	33964	780
6	150	1630	1352	75536	486
7	150	1322	865	47297	920

TABLE XXXIV - SUMMARY OF POST BUCKLING FAILURE DISPLACEMENTS AND ROTATIONS

Specimen No.	Final Pipe Displacement at Buckle (in.)	Total Angular Rotation at Failure
2	30.5	19°15'
3	34	20°35'
4	41	24°44'
6	48*	28°30'*
7	44.8	26°44'

*Specimen did not fail because of test displacement limitations

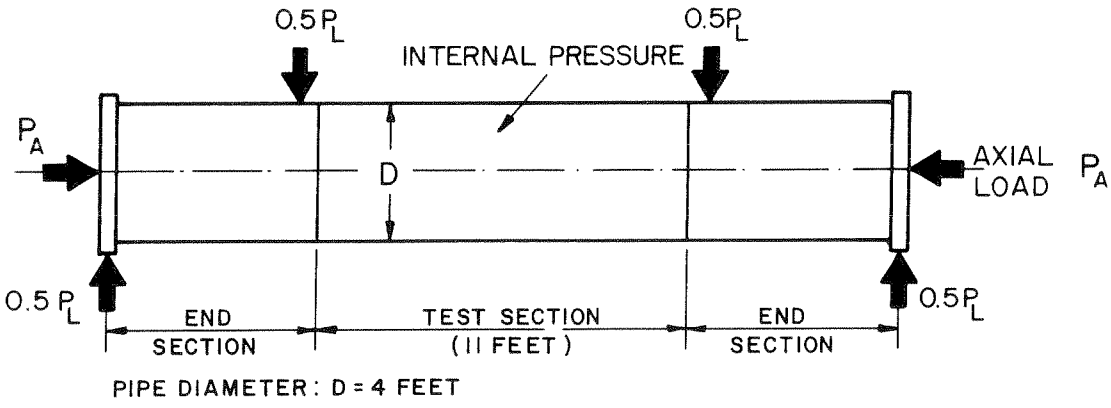

FIG. 1 BASIC TEST SPECIMEN

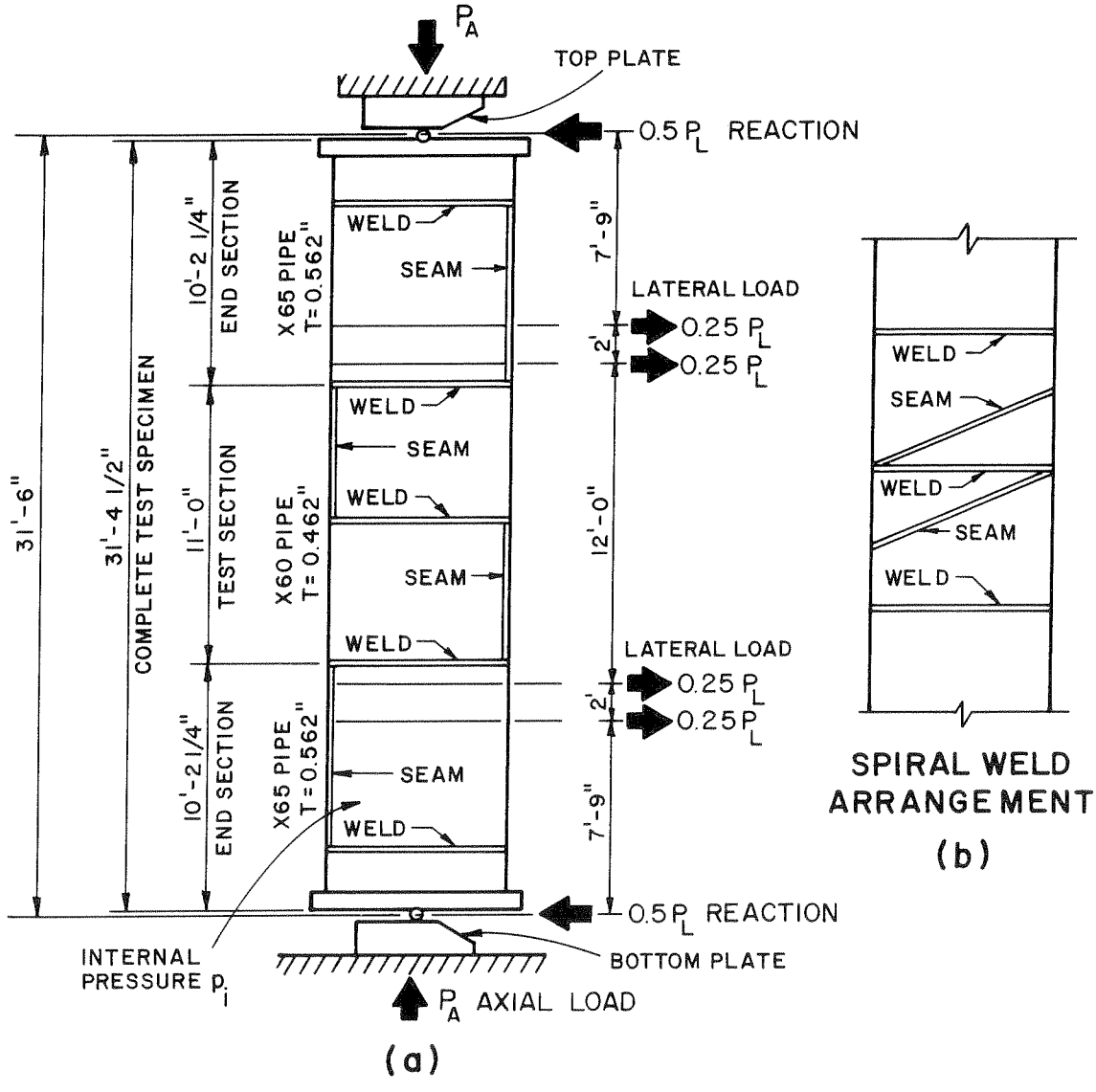

FIG. 2 TYPICAL 48" PIPE TEST SPECIMEN

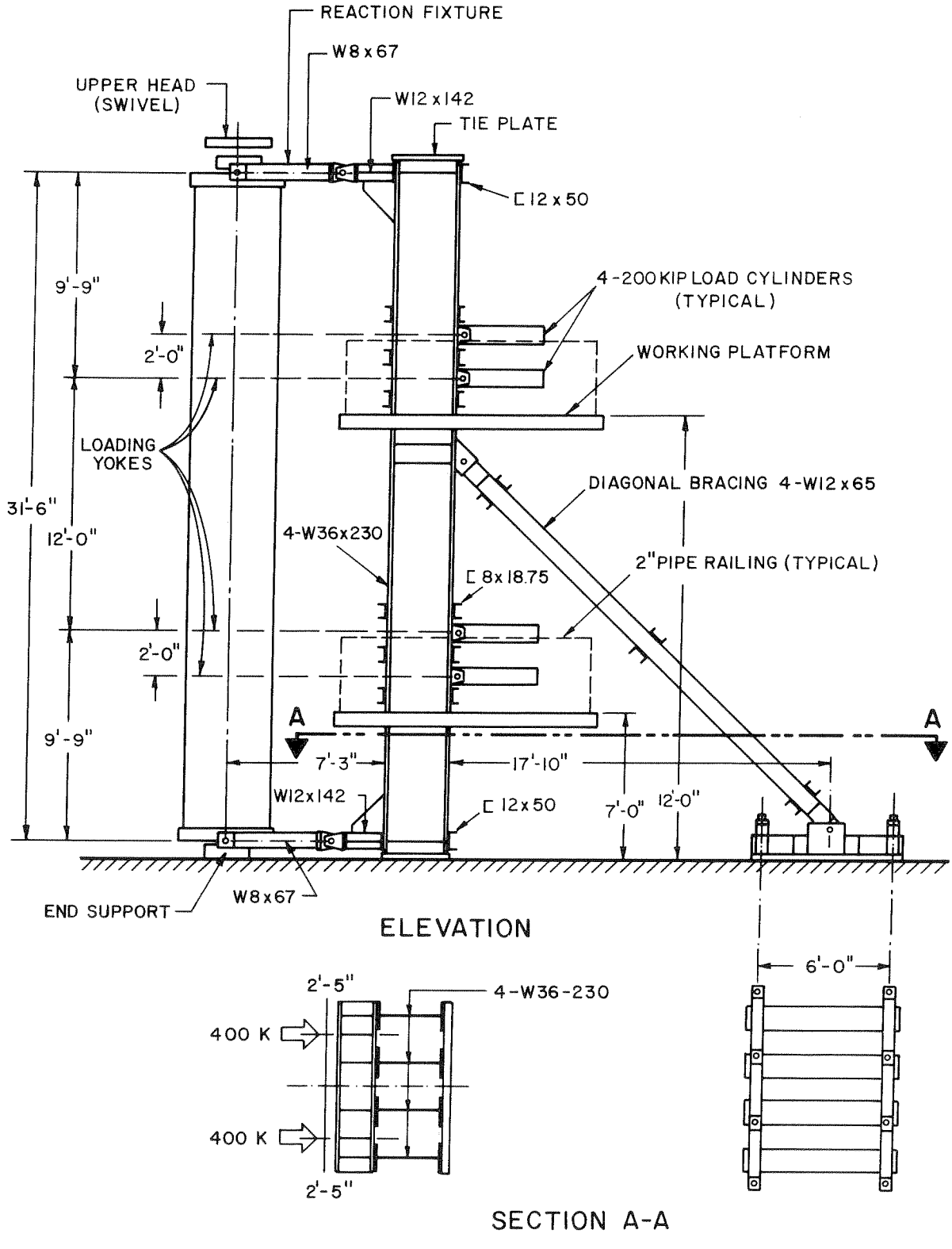

FIG. 3 SELF CONTAINED LATERAL LOADING FRAME, CAPACITY 1600 KIPS

FIG. 4 LATERAL LOAD FRAME

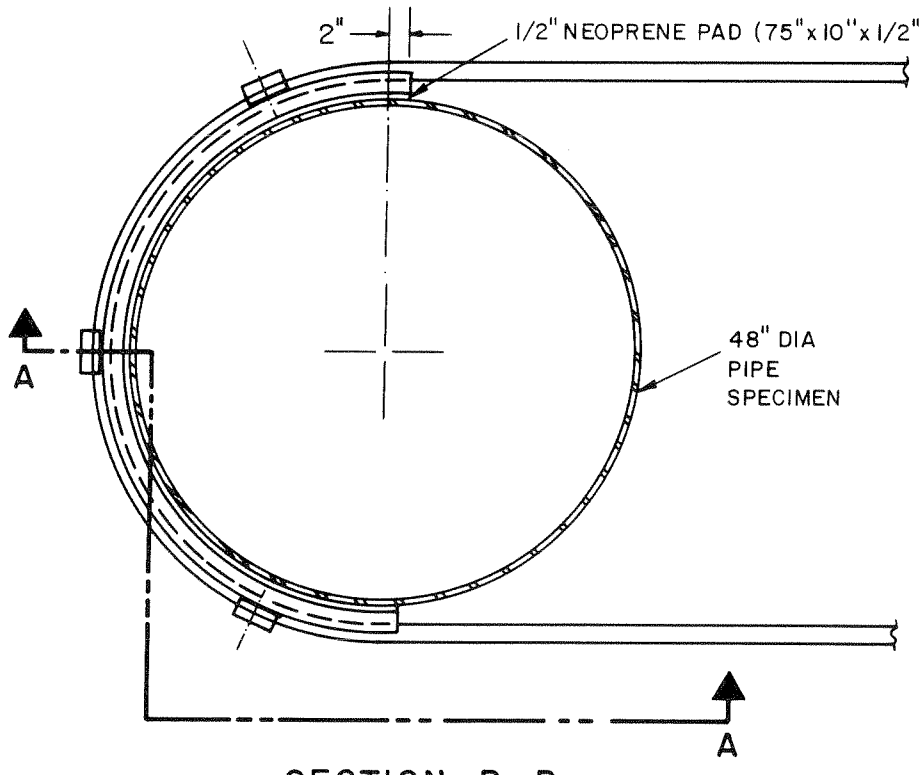

SECTION B-B

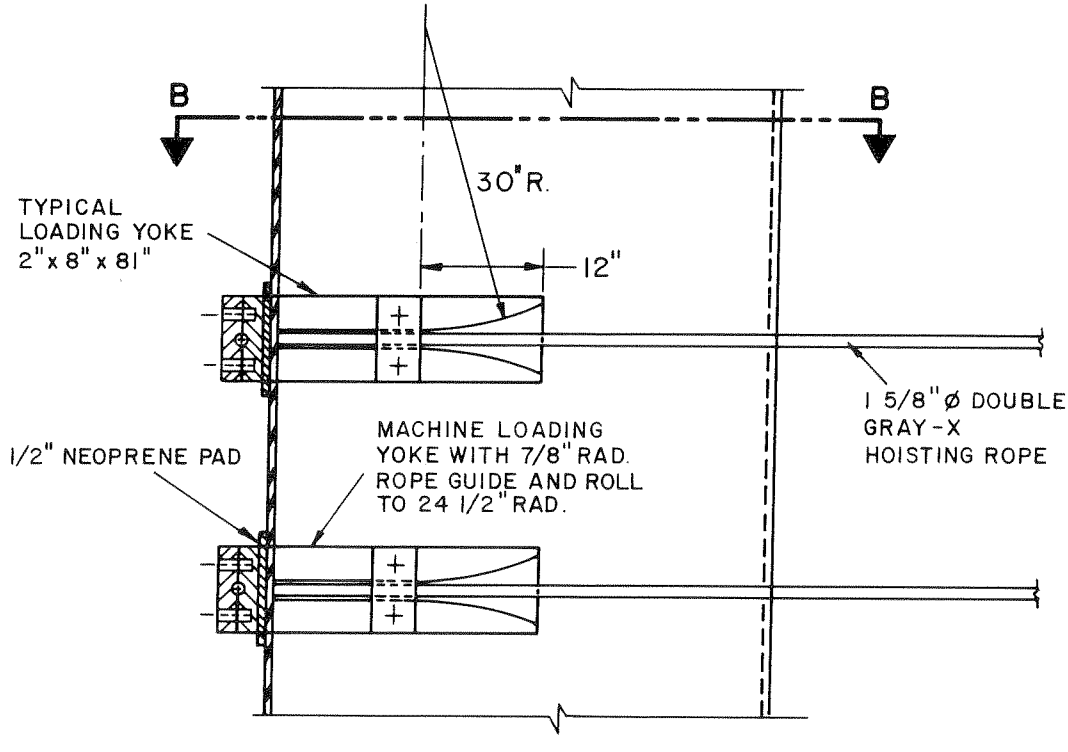

SECTION A-A

FIG. 5 LOADING YOKE ARRANGEMENT

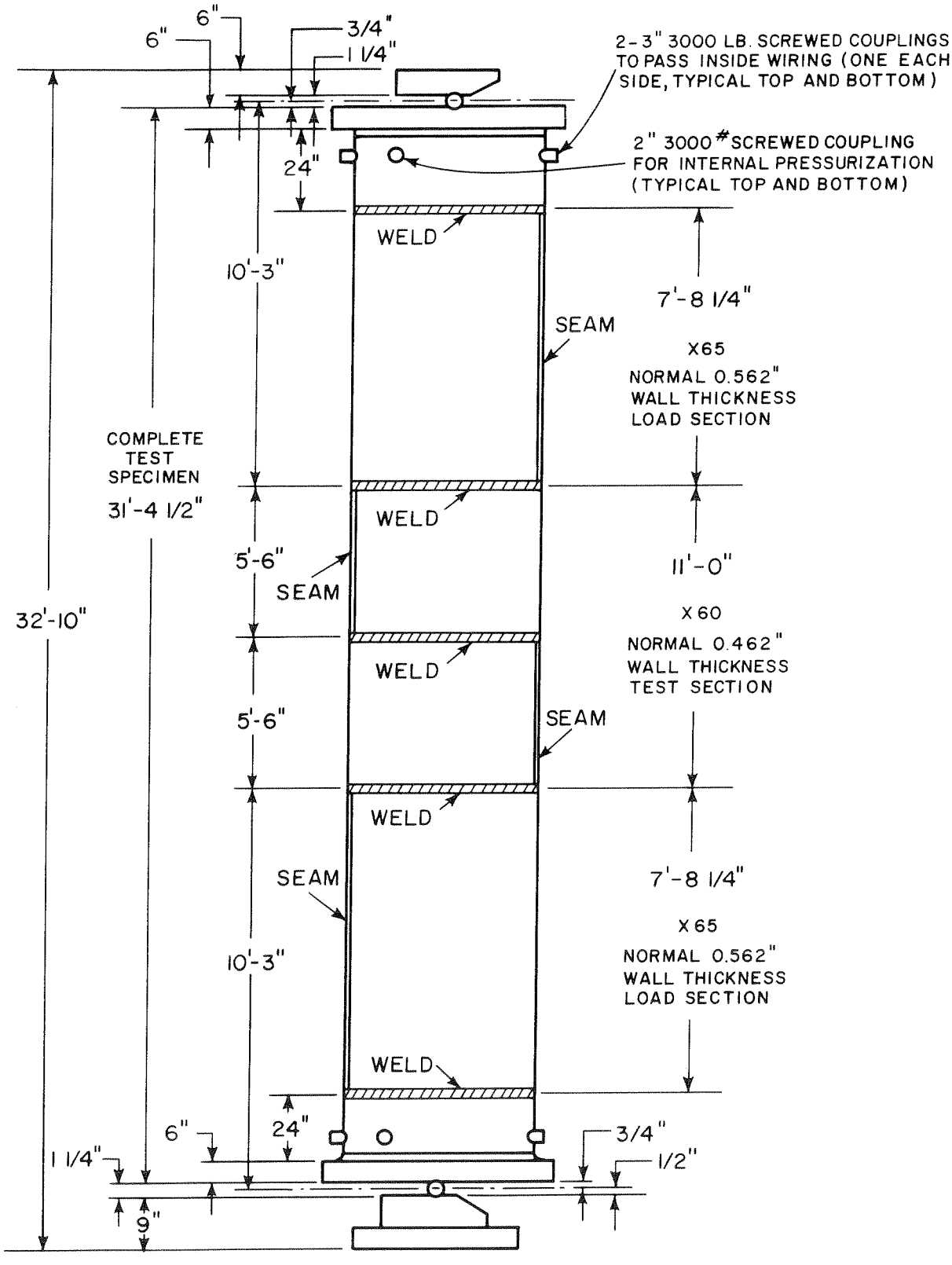

FIG. 6 TYPICAL 48" PIPE TEST SPECIMEN

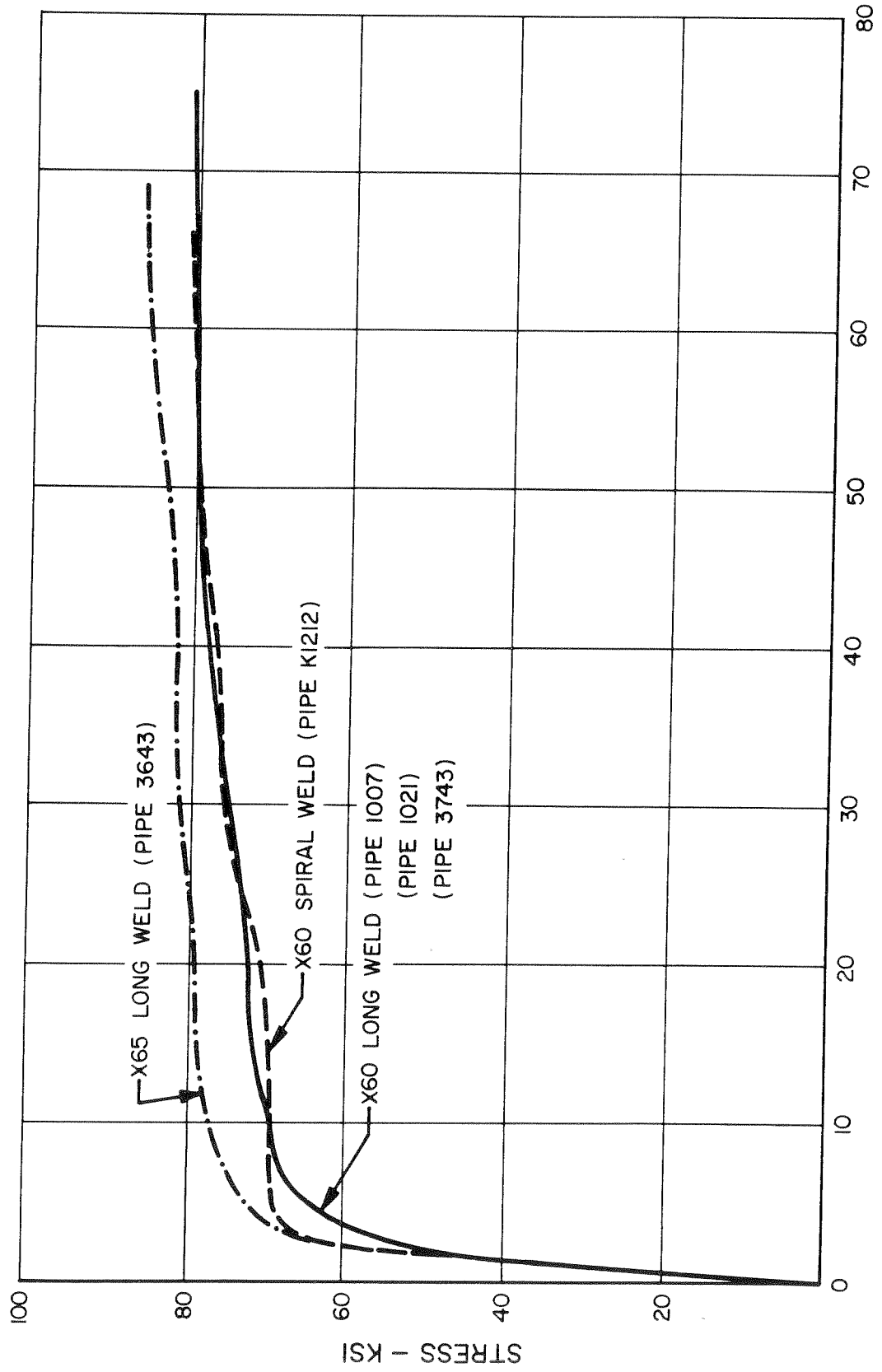

FIG. 7 TYPICAL STRESS–STRAIN CURVES FOR PIPE TENSILE SPECIMENS

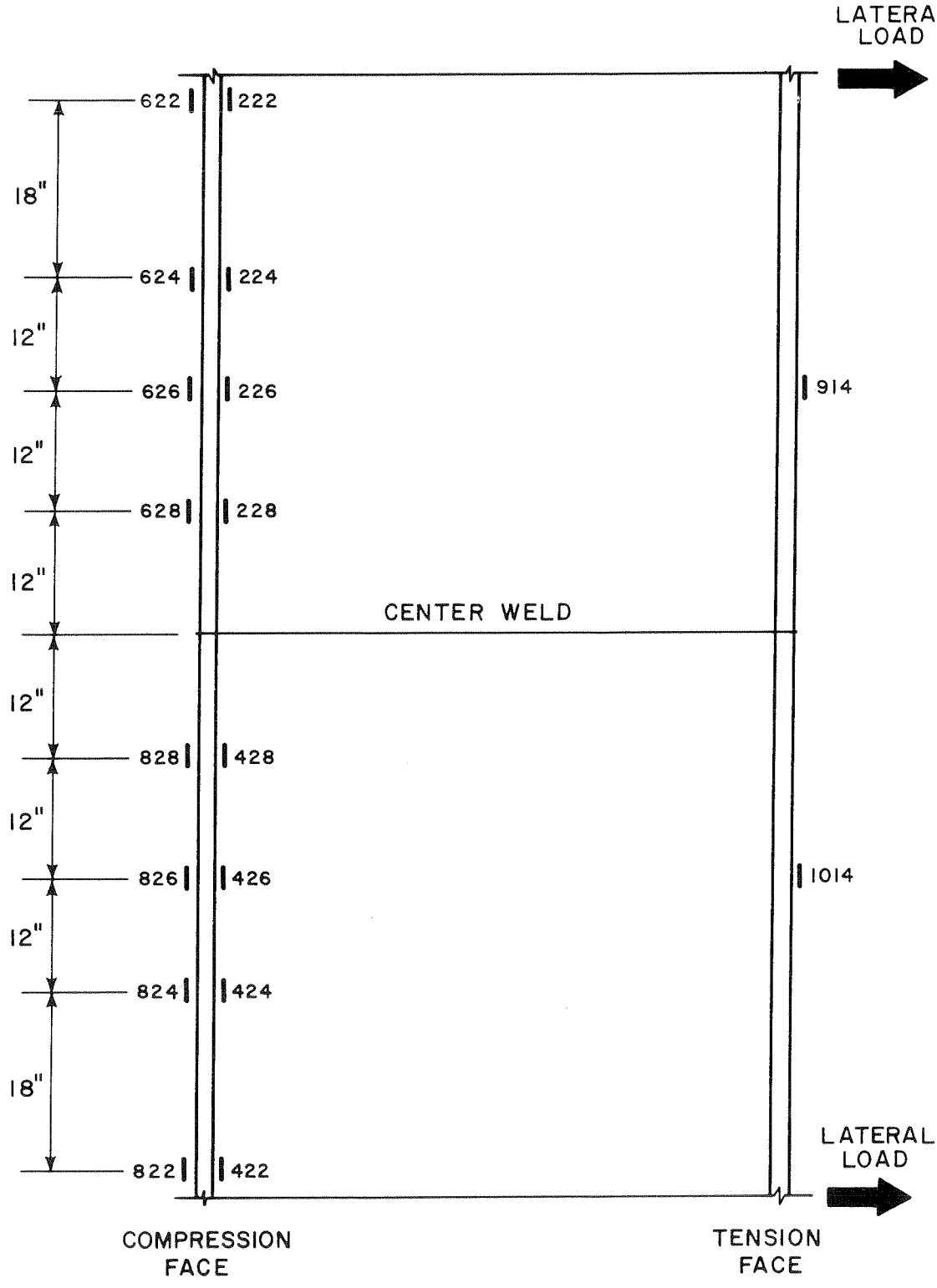

FIG. 8 SPECIMENS NO. 1 AND 2 LOCATION OF SELECTED LONGITUDINAL STRAIN GAGES

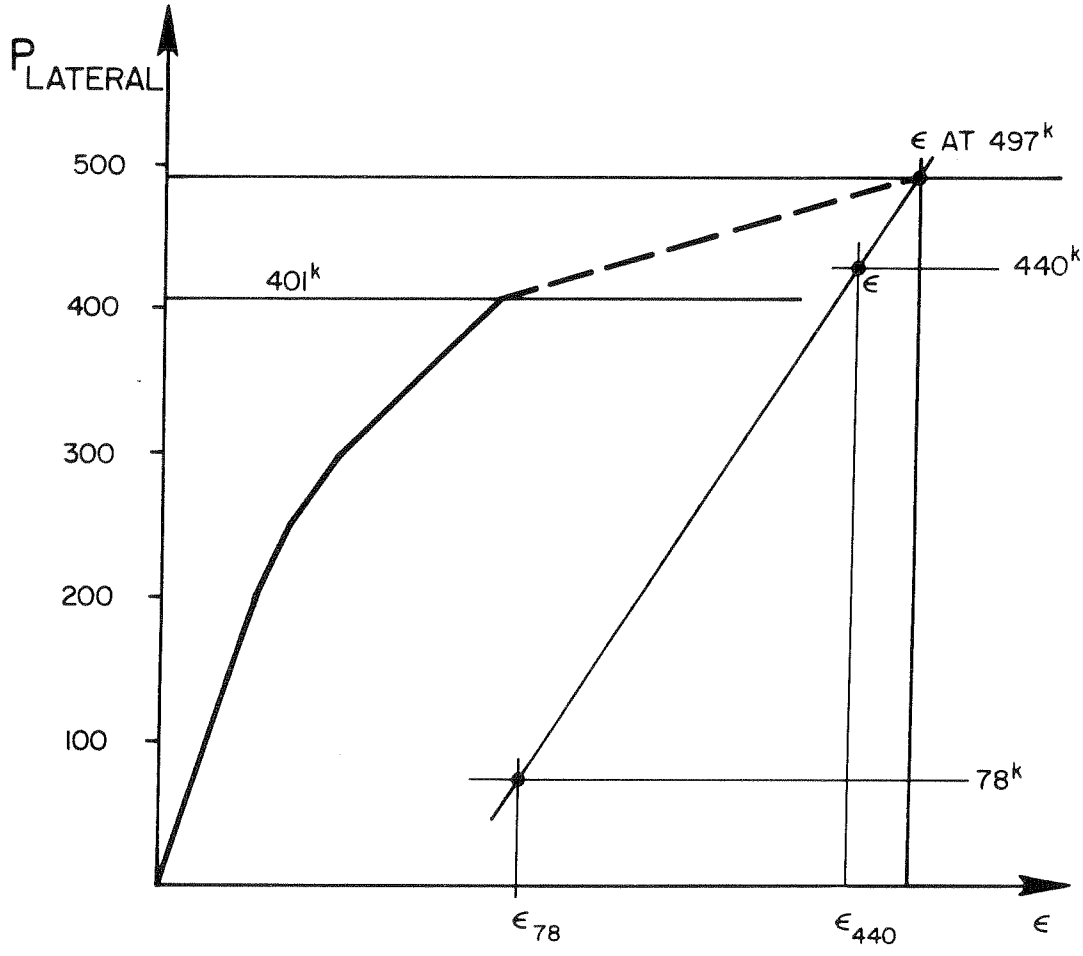

$$\epsilon_{497} = \left[\frac{497-78}{440-78}\right] (\epsilon_{440} - \epsilon_{78}) + \epsilon_{78}$$

FIG. 9 SPECIMEN NO. I STRAIN EXTRAPOLATION PROCEDURE FOR STRAINS AT BUCKLING (497 K)

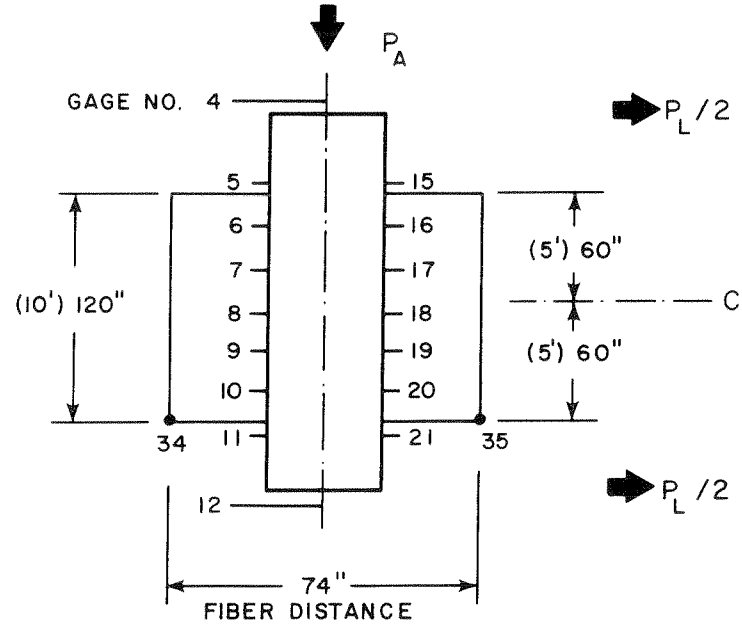

PRINCIPLE POTENTIOMETER LOCATIONS

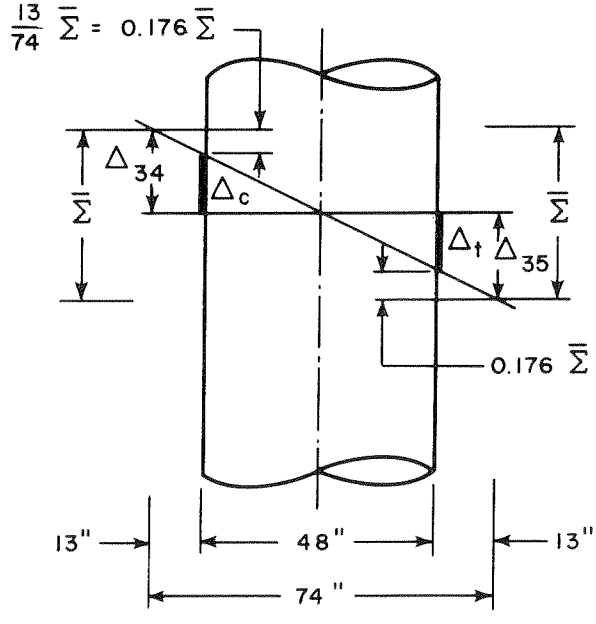

RADIUS OF CURVATURE AND
GROSS-STRAIN EVALUATION

RADIUS OF CURVATURE CALCULATIONS

$$\bar{\Sigma} = |\Delta_{34}| + |\Delta_{35}|$$

$$\frac{10^{FT}}{R^{FT}} = \frac{\bar{\Sigma}}{74} \qquad R^{FT} = \frac{740}{\bar{\Sigma}}$$

GROSS-STRAIN CALCULATIONS

$$\epsilon_t = \frac{|\Delta_{35}| - 0.176\ \bar{\Sigma}}{120}$$

$$\epsilon_c = \frac{|\Delta_{34}| - 0.176\ \bar{\Sigma}}{120}$$

FIG. 10 BASIC DATA REDUCTION CRITERIA

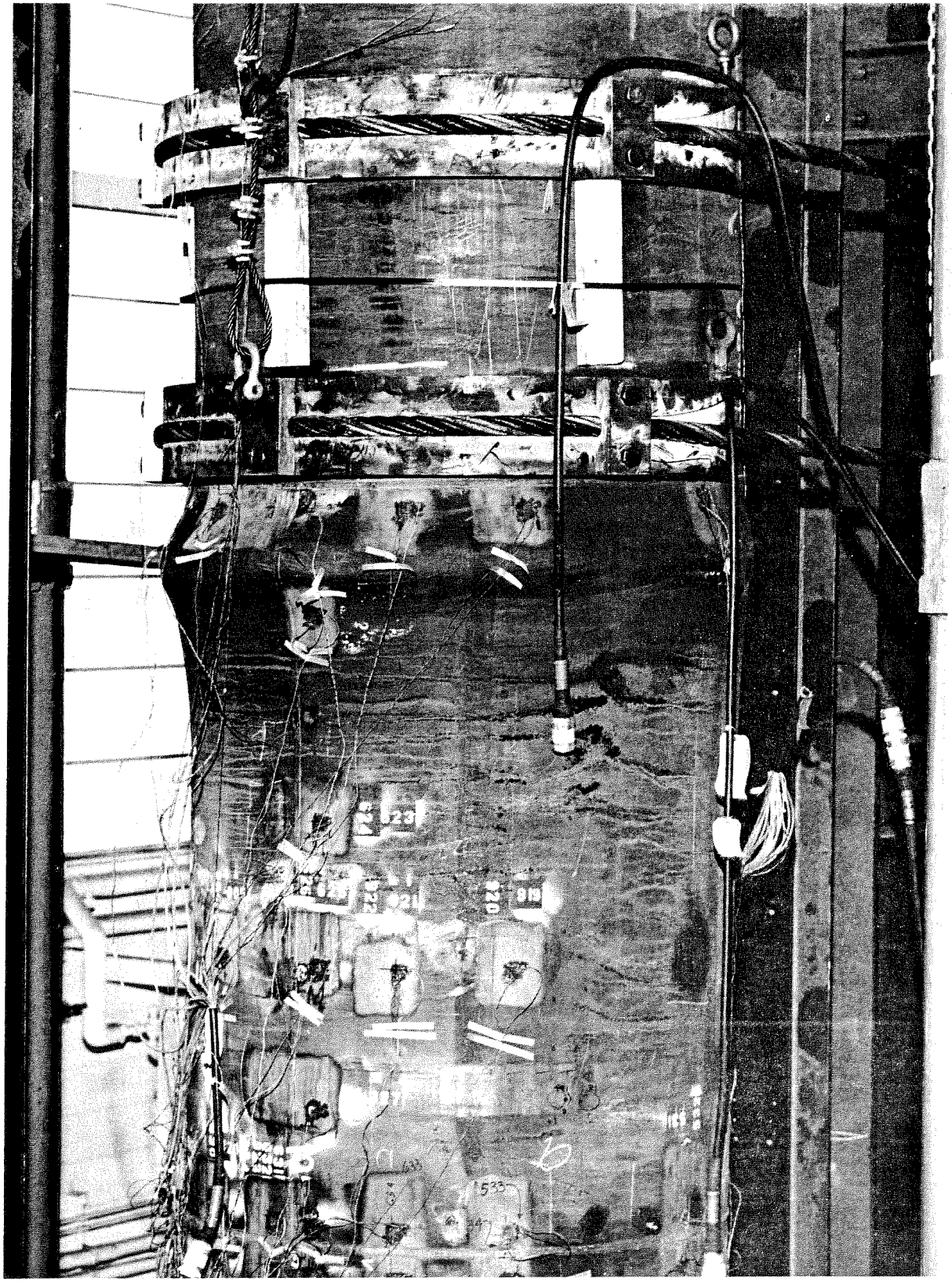

FIG. 11 SPECIMEN NO. 1 -AFTER INITIAL BUCKLING OF COMPRESSION FACE (CENTER DISPLACEMENT ABOUT 9 INCHES)

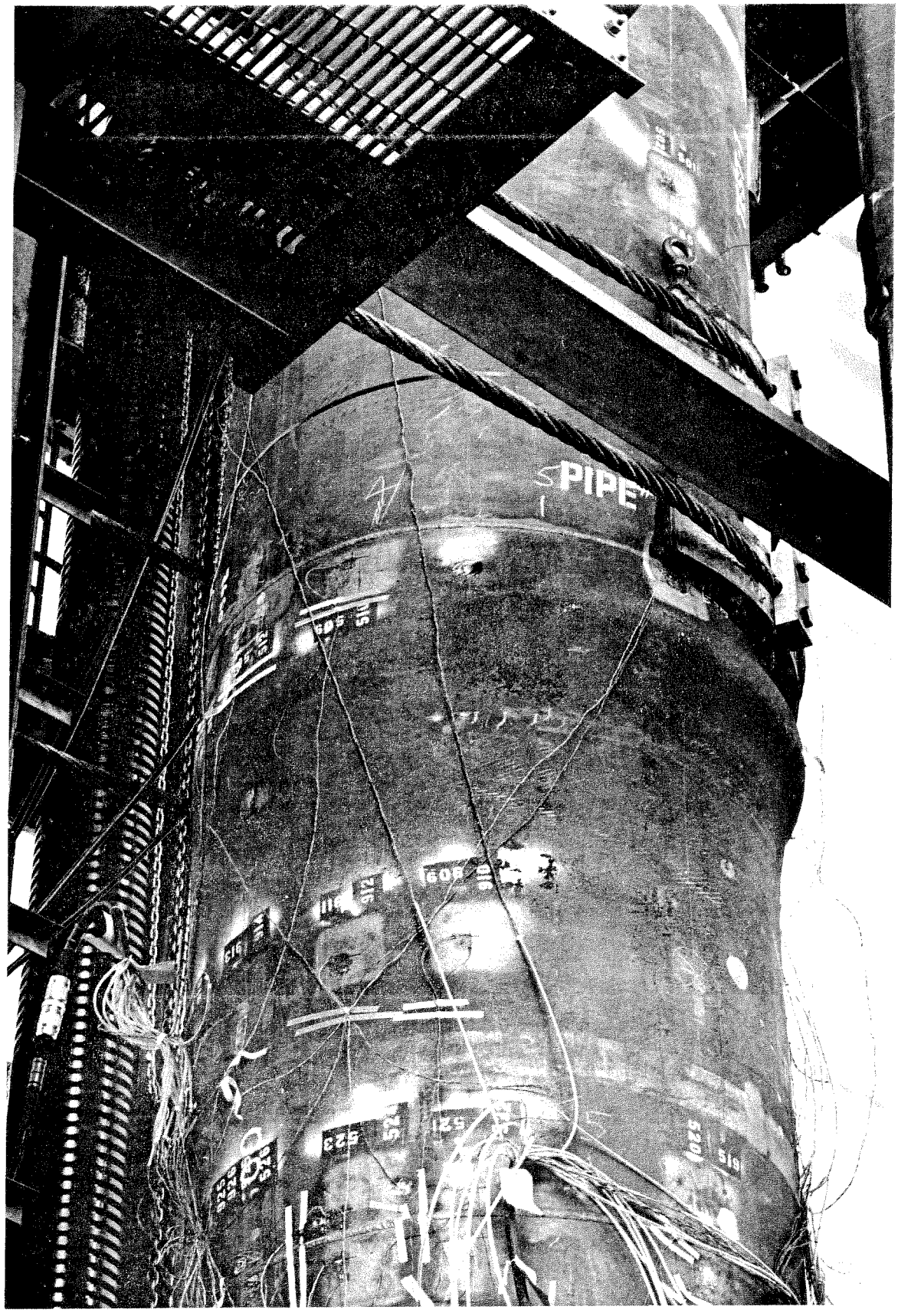

FIG. 12 SPECIMEN NO. 1 - AFTER INITIAL BUCKLING - TENSION FACE (CENTER DISPLACEMENT ABOUT 9 INCHES)

FIG. 13 SPECIMEN NO. 2 - AFTER POST-BUCKLING TEST

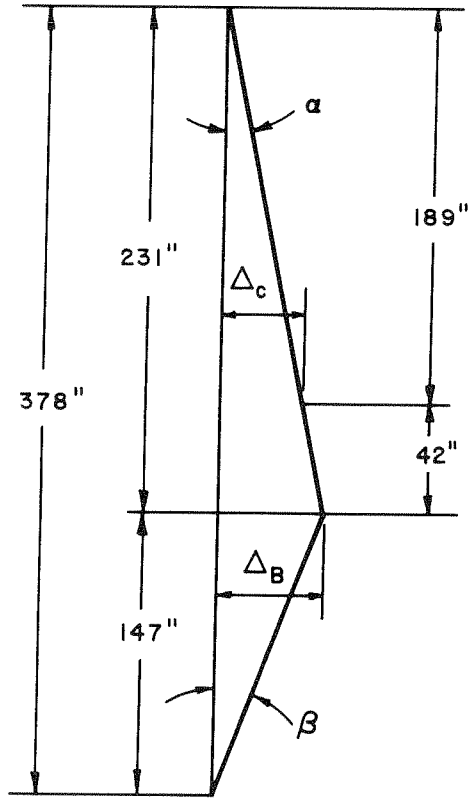

INITIAL ROTATION

$\Delta_{BUCKLE} = \frac{231}{189} \Delta_C = 1.22 \Delta_C$

$\Delta_C = 5.5"$

$\Delta_B = 1.22 \times 5.5 = 6.71$

$\alpha = \tan^{-1} \frac{6.71}{2.31} = 1°40'$

$\beta = \tan^{-1} \frac{6.71}{1.47} = 2°37'$

$\theta = 4°17'$

FINAL FAILURE ROTATION

$\Delta_{BUCKLE} = 30.5"$

$\alpha = \tan^{-1} \frac{30.5}{231} = 7°30'$

$\beta = \tan^{-1} \frac{30.5}{147} = 11°45'$

$\theta = 19°15'$

FIG. 14 SPECIMEN NO. 2 - INITIAL AND FINAL FAILURE ROTATION OF SPECIMEN

FIG. 15 SPECIMEN NO. 2 - AFTER POST-BUCKLING TEST - COMPRESSION FACE

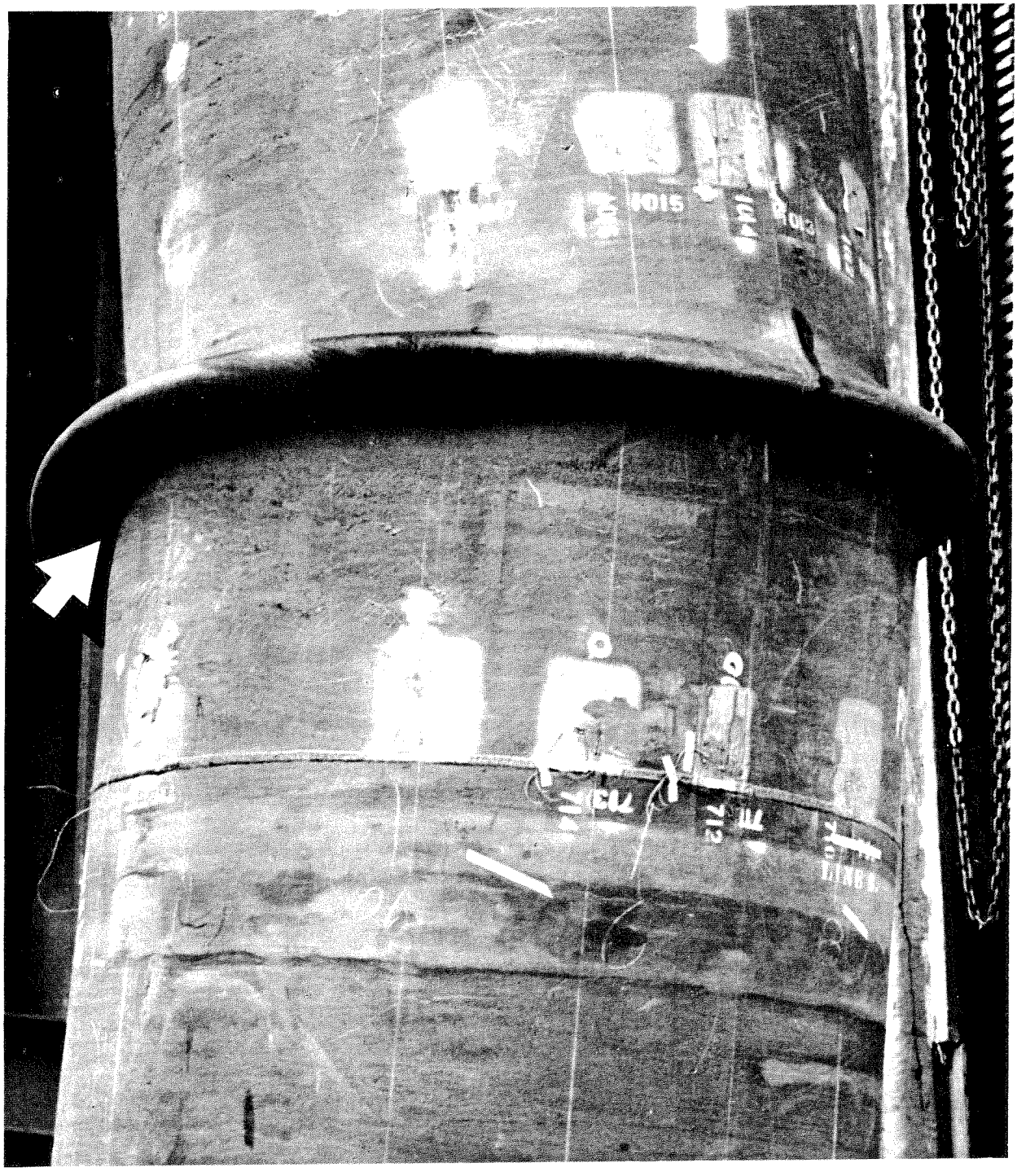

FIG. 16 SPECIMEN NO. 2 - AFTER POST-BUCKLING TEST - TENSION FACE

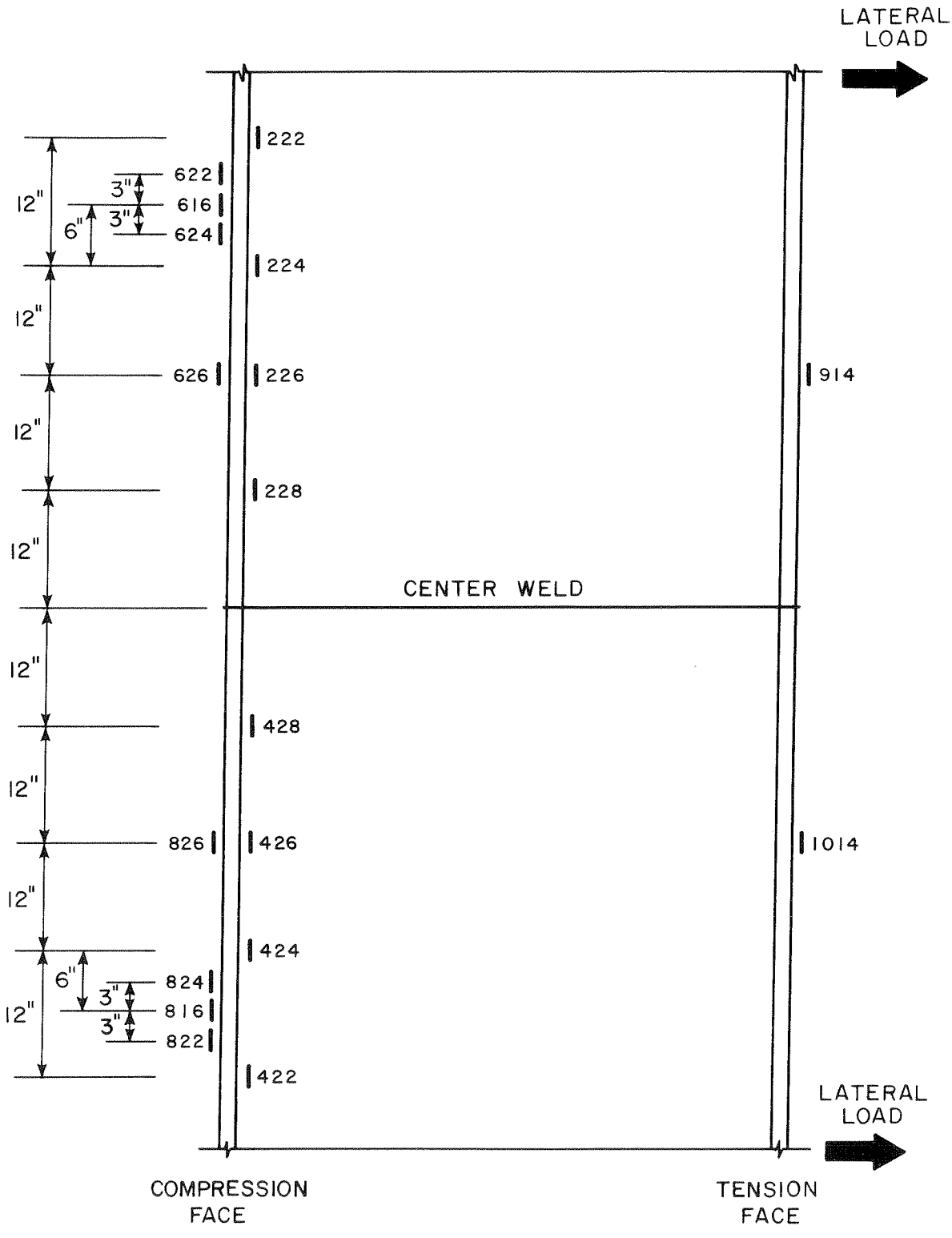

FIG. 17 SPECIMEN NO. 3 LOCATION OF SELECTED LONGITUDINAL STRAIN GAGES

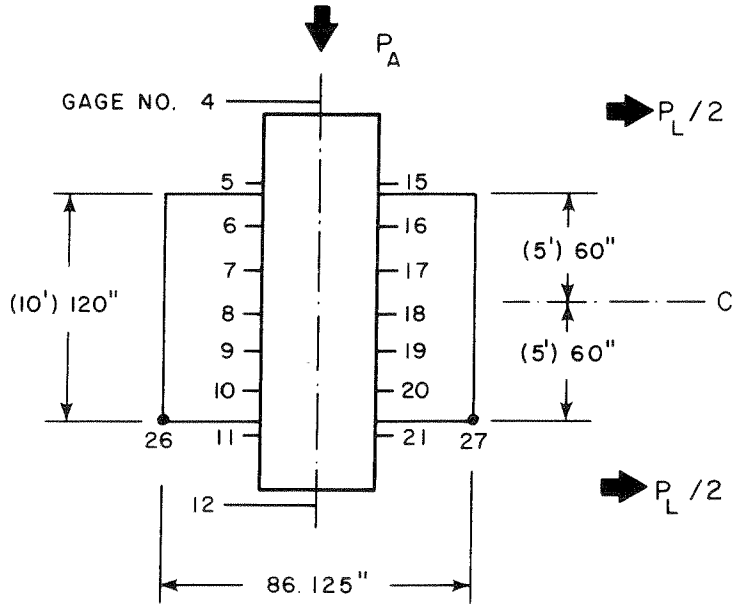

PRINCIPLE POTENTIOMETER LOCATIONS

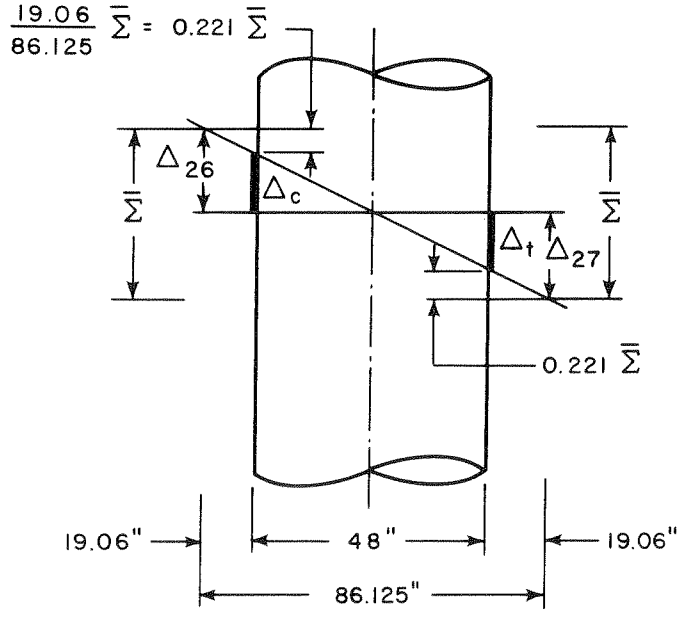

RADIUS OF CURVATURE AND
GROSS-STRAIN EVALUATION

RADIUS OF CURVATURE CALCULATIONS

$$\bar{\Sigma} = |\Delta_{26}| + |\Delta_{27}|$$

$$\frac{10^{FT}}{R^{FT}} = \frac{\bar{\Sigma}}{86.125} \qquad R^{FT} = \frac{861.25}{\bar{\Sigma}}$$

GROSS-STRAIN CALCULATIONS

$$\epsilon_t = \frac{|\Delta_{27}| - 0.221\ \bar{\Sigma}}{120}$$

$$\epsilon_c = \frac{|\Delta_{26}| - 0.221\ \bar{\Sigma}}{120}$$

FIG. 18 SPECIMEN NO. 3 BASIC DATA REDUCTION CRITERIA

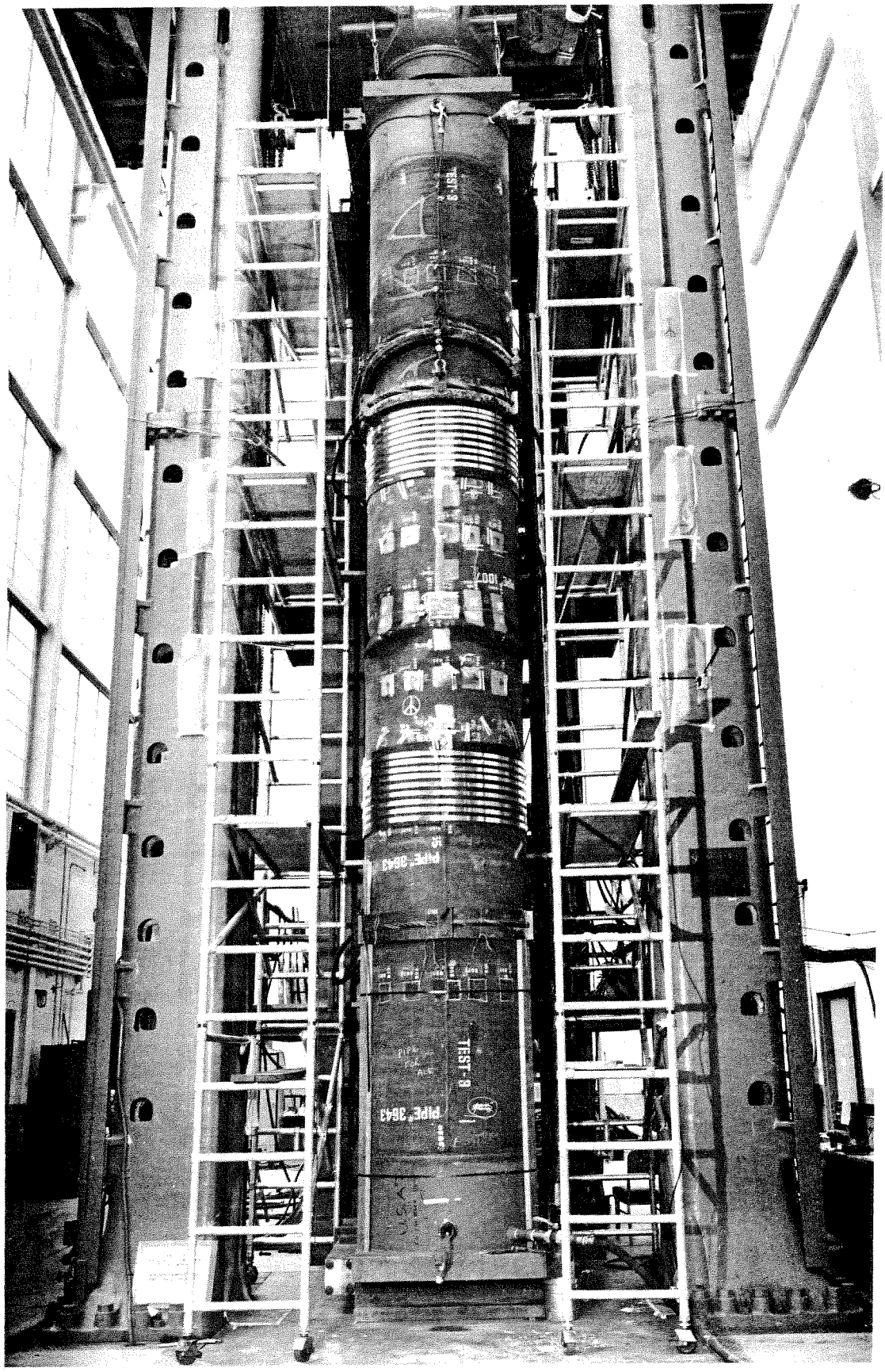

FIG. 19 SPECIMEM NO. 3 - AFTER INITIAL BUCKLING - COMPRESSION FACE (CENTER DISPLACEMENT ABOUT 5 3/4 INCHES)

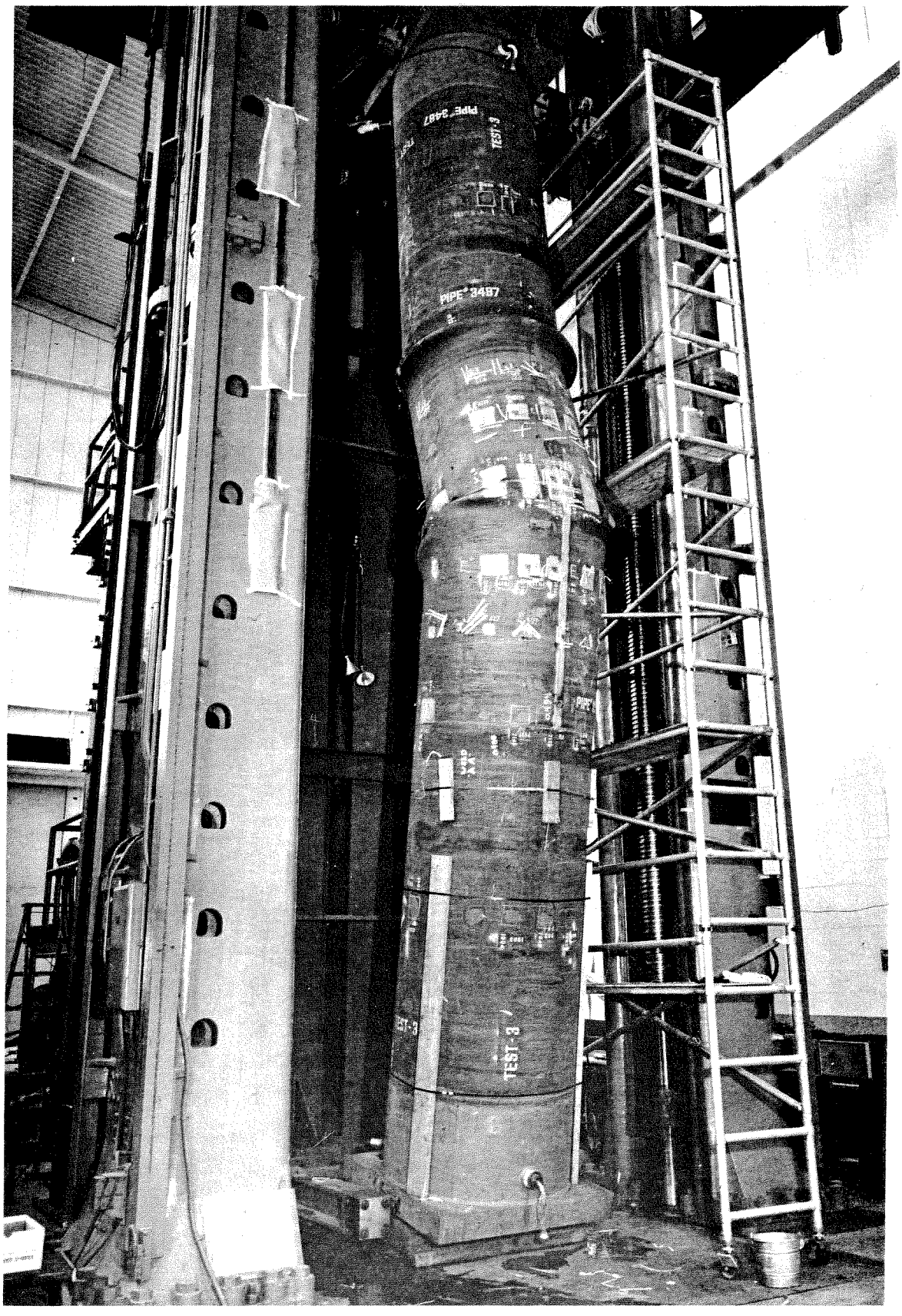

FIG. 20 SPECIMEN NO. 3 - AFTER POST-BUCKLING TEST

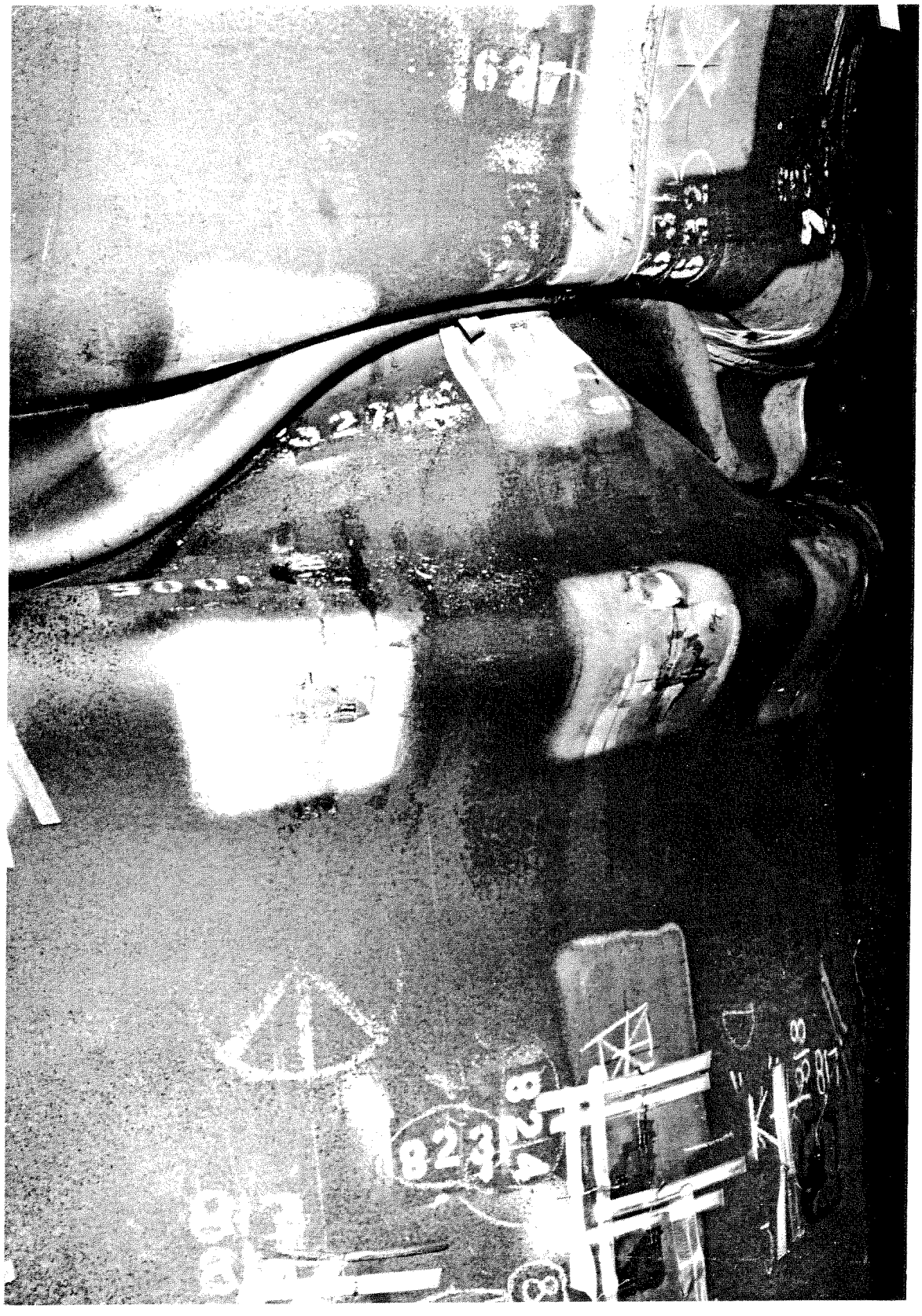

FIG. 21 SPECIMEN NO. 3 -AFTER POST-BUCKLING TEST - COMPRESSION FACE

FIG. 22 SPECIMEN NO. 3 -AFTER POST-BUCKLING TEST - COMPRESSION FACE

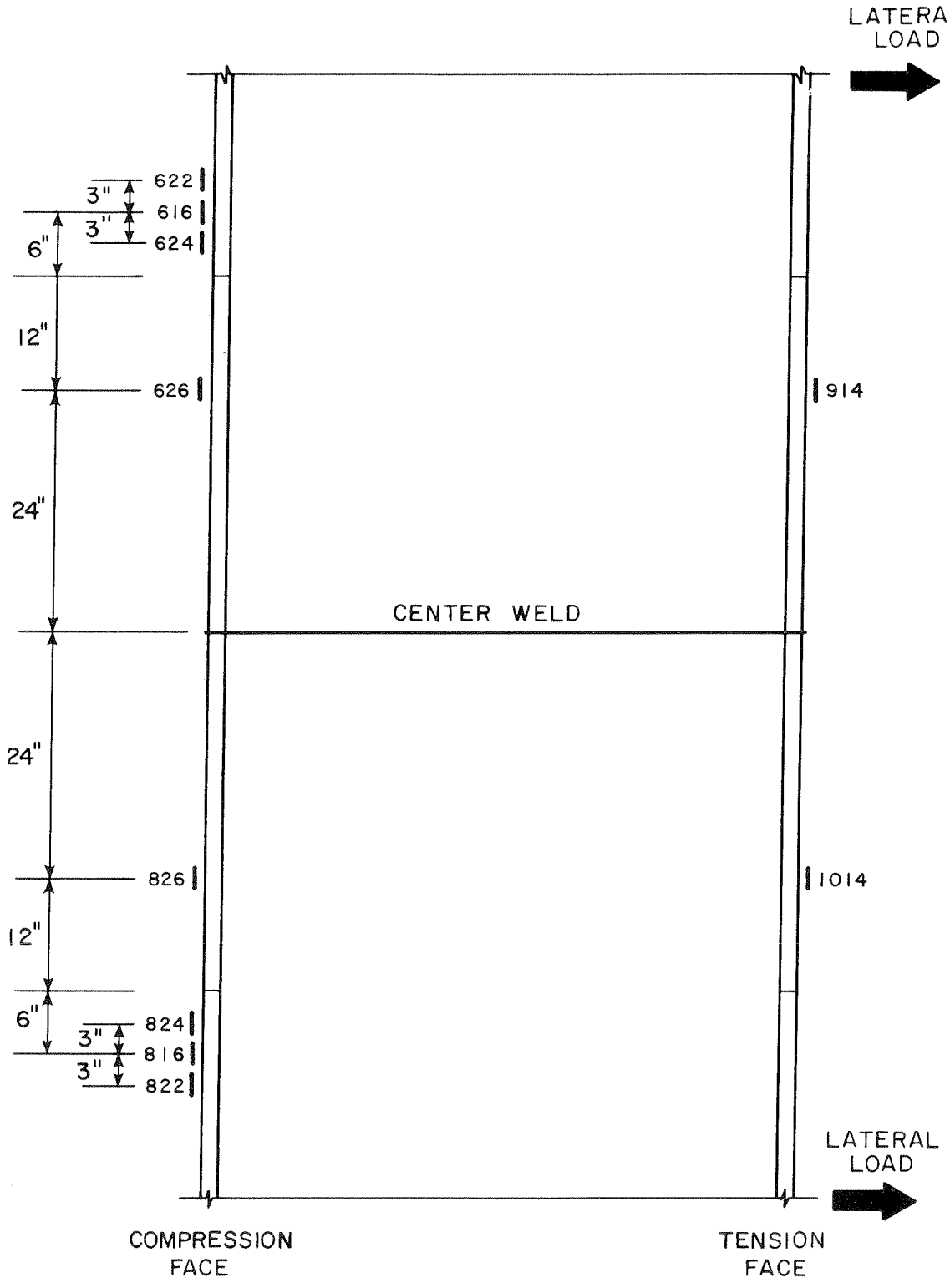

FIG. 23 SPECIMEN NO. 4 LOCATION OF SELECTED LONGITUDINAL STRAIN GAGES

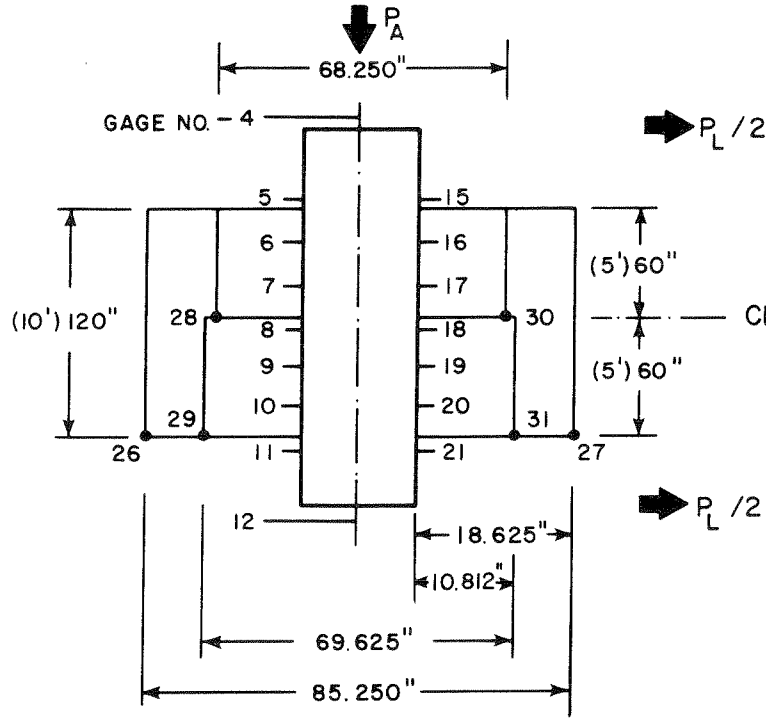

CENTER DISPLACEMENT Δ_{av}

$$\Delta_{av} = \frac{|\Delta_8| + |\Delta_{18}|}{2}$$

$$M_T = 52.5\, P_L + P_A \Delta_{av}$$

PRINCIPLE POTENTIOMETER LOCATIONS

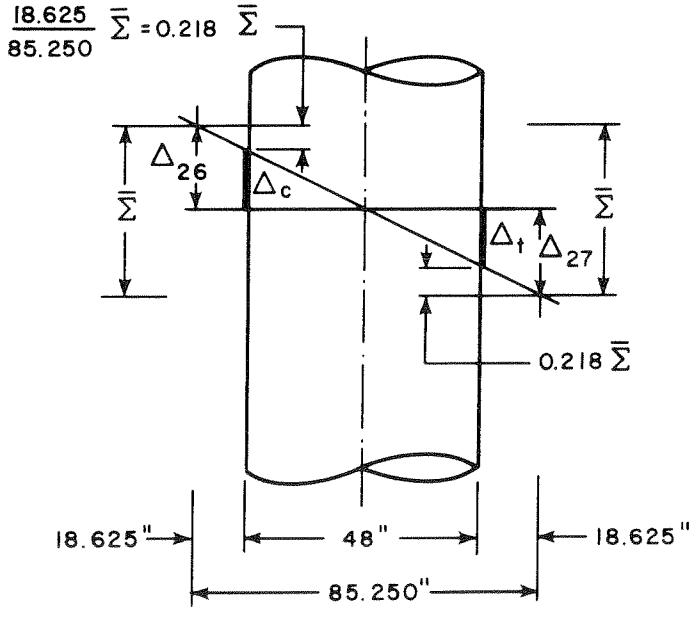

RADIUS OF CURVATURE AND GROSS-STRAIN EVALUATION

RADIUS OF CURVATURE CALCULATIONS

TOTAL SECTION

$$\bar{\Sigma}_T = |\Delta_{26}| + |\Delta_{27}|$$

$$R_{TOTAL} = \frac{852.5}{\bar{\Sigma}_T}$$

UPPER SECTION

$$\bar{\Sigma}_u = |\Delta_{28}| + |\Delta_{30}|$$

$$R_{UPPER} = \frac{341}{\bar{\Sigma}_u}$$

LOWER SECTION

$$\bar{\Sigma}_L = |\Delta_{29}| + |\Delta_{31}|$$

$$R_{LOWER} = \frac{348}{\bar{\Sigma}_L}$$

GROSS-STRAIN CALCULATIONS

$$\epsilon_t = \frac{|\Delta_{27}| - 0.218\, \bar{\Sigma}_T}{120}$$

$$\epsilon_c = \frac{|\Delta_{26}| - 0.218\, \bar{\Sigma}_T}{120}$$

FIG. 24 SPECIMEN NO. 4 BASIC DATA REDUCTION CRITERIA

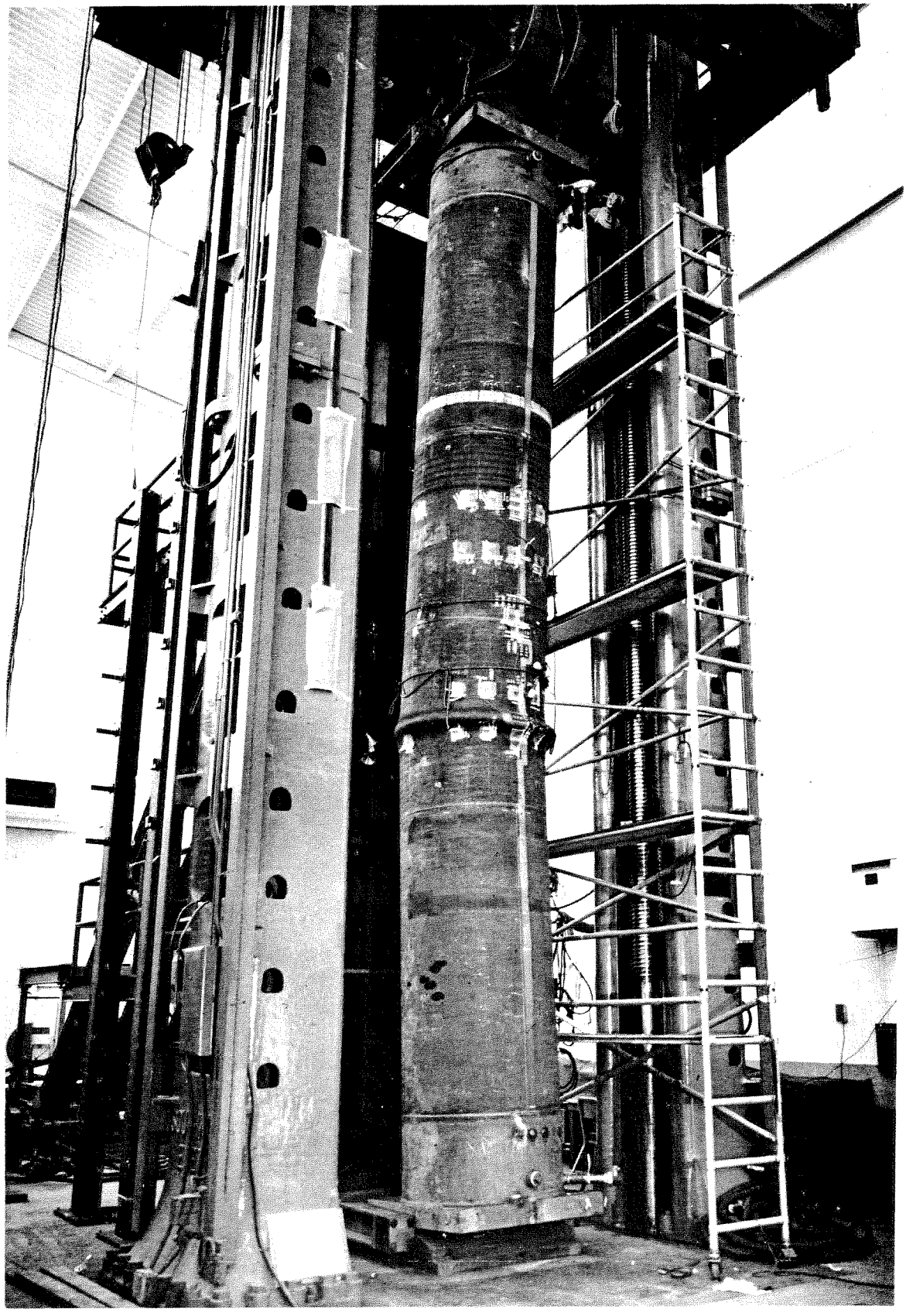

FIG. 25 SPECIMEN NO. 4 - AFTER INITIAL BUCKLING - COMPRESSION FACE (CENTER DISPLACEMENT ABOUT 8 1/2 INCHES)

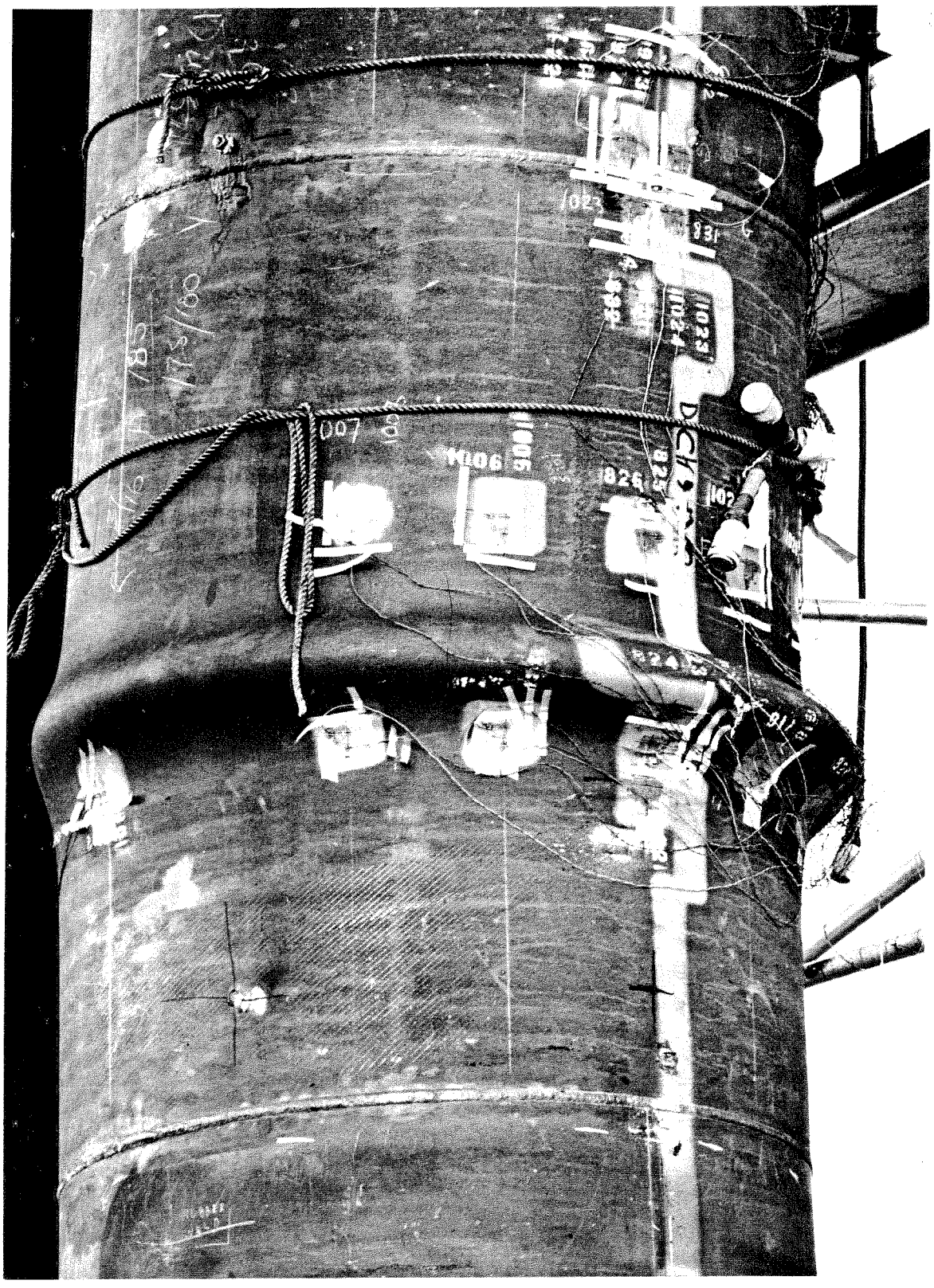

FIG. 26 SPECIMEN NO. 4 - AFTER INITIAL BUCKLING - COMPRESSION FACE (CENTER DISPLACEMENT ABOUT 8 1/2 INCHES)

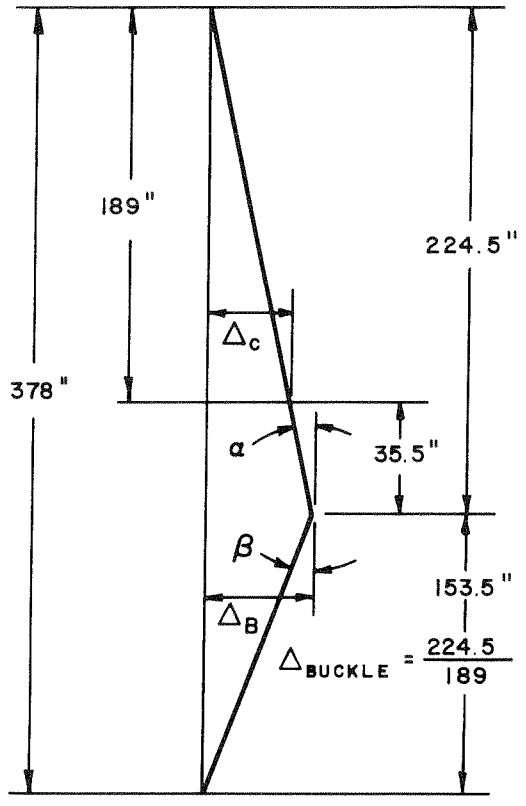

INITIAL ROTATION:

$\Delta_C = 8.5"$

$\Delta_B = 1.188 \times 8.5 = 10.1"$

$\tan\alpha = \frac{10.1}{224.5} = 0.0449 \quad \alpha = 2°34'$

$\tan\beta = \frac{10.1}{153.5} = 0.0658 \quad \beta = 3°46'$

$\theta = 6°20'$

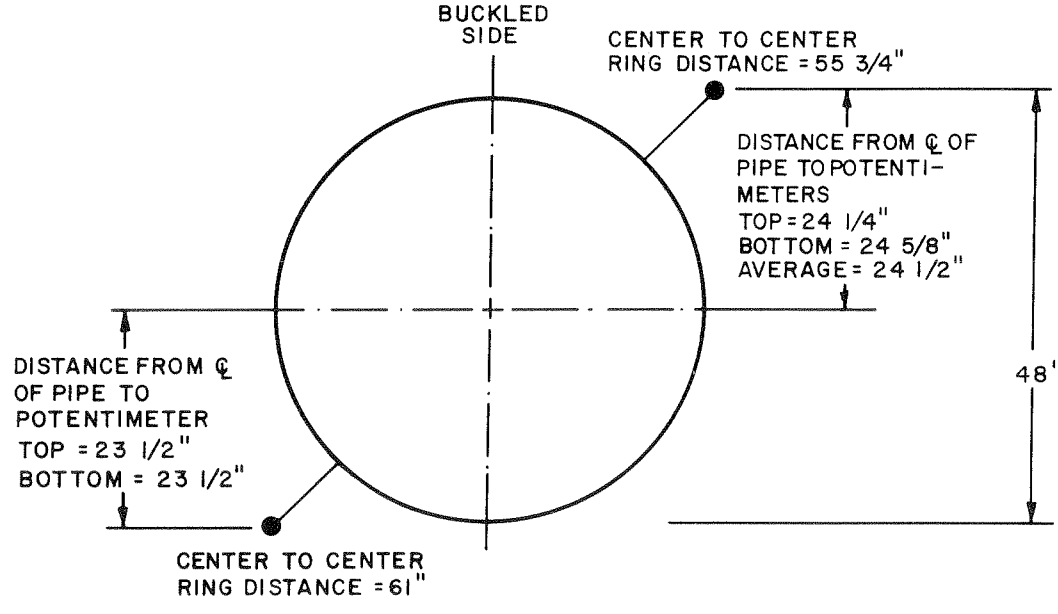

CLIP GAGE ARRANGEMENT FOR ROTATION MEASUREMENT

FIG. 27 SPECIMEN NO. 4 - PIPE DEFORMATION PRIOR TO POST-BUCKLING TEST

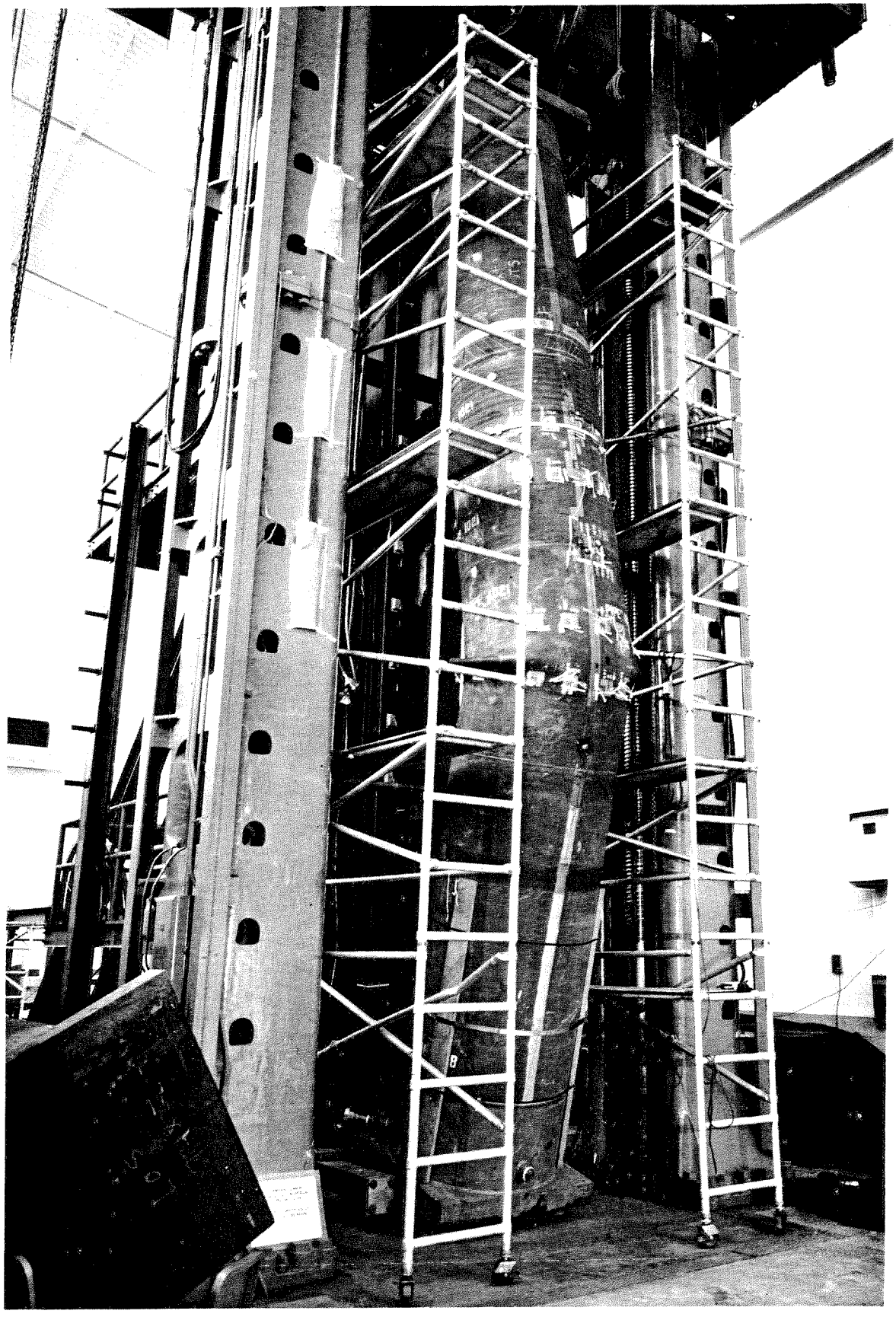

FIG. 28 SPECIMEN NO. 4 - AFTER POST-BUCKLING TEST

FIG. 29 SPECIMEN NO. 4 - AFTER POST-BUCKLING TEST - COMPRESSION FACE

FIG. 30 SPECIMEN NO. 4 - AFTER POST-BUCKLING TEST - COMPRESSION FACE

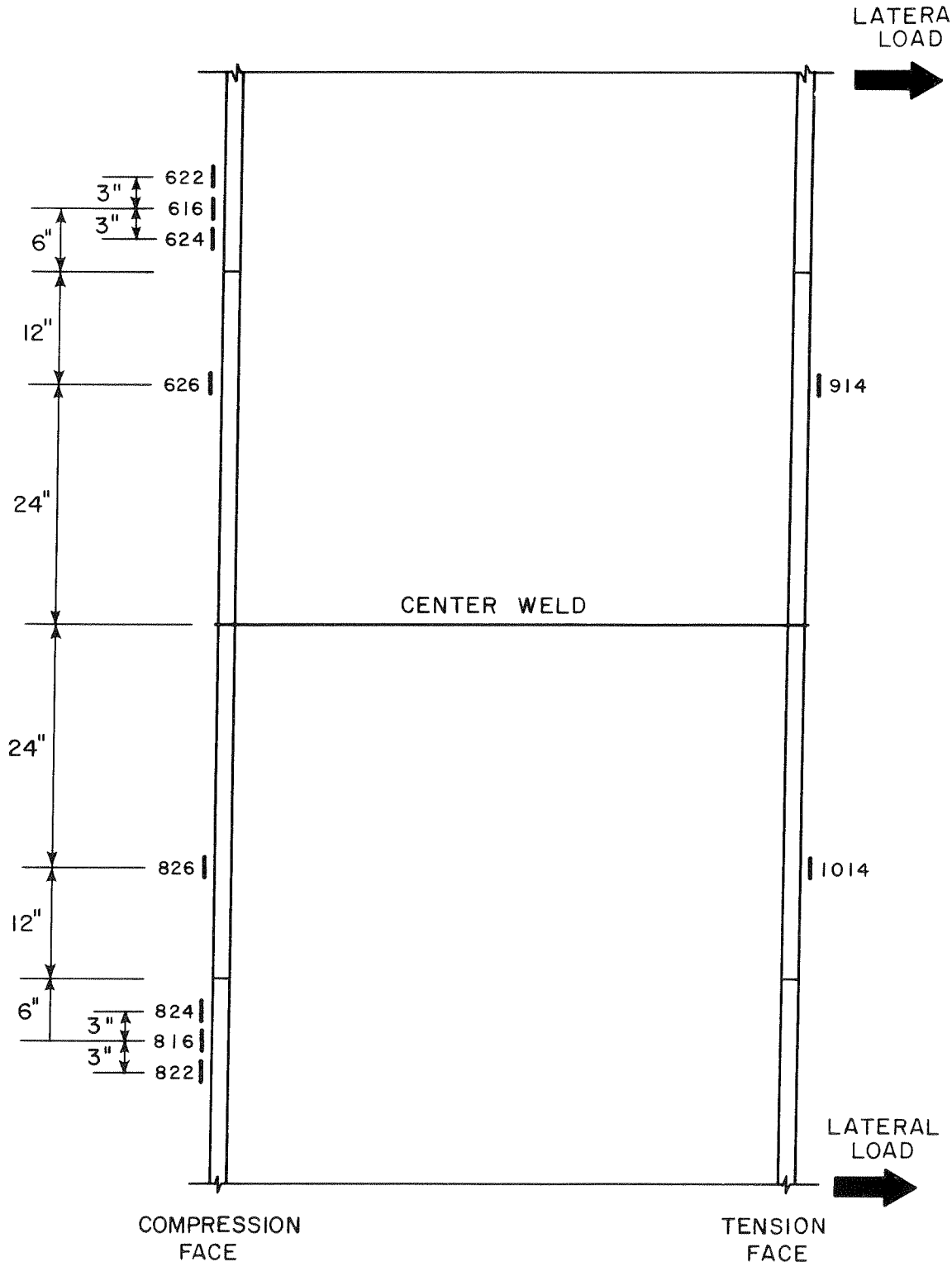

FIG. 31 SPECIMEN NO. 5 LOCATION OF SELECTED LONGITUDINAL STRAIN GAGES

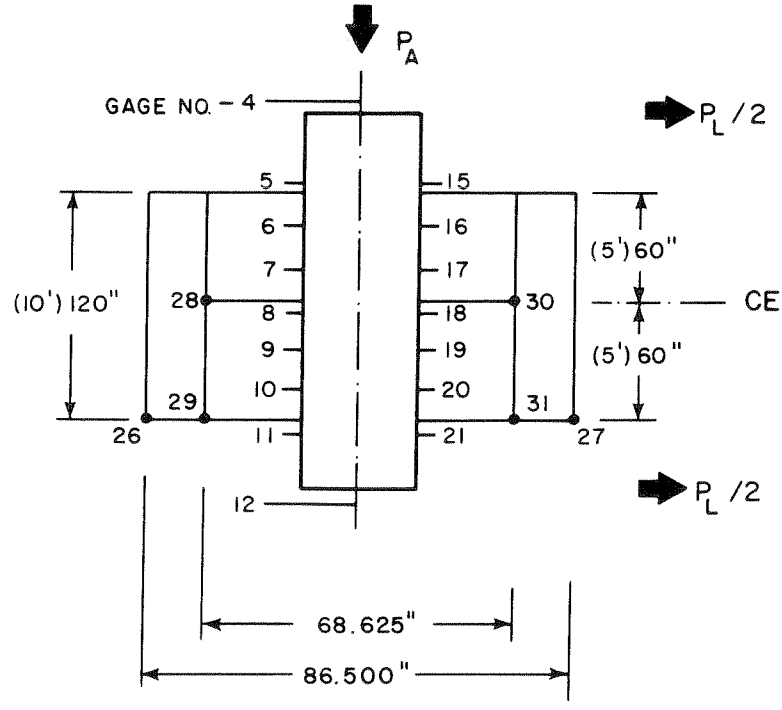

PRINCIPLE POTENTIOMETER LOCATIONS

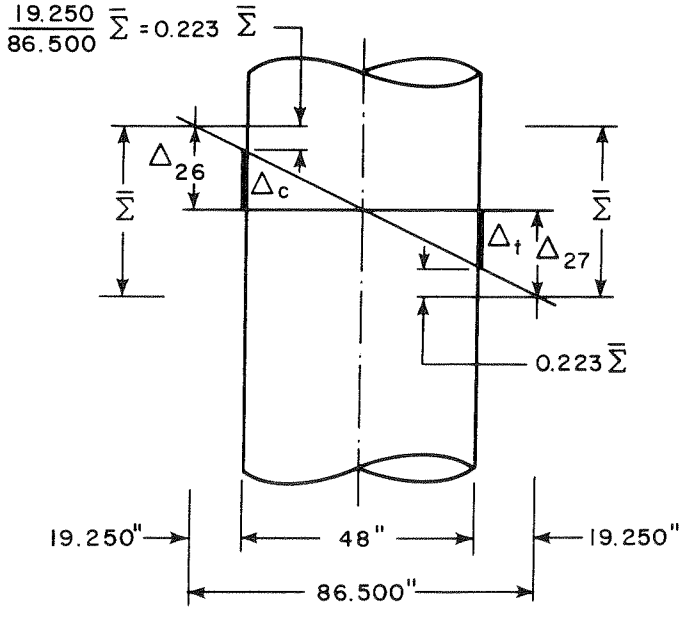

RADIUS OF CURVATURE AND GROSS-STRAIN EVALUATION

RADIUS OF CURVATURE CALCULATIONS

TOTAL SECTION

$$\bar{\Sigma}_T = |\Delta_{26}| + |\Delta_{27}|$$

$$R_{TOTAL} = \frac{865}{\bar{\Sigma}_T}$$

UPPER SECTION

$$\bar{\Sigma}_u = |\Delta_{28}| + |\Delta_{30}|$$

$$R_{UPPER} = \frac{343}{\bar{\Sigma}_u}$$

LOWER SECTION

$$\bar{\Sigma}_L = |\Delta_{29}| + |\Delta_{31}|$$

$$R_{LOWER} = \frac{343}{\bar{\Sigma}_L}$$

GROSS-STRAIN CALCULATIONS

$$\epsilon_t = \frac{|\Delta_{27}| - 0.223\,\bar{\Sigma}_T}{120}$$

$$\epsilon_c = \frac{|\Delta_{26}| - 0.223\,\bar{\Sigma}_T}{120}$$

FIG. 32 SPECIMEN NO.5 BASIC DATA REDUCTION CRITERIA

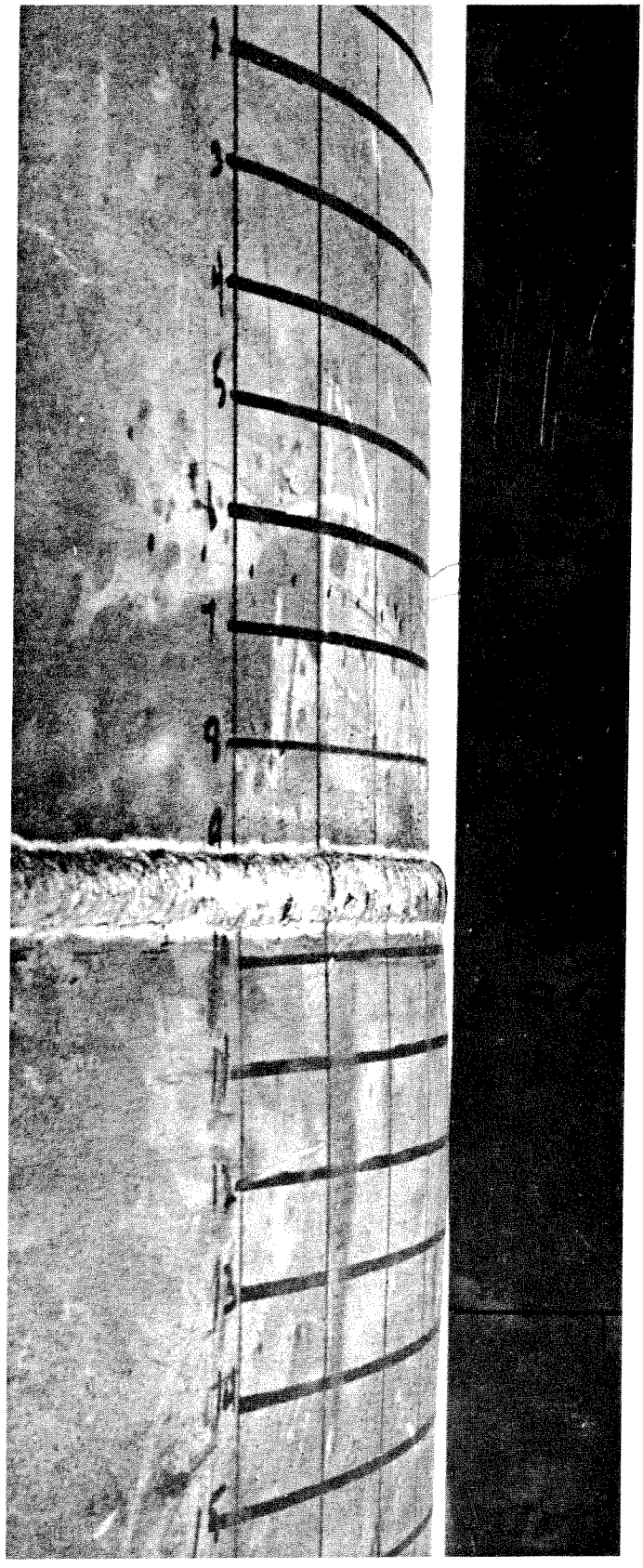

FIG. 33 SPECIMEN NO. 5 - AFTER INITIAL BUCKLING - COMPRESSION FACE

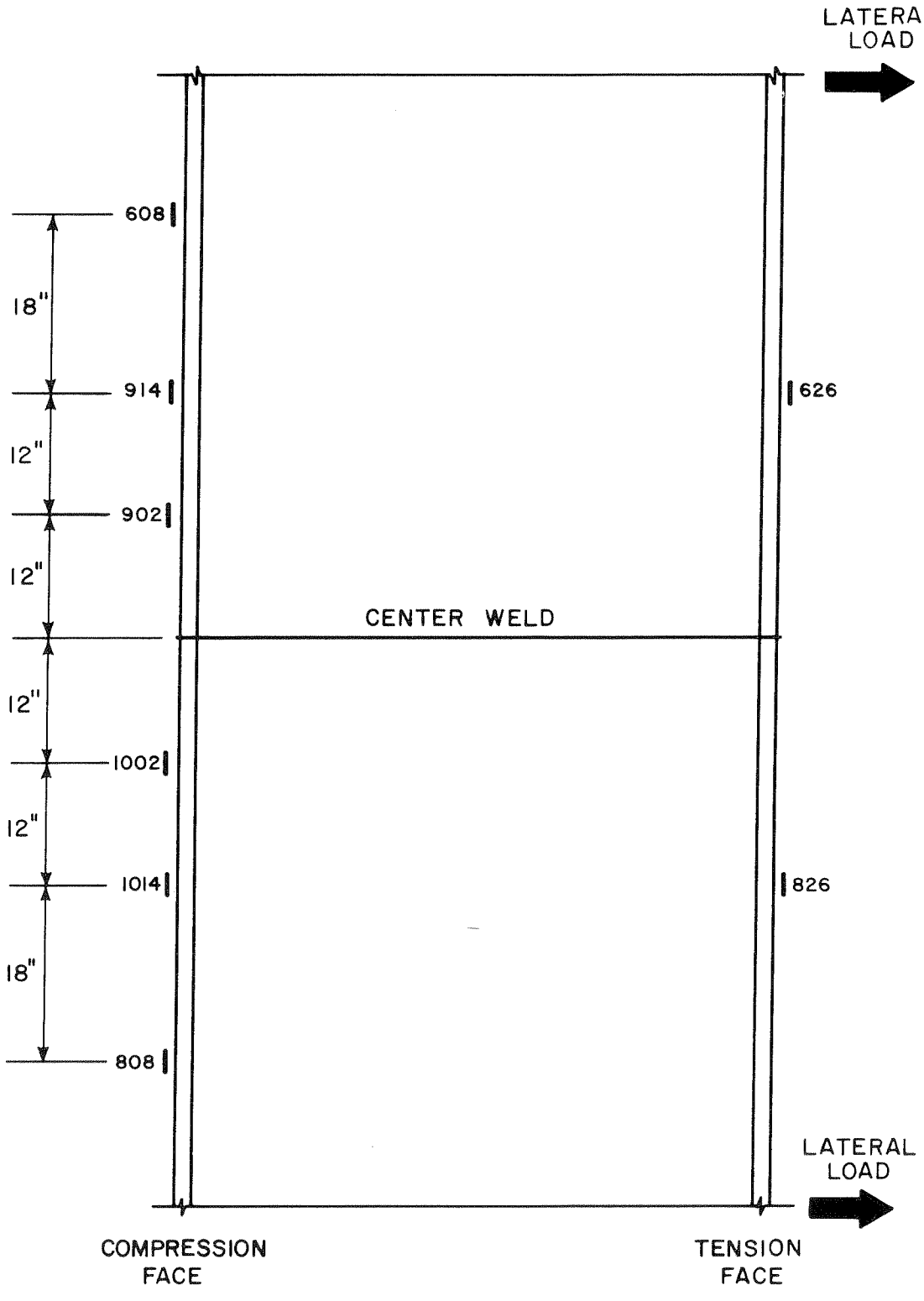

FIG. 34 SPECIMEN NO. 5A LOCATION OF SELECTED LONGITUDINAL STRAIN GAGES

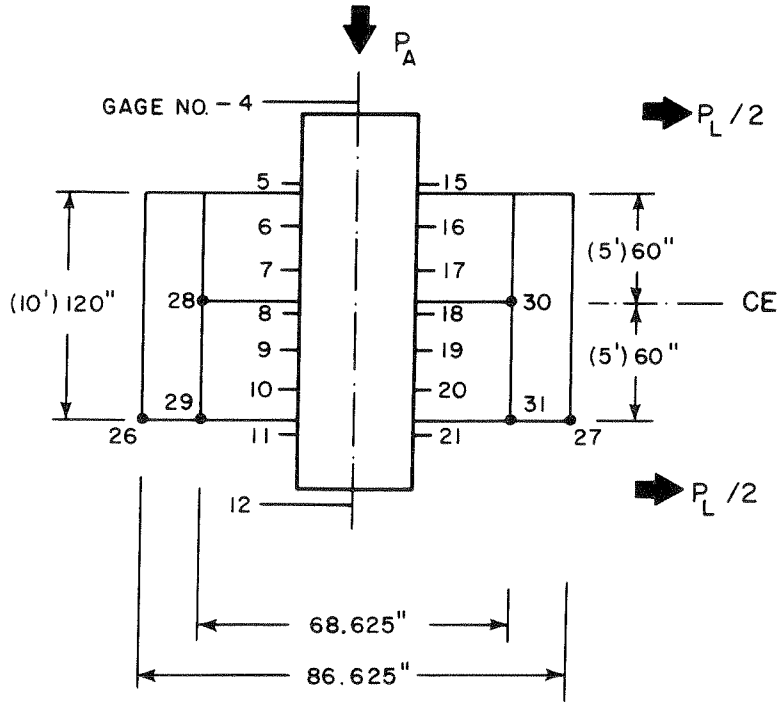

PRINCIPLE POTENTIOMETER LOCATIONS

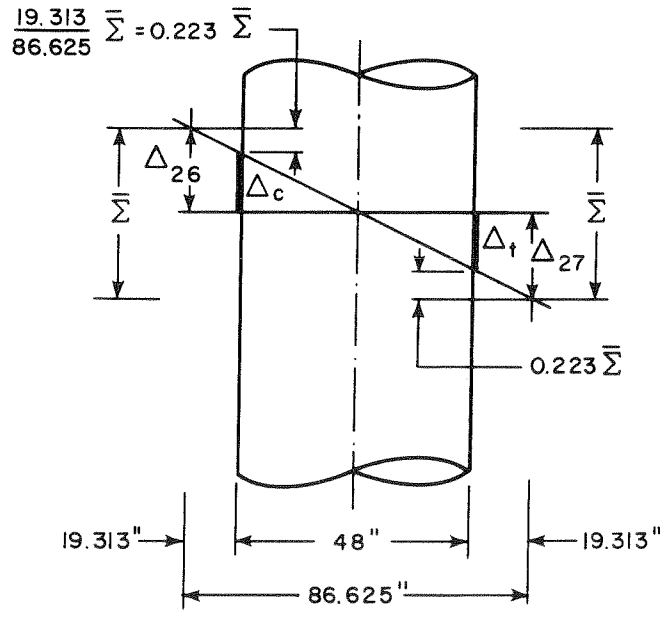

RADIUS OF CURVATURE AND GROSS-STRAIN EVALUATION

RADIUS OF CURVATURE CALCULATIONS

TOTAL SECTION

$$\bar{\Sigma}_T = |\Delta_{26}| + |\Delta_{27}|$$

$$R_{TOTAL} = \frac{866}{\bar{\Sigma}_T}$$

UPPER SECTION

$$\bar{\Sigma}_u = |\Delta_{28}| + |\Delta_{30}|$$

$$R_{UPPER} = \frac{343}{\bar{\Sigma}_u}$$

LOWER SECTION

$$\bar{\Sigma}_L = |\Delta_{29}| + |\Delta_{31}|$$

$$R_{LOWER} = \frac{343}{\bar{\Sigma}_L}$$

GROSS-STRAIN CALCULATIONS

$$\epsilon_t = \frac{|\Delta_{27}| - 0.223\,\bar{\Sigma}_T}{120}$$

$$\epsilon_c = \frac{|\Delta_{26}| - 0.223\,\bar{\Sigma}_T}{120}$$

FIG. 35 SPECIMEN NO.5A BASIC DATA REDUCTION CRITERIA

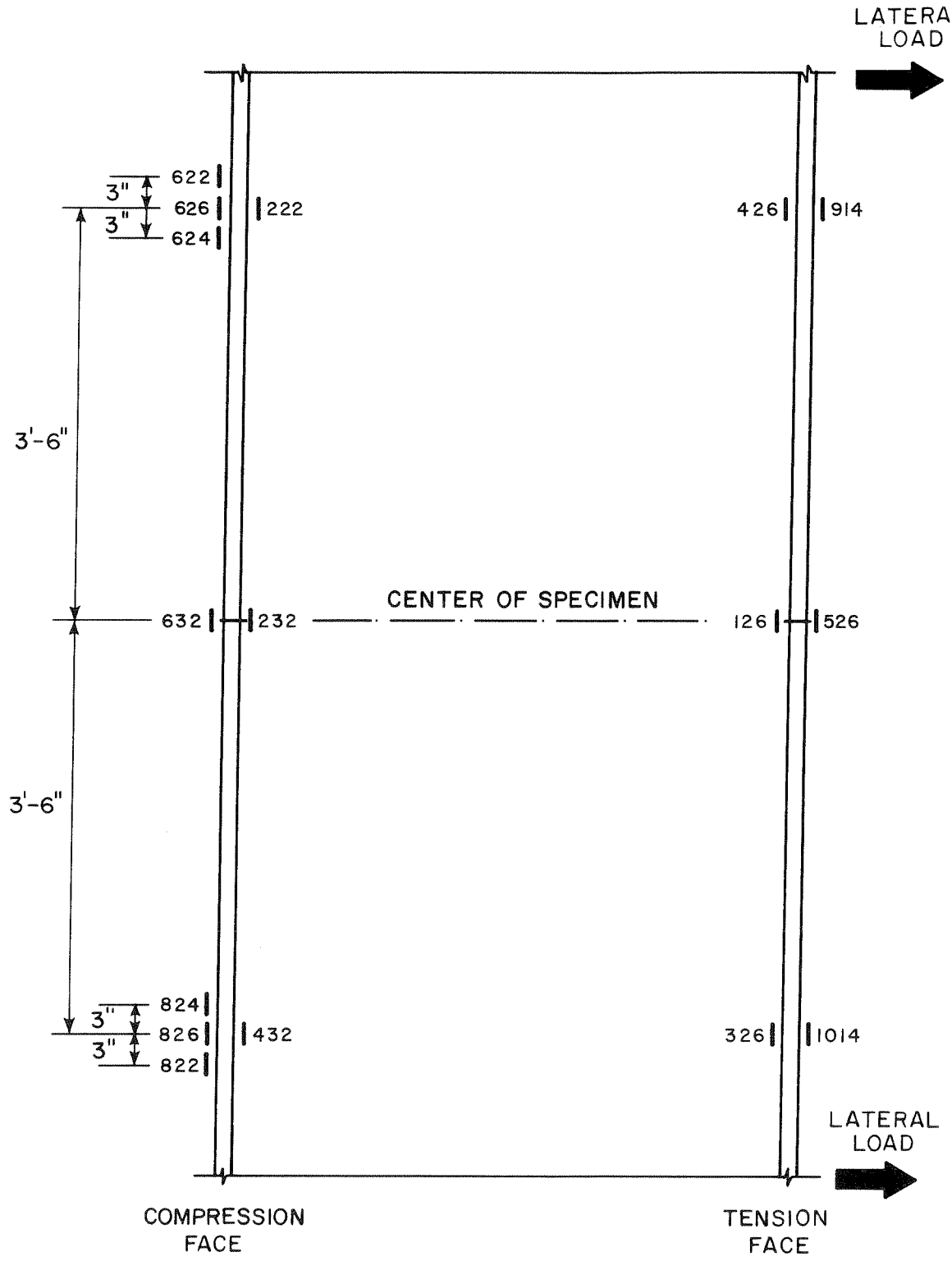

FIG.36 SPECIMEN NO.6 LOCATION OF SELECTED LONGITUDINAL STRAIN GAGES

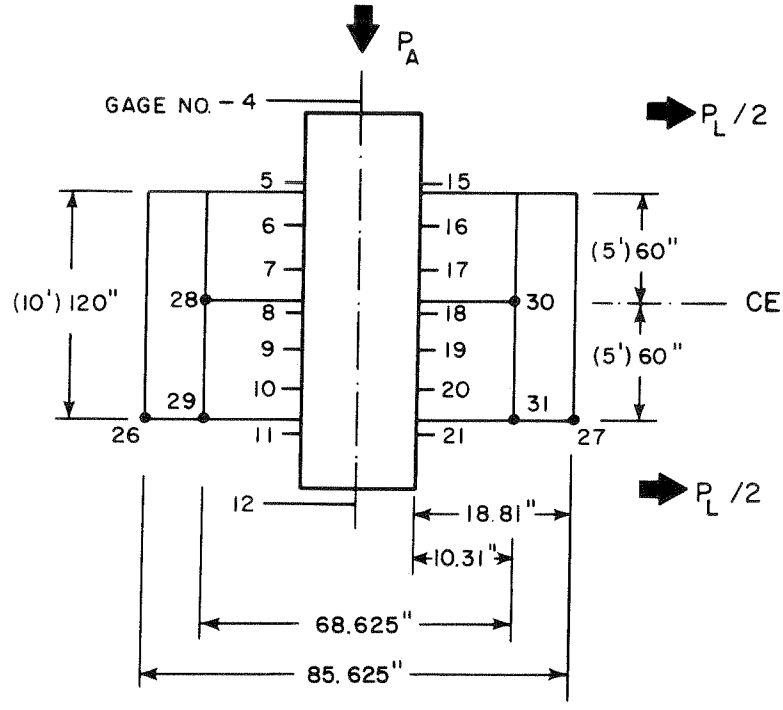

$$\Delta_{av} = \frac{|\Delta_8| + |\Delta_{18}|}{2}$$

$$M_T = 52.5\, P_L + P_A \Delta_{av}$$

PRINCIPLE POTENTIOMETER LOCATIONS

RADIUS OF CURVATURE CALCULATIONS

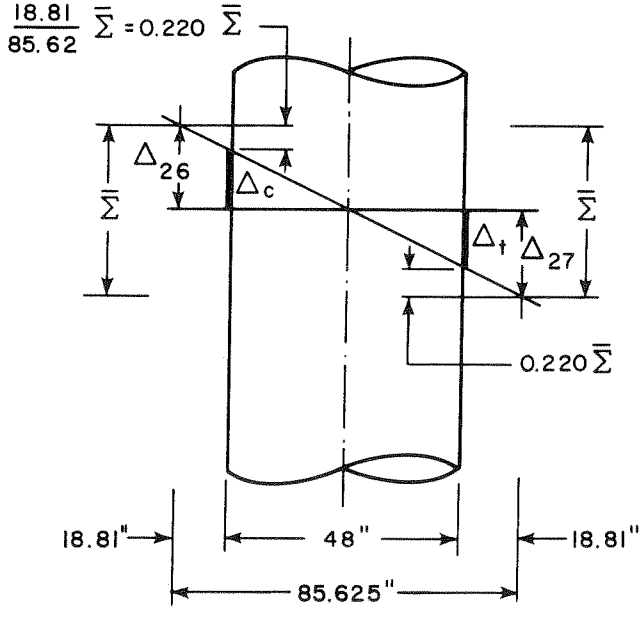

RADIUS OF CURVATURE AND GROSS-STRAIN EVALUATION

TOTAL SECTION

$$\bar{\Sigma}_T = |\Delta_{26}| + |\Delta_{27}|$$

$$R_{TOTAL} = \frac{856}{\bar{\Sigma}_T}$$

UPPER SECTION

$$\bar{\Sigma}_u = |\Delta_{28}| + |\Delta_{30}|$$

$$R_{UPPER} = \frac{343}{\bar{\Sigma}_u}$$

LOWER SECTION

$$\bar{\Sigma}_L = |\Delta_{29}| + |\Delta_{31}|$$

$$R_{LOWER} = \frac{343}{\bar{\Sigma}_L}$$

GROSS-STRAIN CALCULATIONS

$$\epsilon_t = \frac{|\Delta_{27}| - 0.220\,\bar{\Sigma}_T}{120}$$

$$\epsilon_c = \frac{|\Delta_{26}| - 0.220\,\bar{\Sigma}_T}{120}$$

FIG. 37 SPECIMEN NO. 6 BASIC DATA REDUCTION CRITERIA

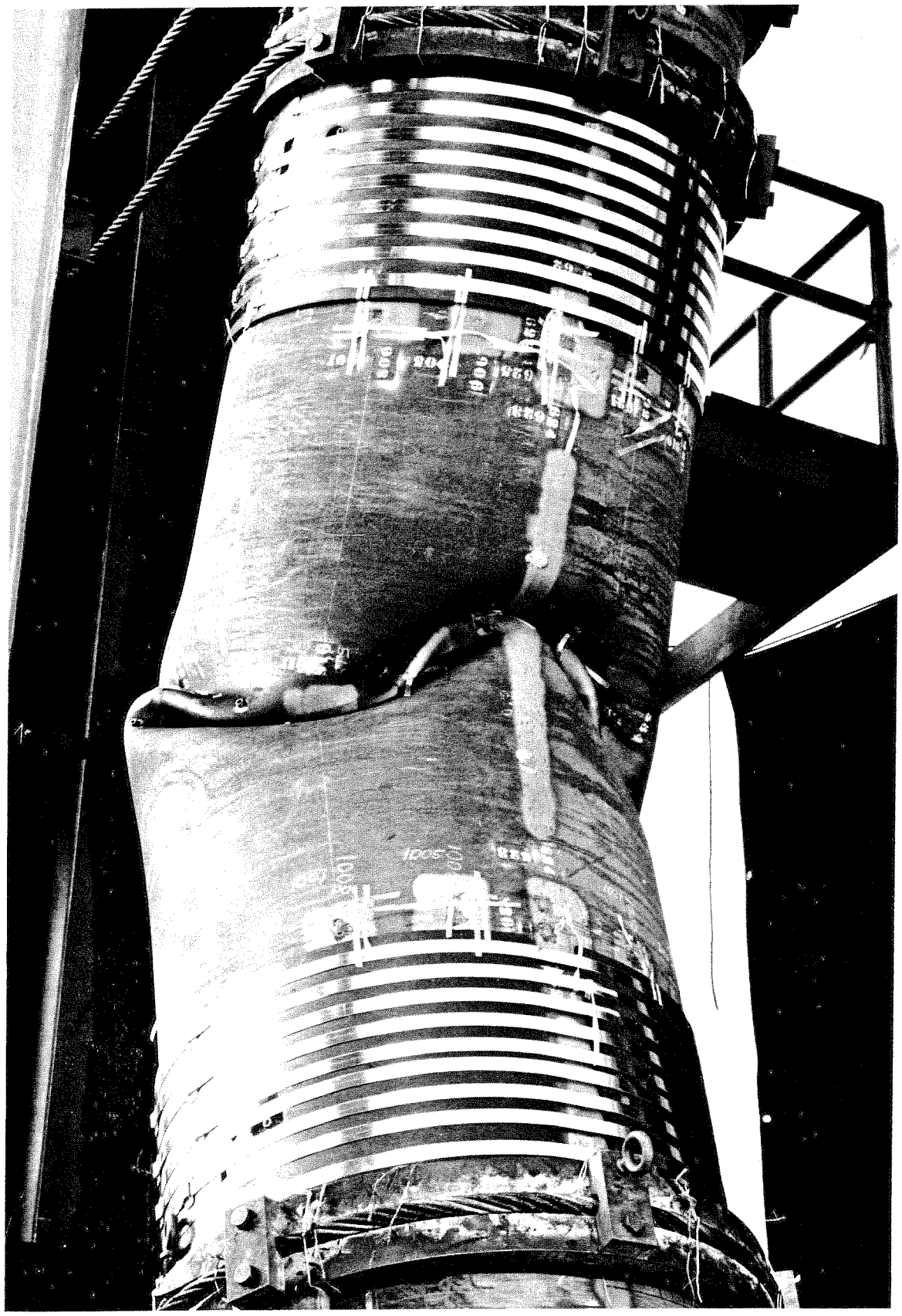

FIG. 38 SPECIMEN NO. 6 VIEW OF BUCKLE

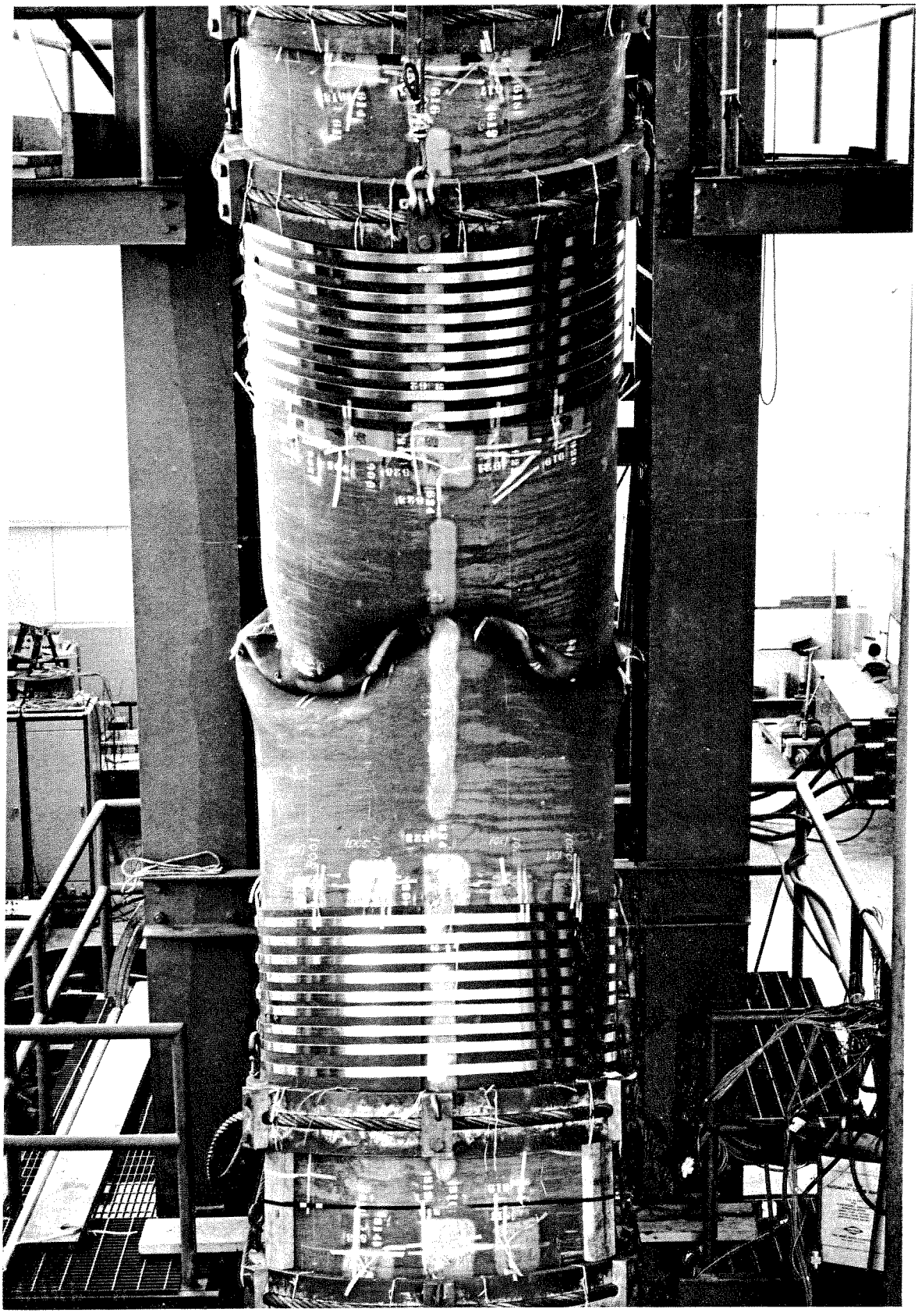

FIG. 39 SPECIMEN NO. 6 GENERAL VIEW AFTER POST-BUCKLING TEST

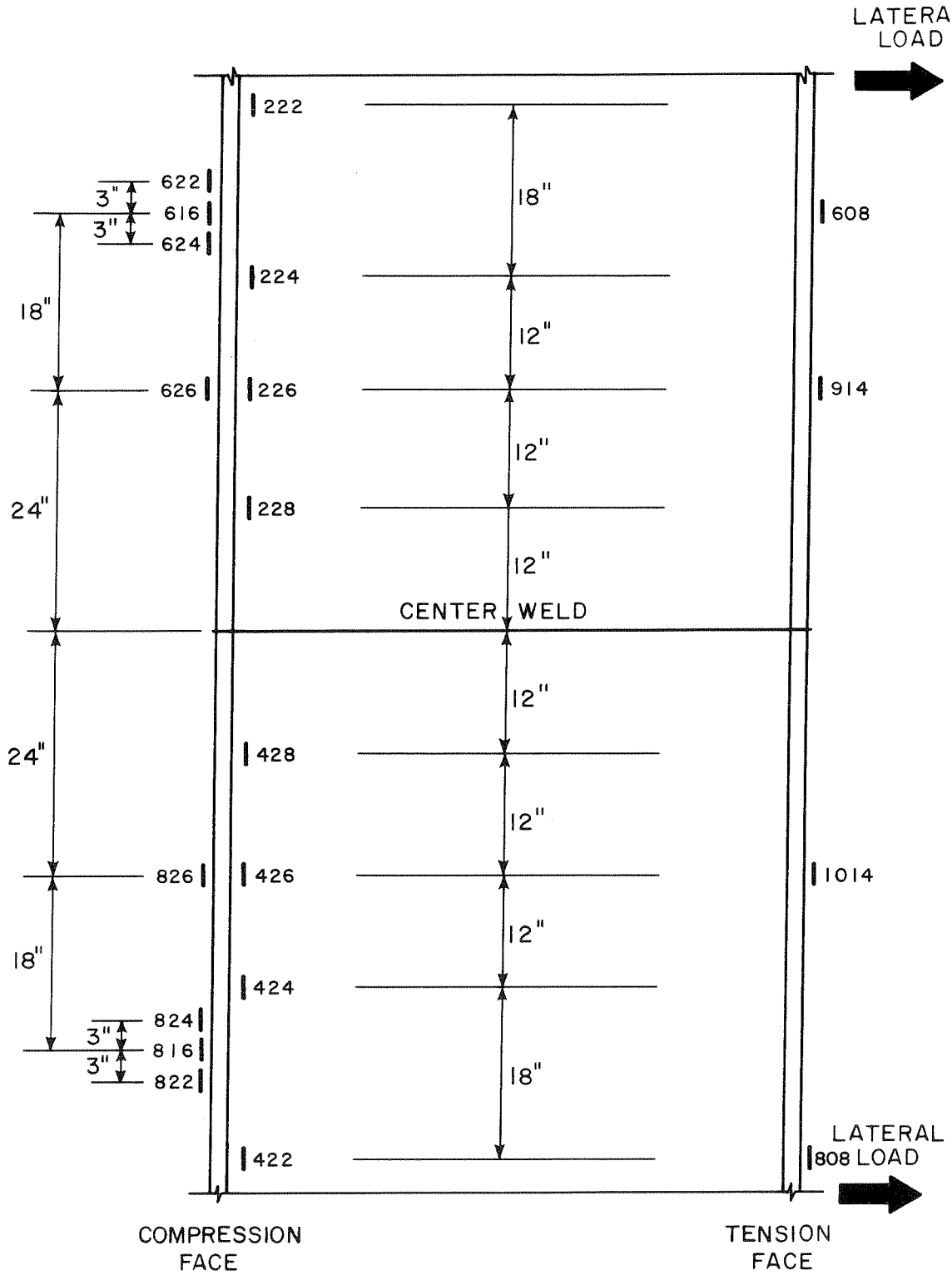

FIG. 40 SPECIMEN NO. 7 LOCATION OF SELECTED LONGITUDINAL STRAIN GAGES

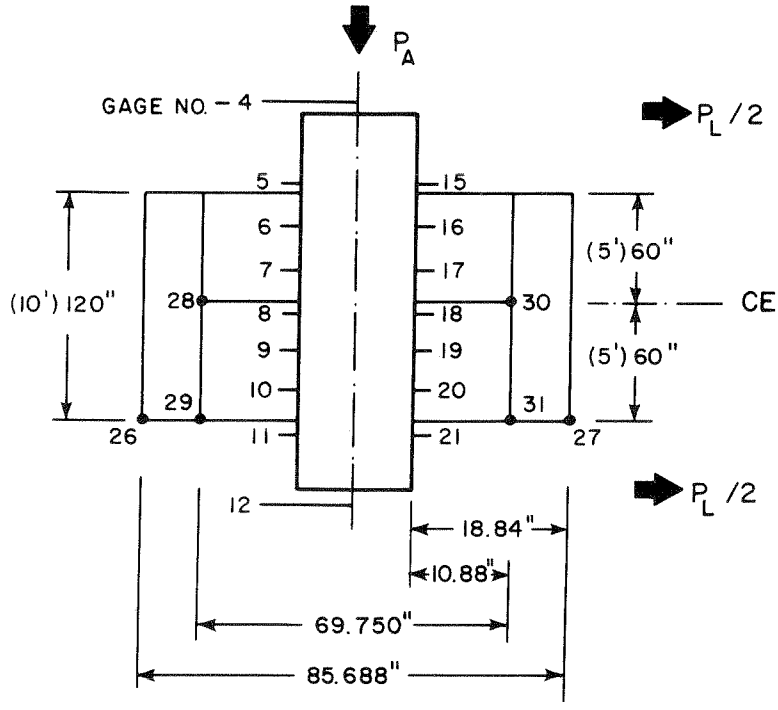

$$\Delta_{av} = \frac{|\Delta_8| + |\Delta_{18}|}{2}$$

$$M_T = 52.5\, P_L + P_A \Delta_{av}$$

PRINCIPLE POTENTIOMETER LOCATIONS

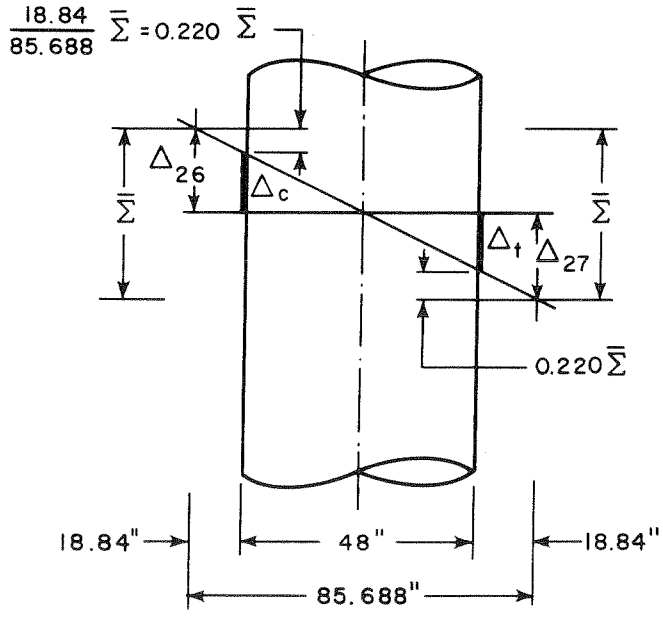

RADIUS OF CURVATURE AND GROSS-STRAIN EVALUATION

RADIUS OF CURVATURE CALCULATIONS

TOTAL SECTION

$$\bar{\Sigma}_T = |\Delta_{26}| + |\Delta_{27}|$$

$$R_{TOTAL} = \frac{856.9}{\bar{\Sigma}_T}$$

UPPER SECTION

$$\bar{\Sigma}_u = |\Delta_{28}| + |\Delta_{30}|$$

$$R_{UPPER} = \frac{348.8}{\bar{\Sigma}_u}$$

LOWER SECTION

$$\bar{\Sigma}_L = |\Delta_{29}| + |\Delta_{31}|$$

$$R_{LOWER} = \frac{348.8}{\bar{\Sigma}_L}$$

GROSS-STRAIN CALCULATIONS

$$\epsilon_t = \frac{|\Delta_{27}| - 0.220\,\bar{\Sigma}_T}{120}$$

$$\epsilon_c = \frac{|\Delta_{26}| - 0.220\,\bar{\Sigma}_T}{120}$$

FIG. 41 SPECIMEN NO. 7 BASIC DATA REDUCTION CRITERIA

FIG. 42 SPECIMEN NO. 7 SIDE VIEW AFTER POST-BUCKLING TEST

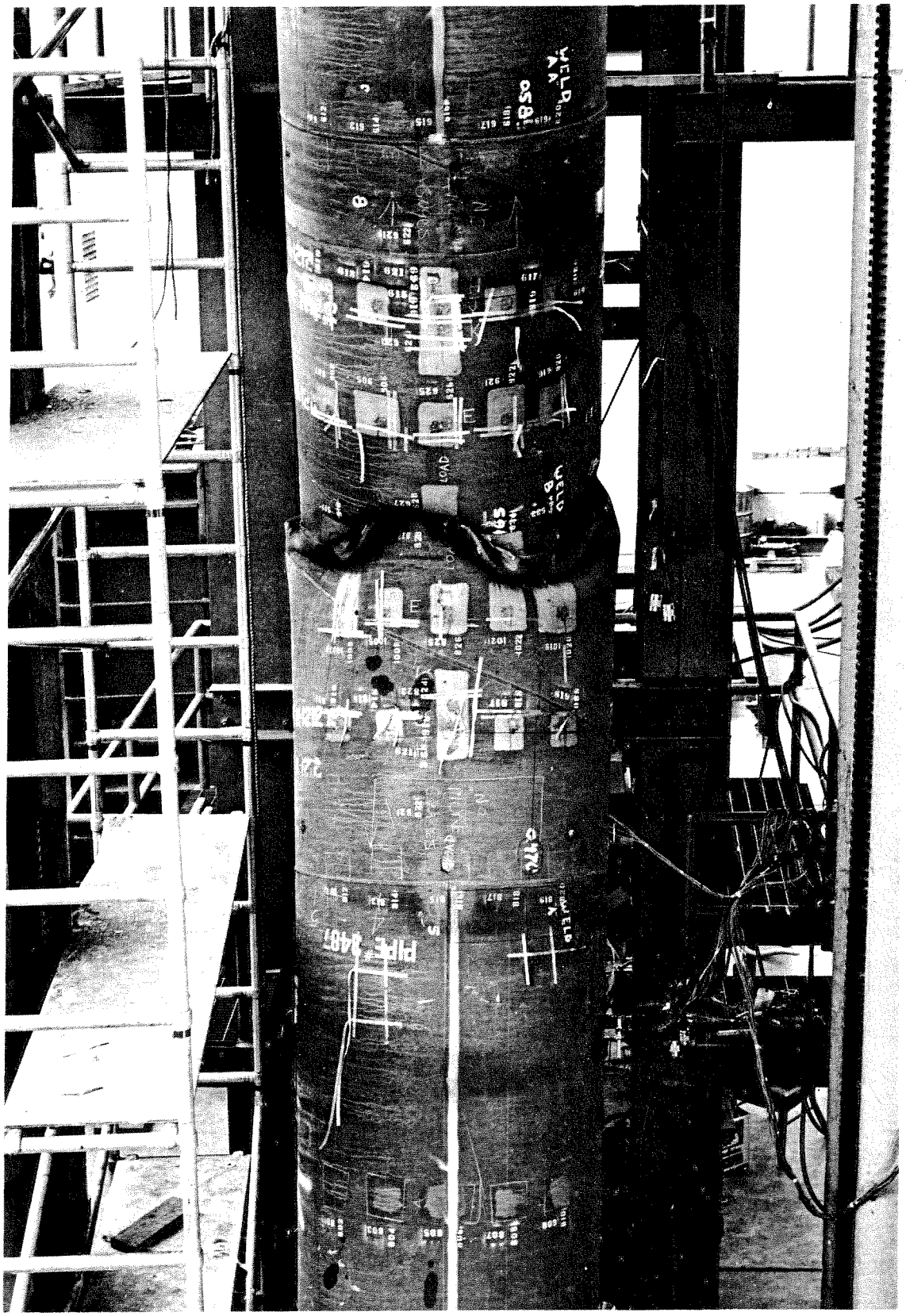

FIG. 43 SPECIMEN NO. 7 OVERALL VIEW AFTER POST-BUCKLING TEST

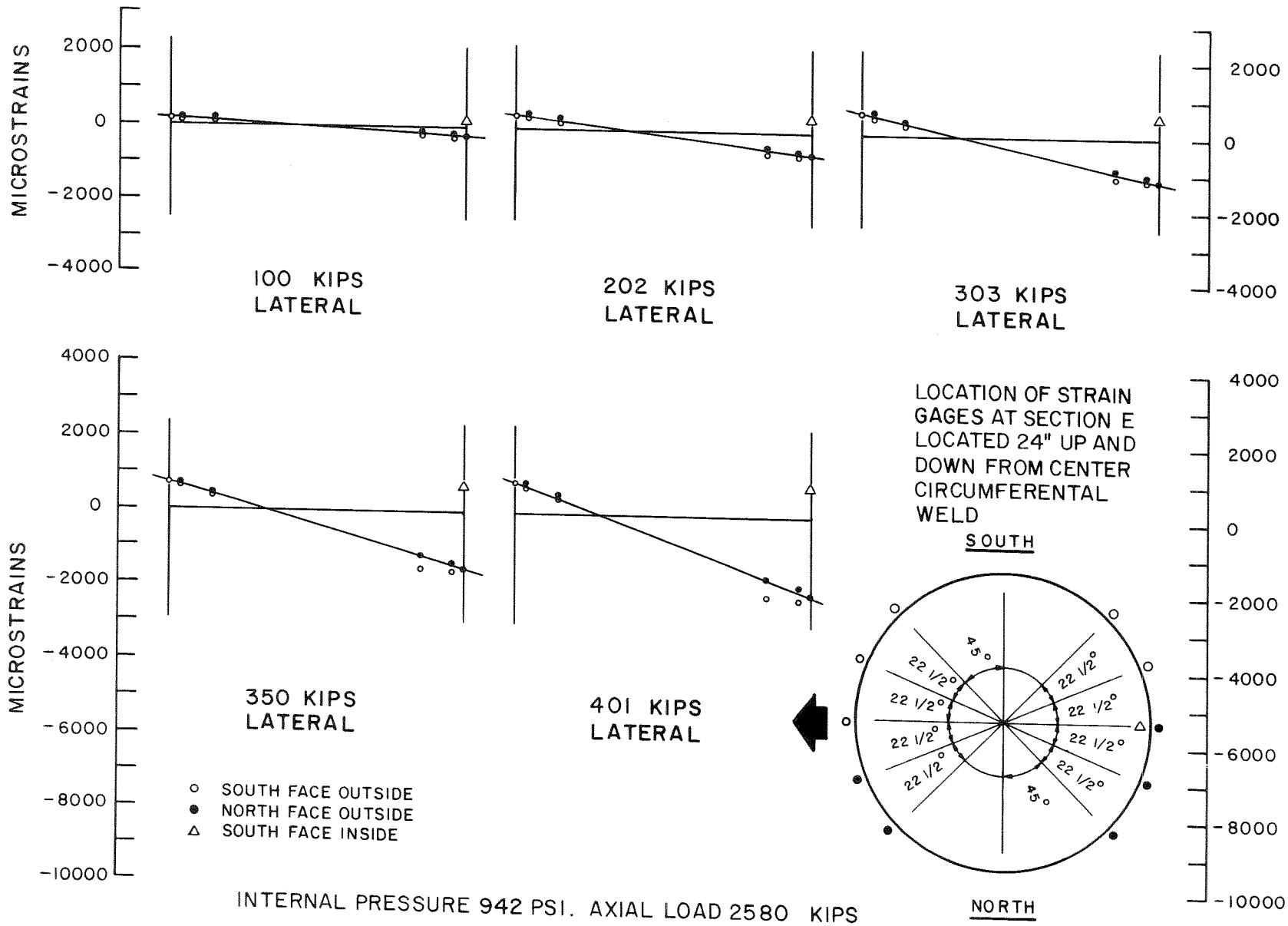

FIG. 44 SPECIMEN I-UPPER SECTION E PLOT OF LONGITUDINAL STRAINS

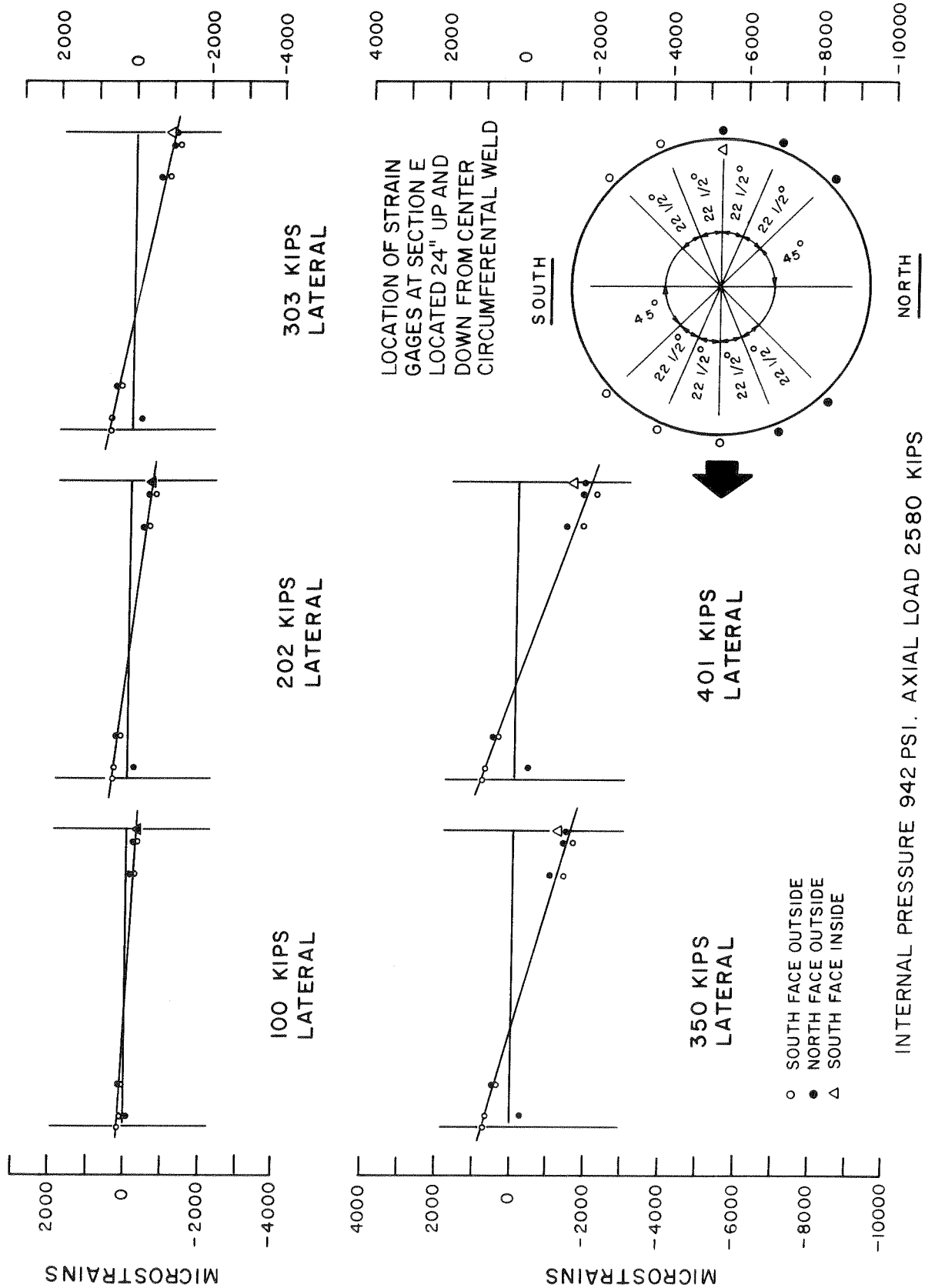

FIG. 45 SPECIMEN I - LOWER SECTION E PLOT OF LONGITUDINAL STRAINS

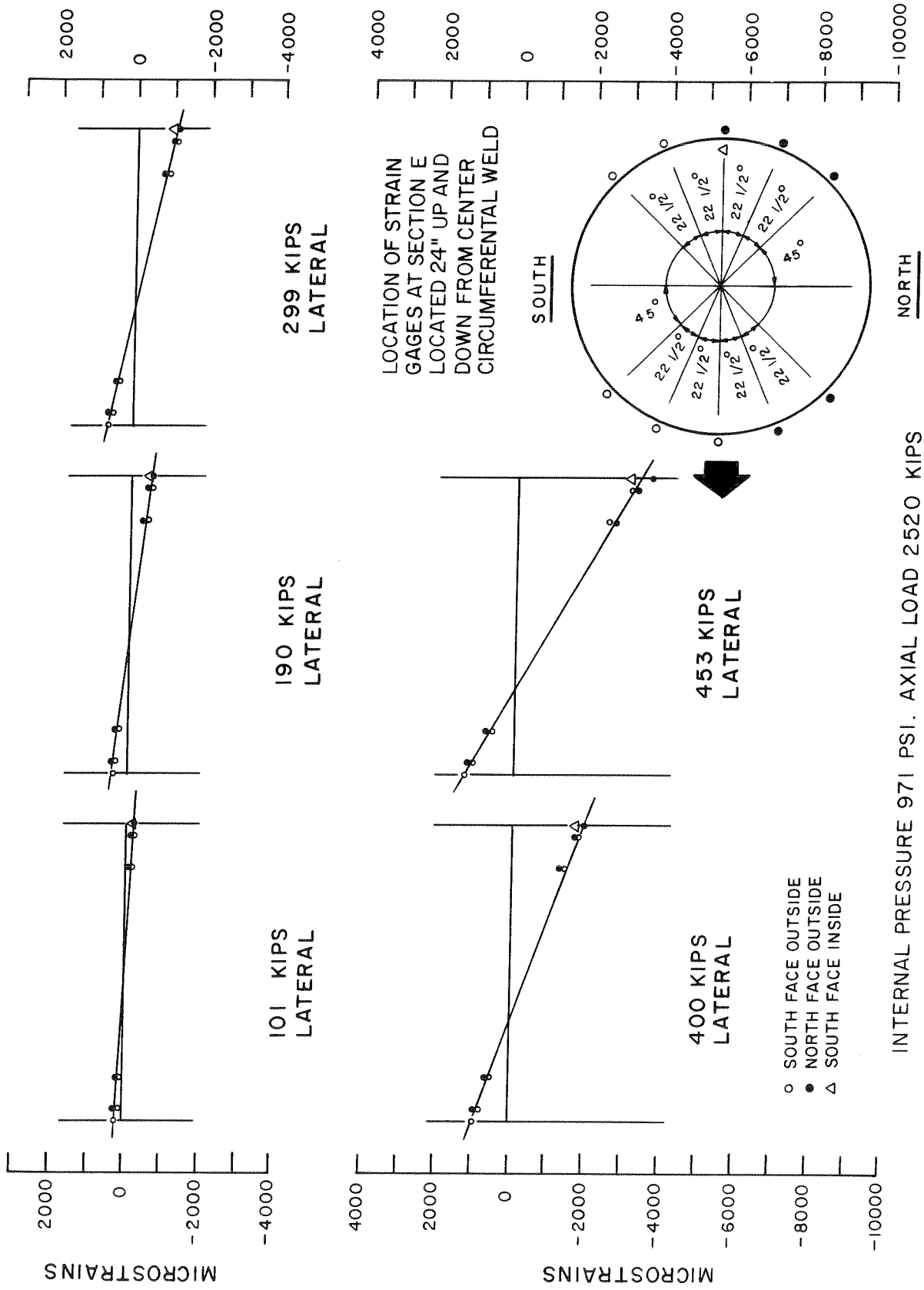

FIG. 46 SPECIMEN 2-UPPER SECTION E PLOT OF LONGITUDINAL STRAINS

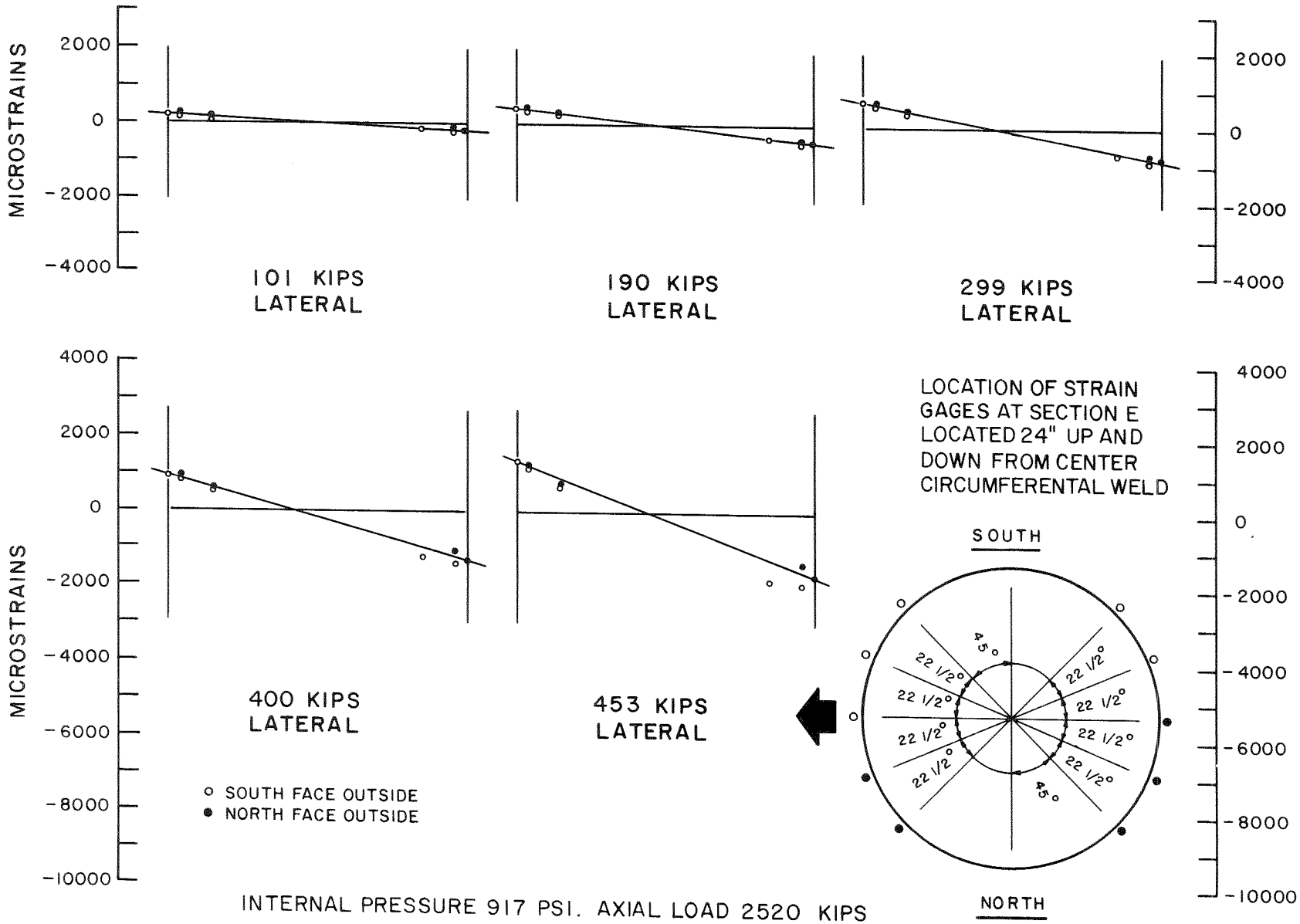

FIG. 47 SPECIMEN 2 - LOWER SECTION E PLOT OF LONGITUDINAL STRAINS

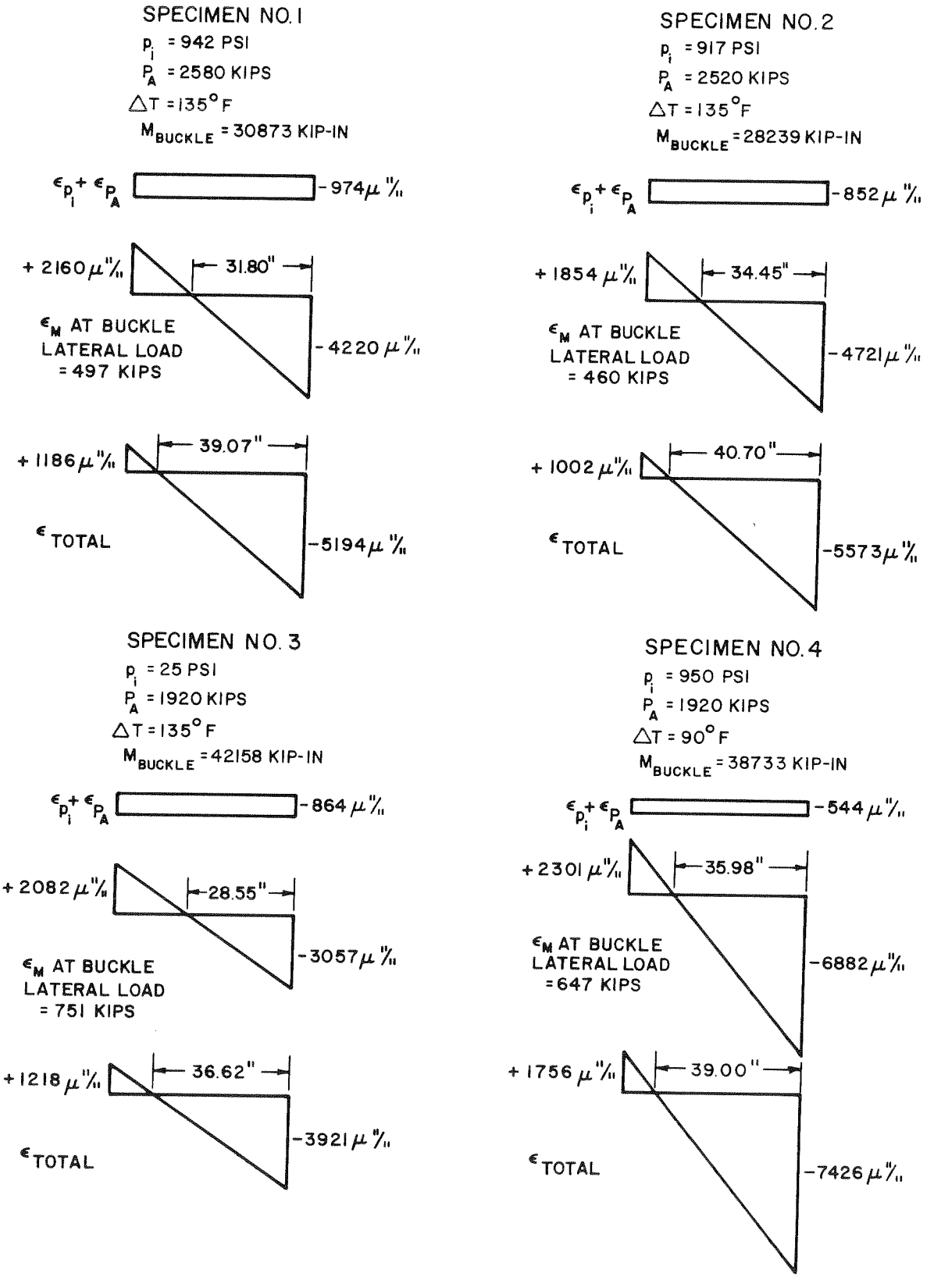

FIG. 48 RELATIONSHIPS OF CLIP-GAGE STRAINS AT THE MAXIMUM OR BUCKLING LOAD BASED ON TOTAL TEST SECTION

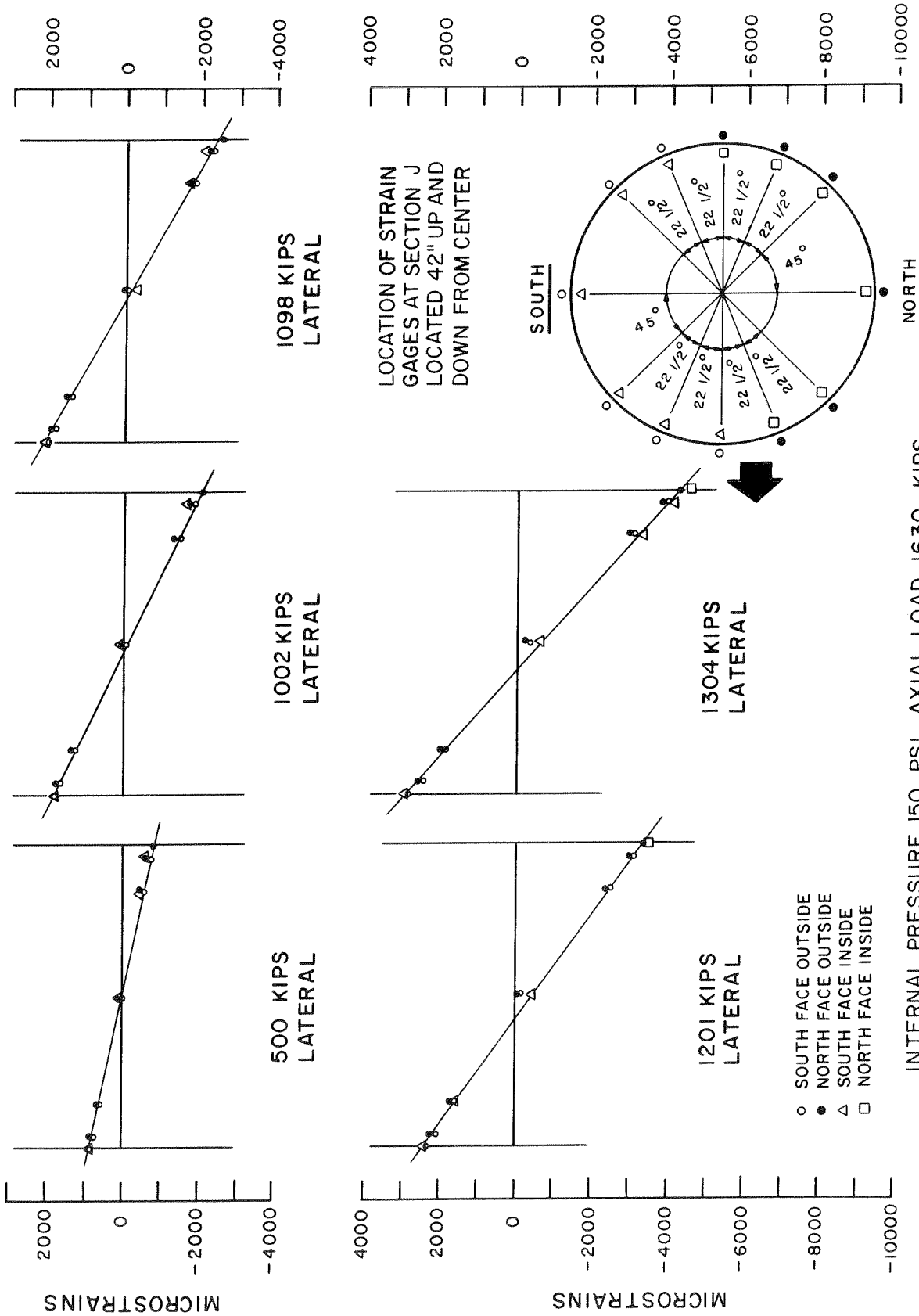

FIG. 49 SPECIMEN 6 - UPPER SECTION J PLOT OF LONGITUDINAL STRAINS

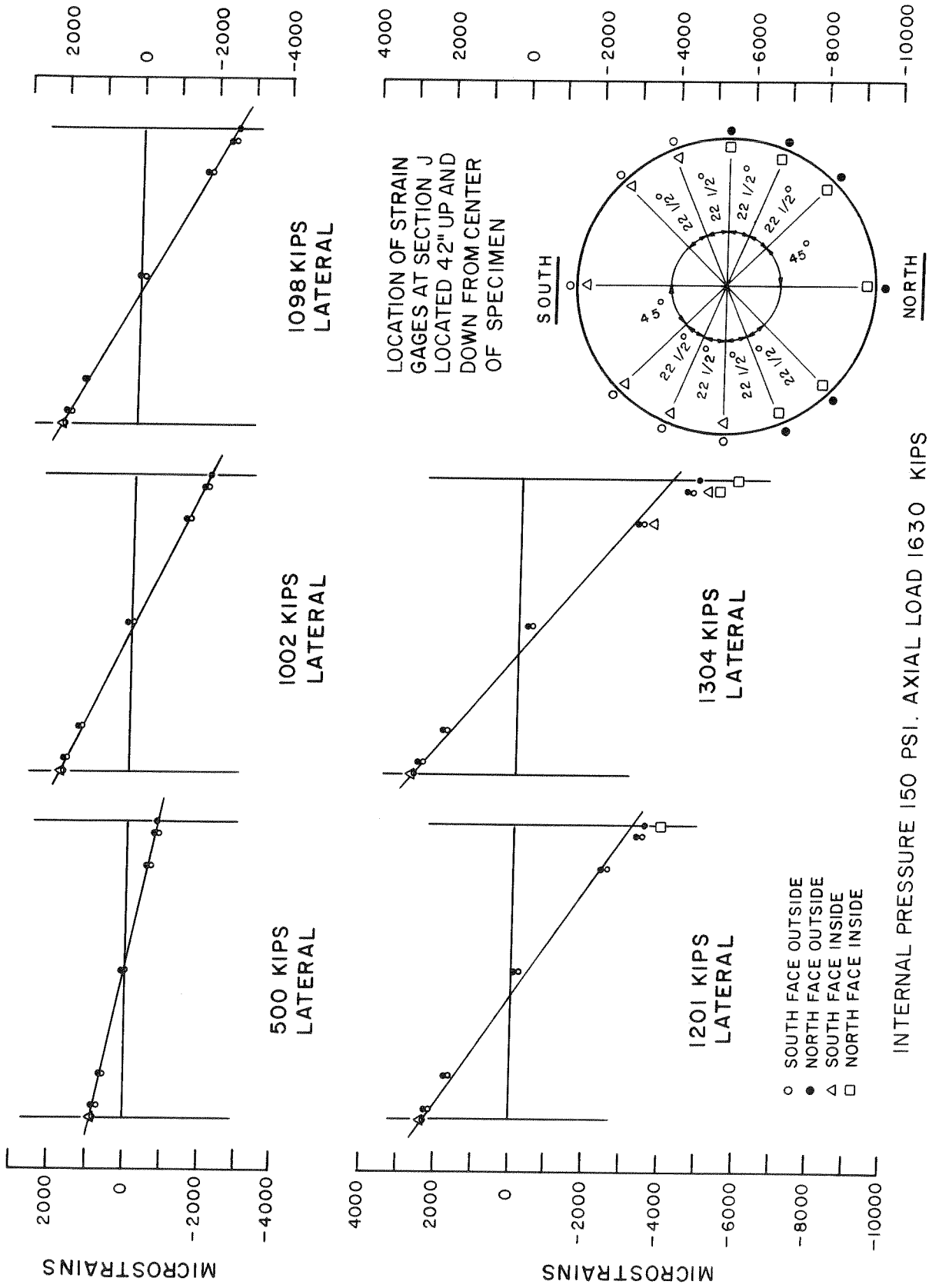

FIG. 50 SPECIMEN 6 - LOWER SECTION J PLOT OF LONGITUDINAL STRAINS

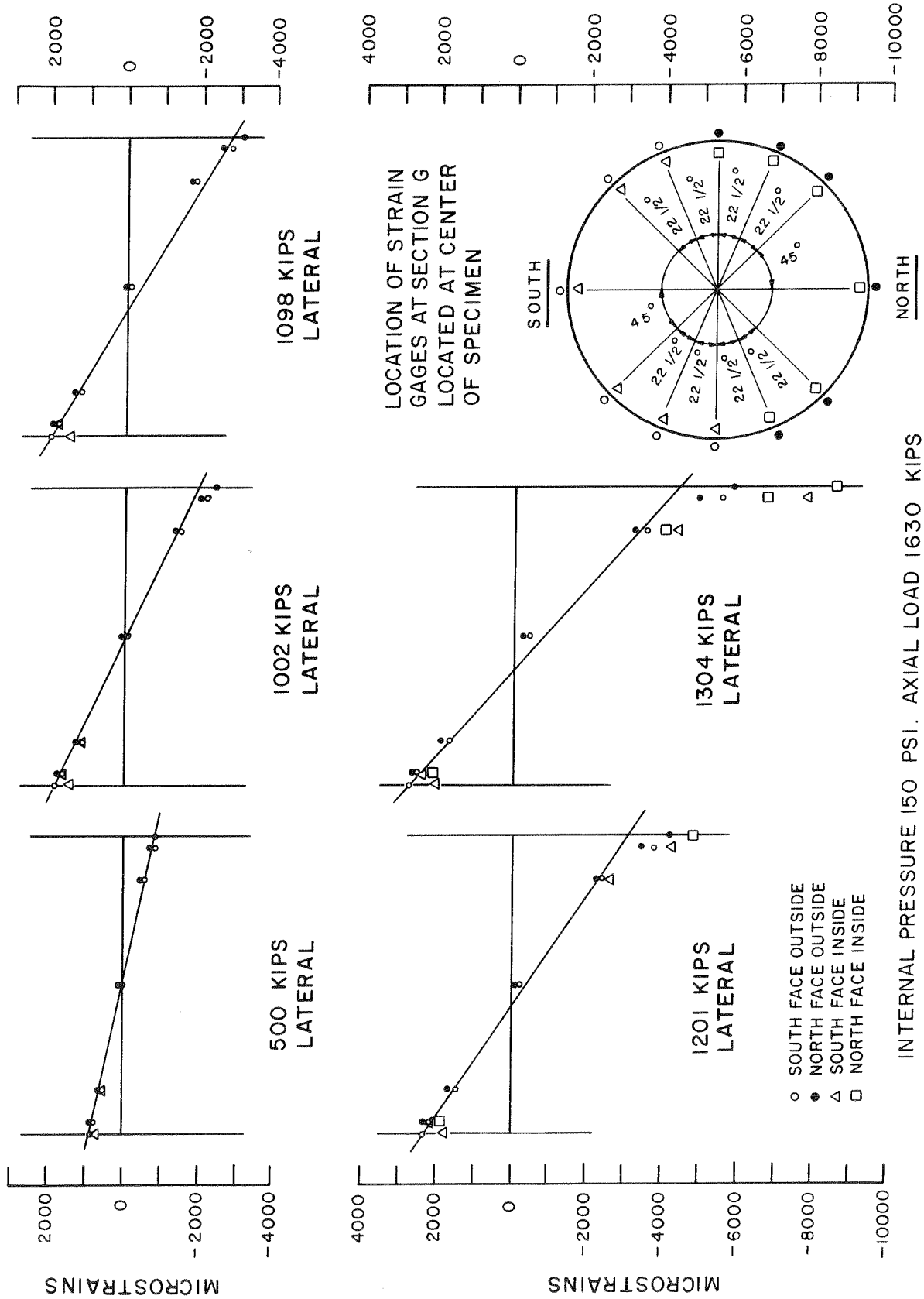

FIG. 51 SPECIMEN 6 - CENTER SECTION G PLOT OF LONGITUDINAL STRAINS

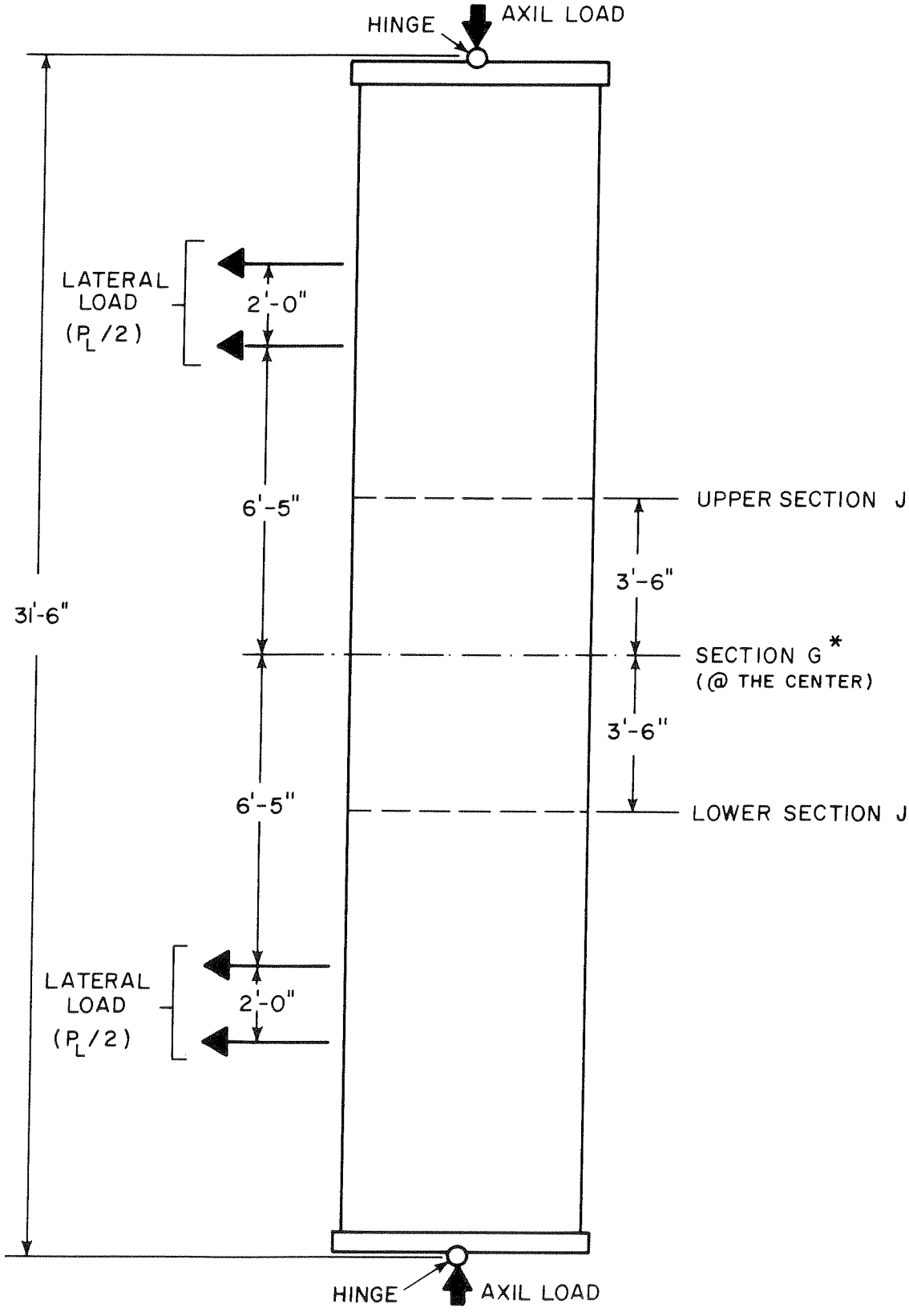

FIG. 52 SPECIMEN NO.6 WITH SECTION IDENTIFICATION

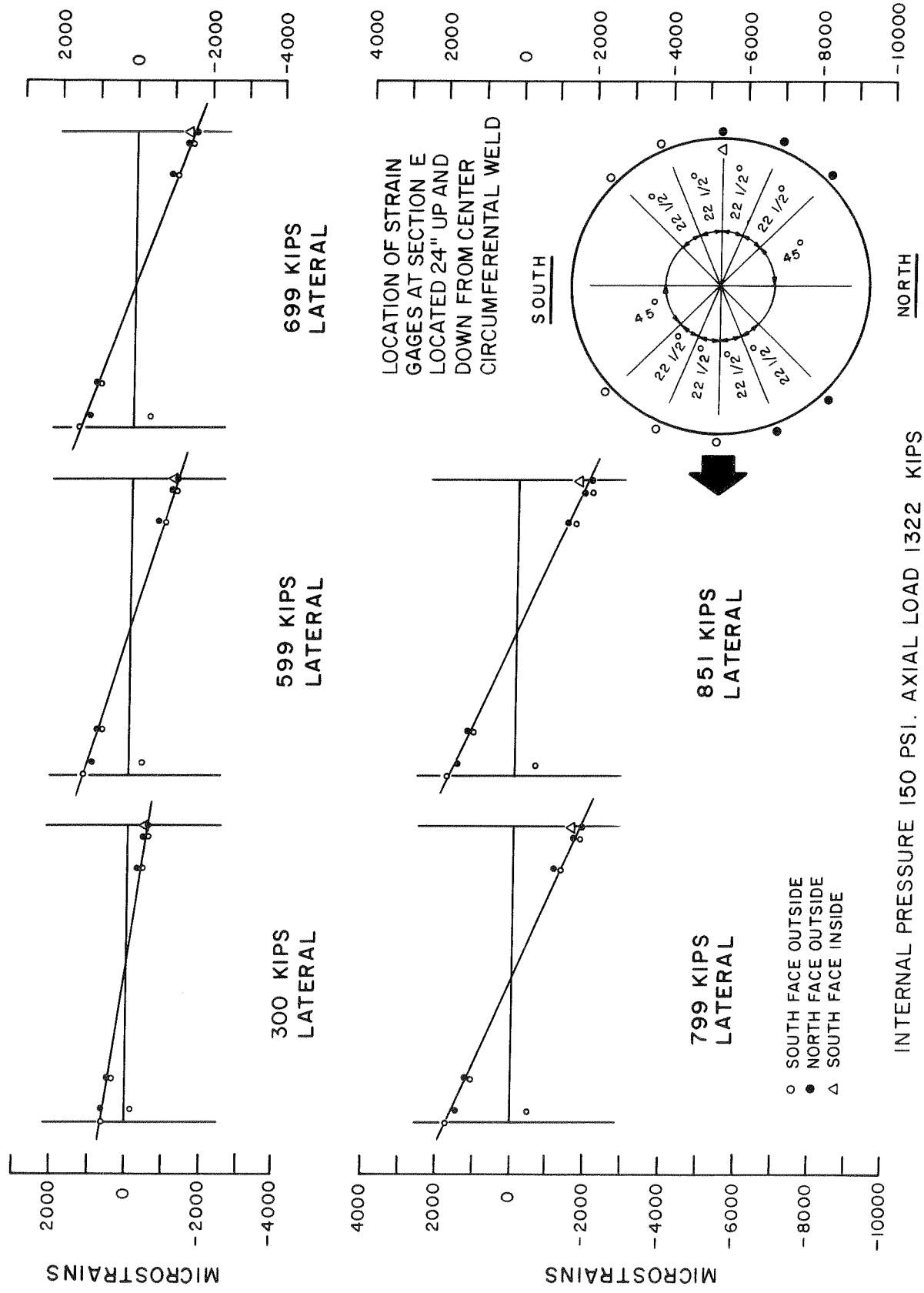

FIG. 53 SPECIMEN 7-UPPER SECTION E PLOT OF LONGITUDINAL STRAINS

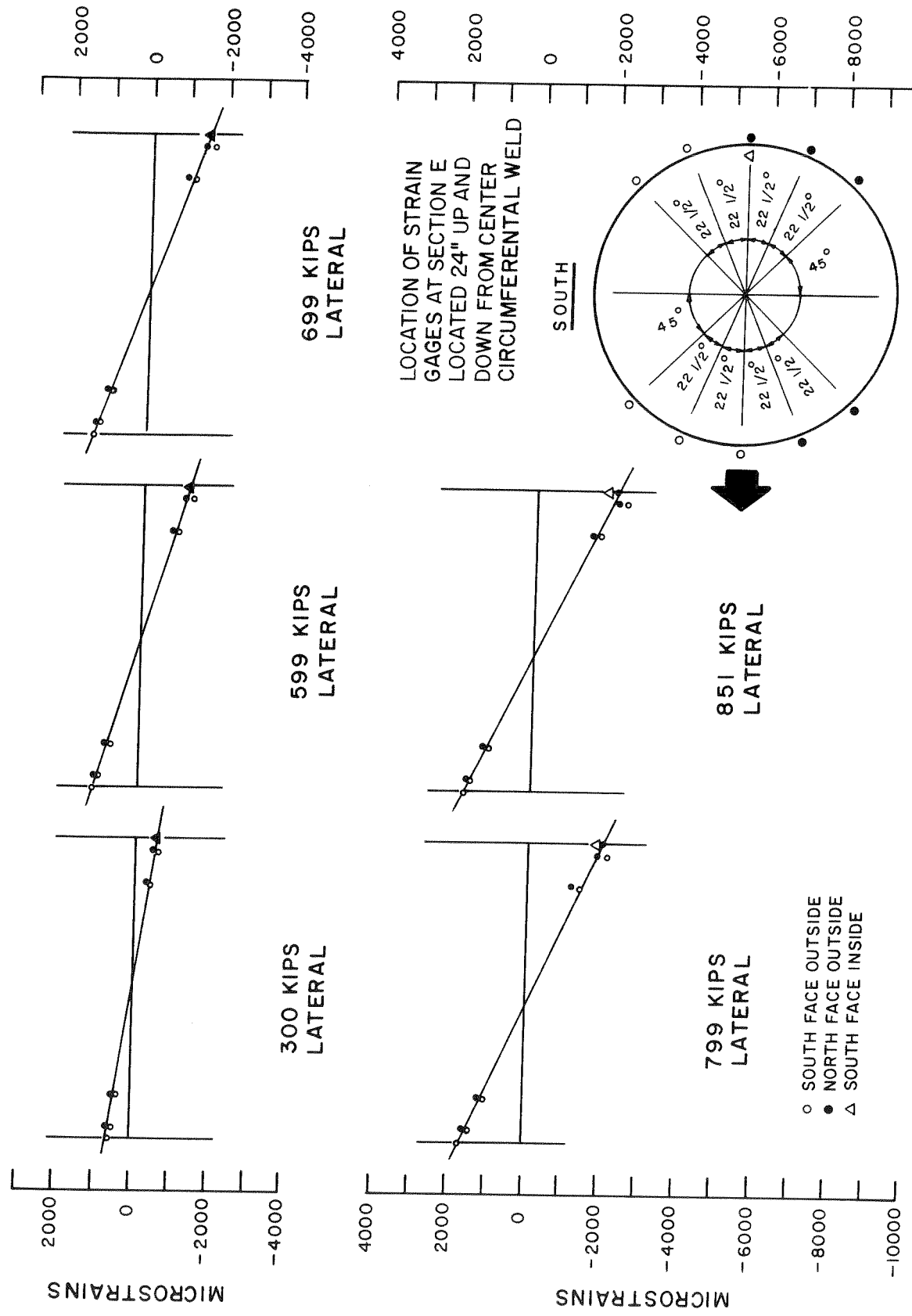

FIG. 54 SPECIMEN 7 - LOWER SECTION E PLOT OF LONGITUDINAL STRAINS

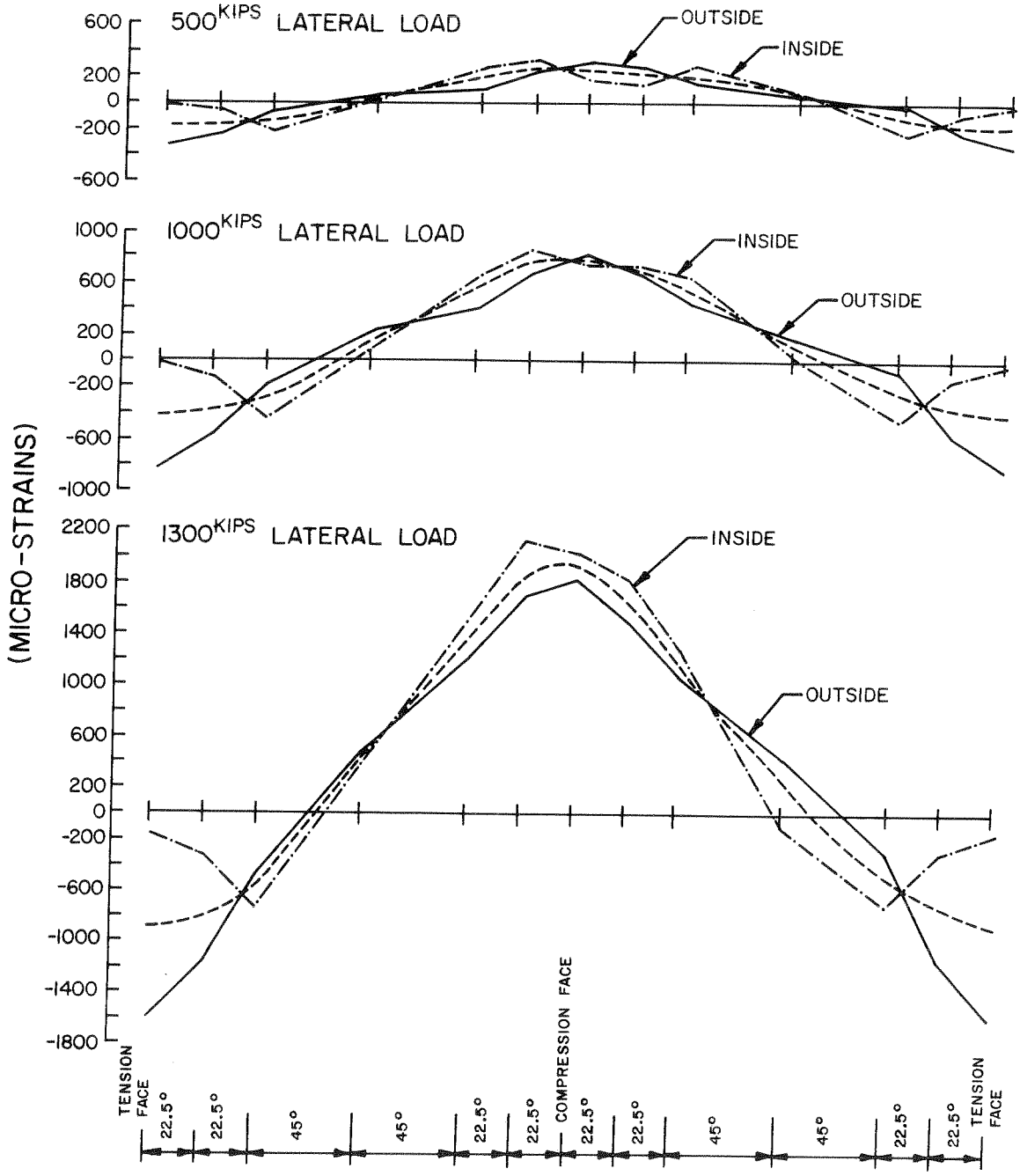

FIG. 55 SPECIMEN NO. 6 - UPPER SECTION J
CIRCUMFERENTIAL STRAINS

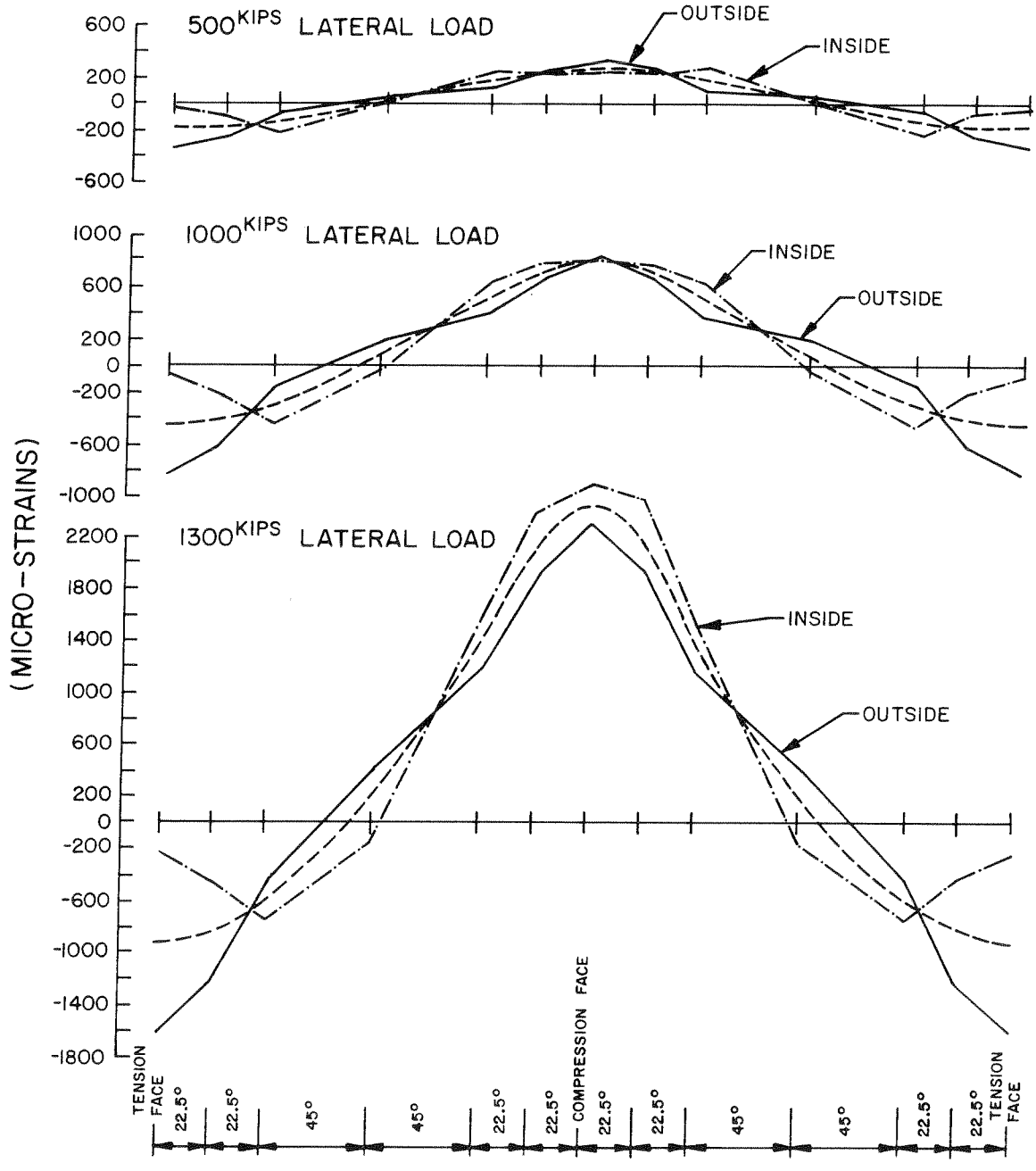

FIG. 56 SPECIMEN NO.6 - LOWER SECTION J
CIRCUMFERENTIAL STRAINS

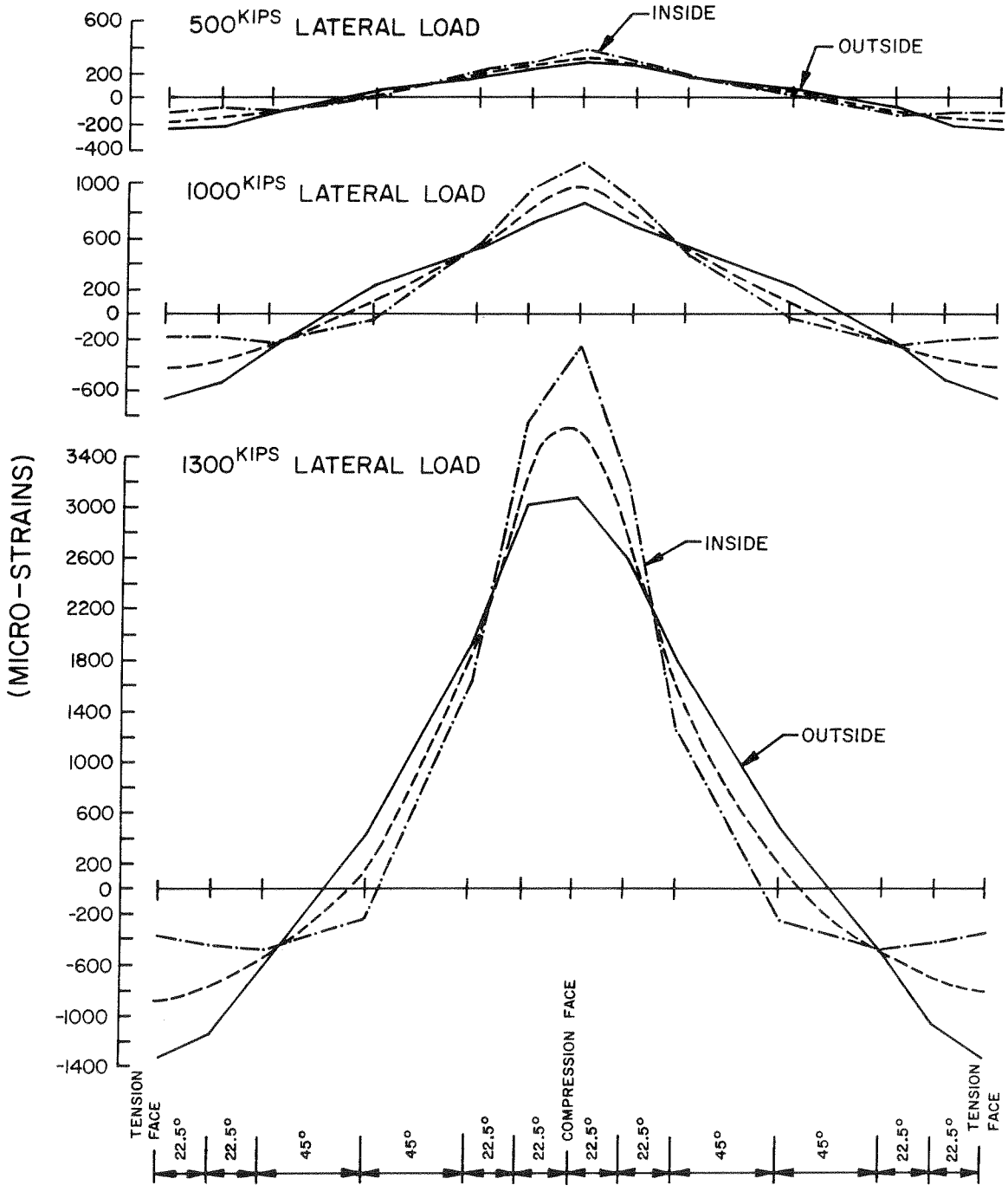

FIG. 57 SPECIMEN NO. 6 - CENTER SECTION G
CIRCUMFERENTIAL STRAINS

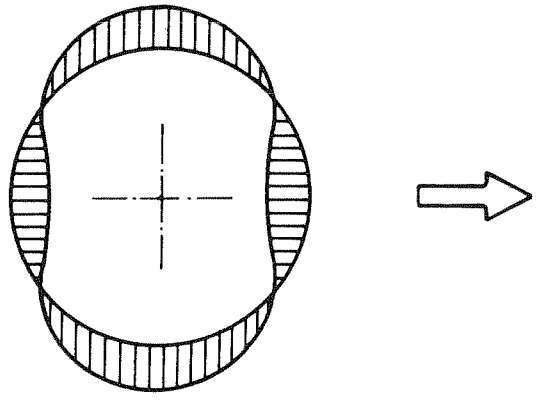

GENERAL CIRCUMFERENTIAL BENDING PATTERN

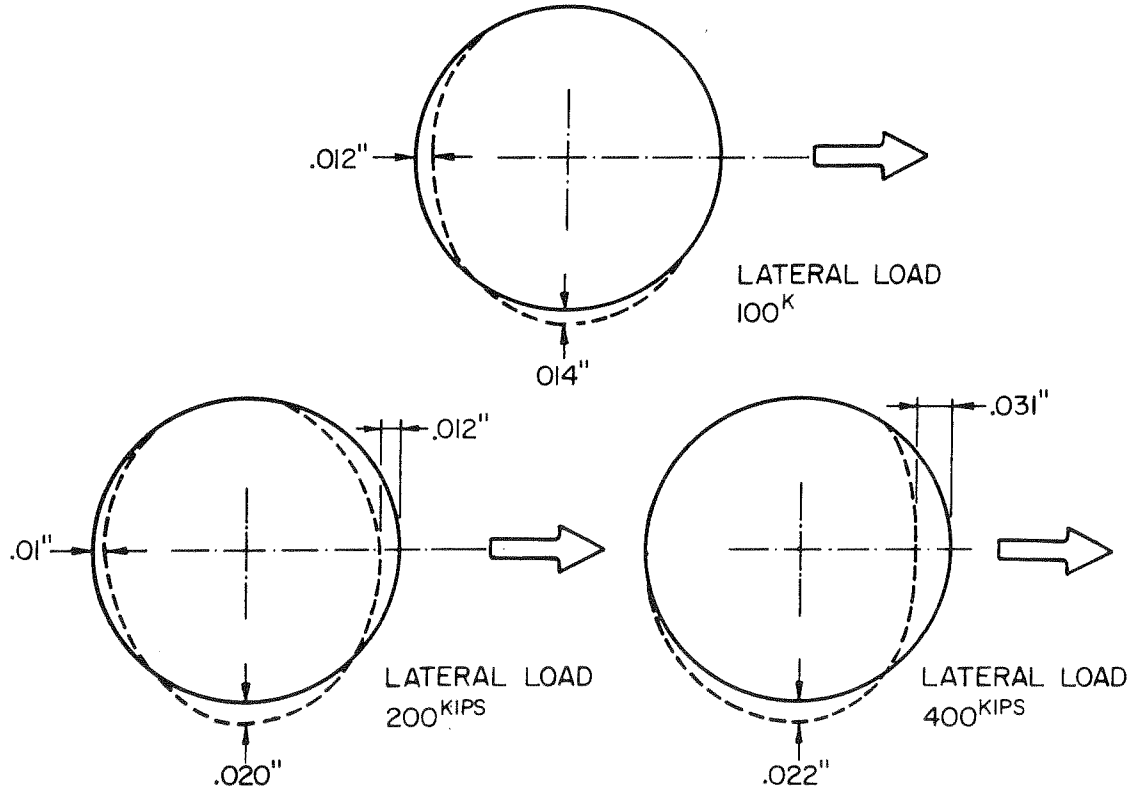

TYPICAL RADIAL DEFORMATION PATTERNS

FIG. 58 TYPICAL CROSS-SECTIONAL PIPE DEFORMATION DATA

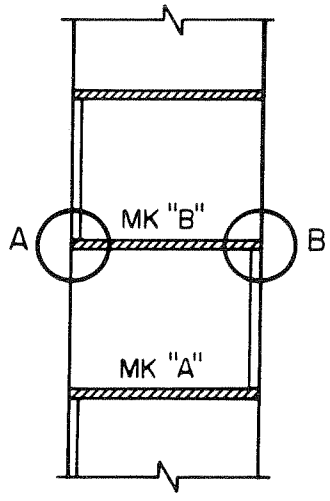

PIPE ELEVATION SHOWING
LOCATIONS OF WELD NOTCHES

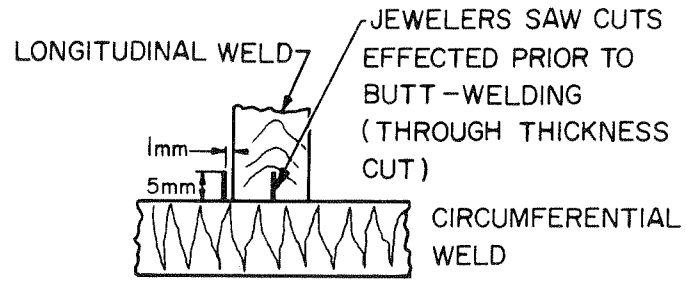

NOTCHES IN CERCUMFERENTIALLY
WELDED PIPE

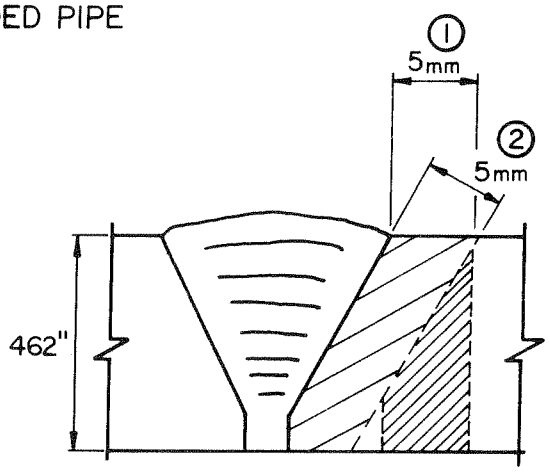

SECTION A-A

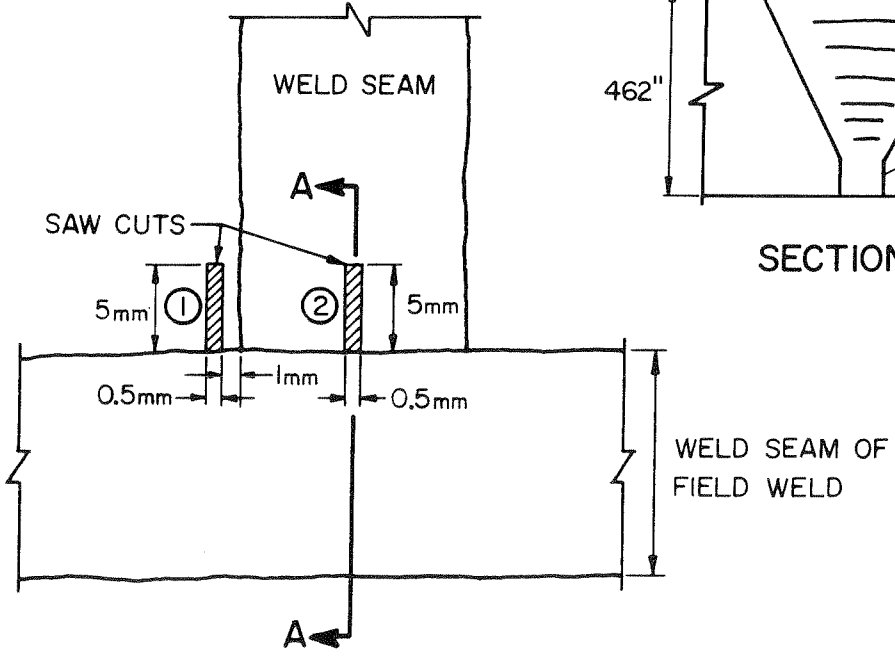

DETAIL OF WELD NOTCH LOCATIONS

FIG. 59 DETAIL OF NOTCHES IN CIRCUMFERENTIALLY WELDED PIPE SPECIMEN

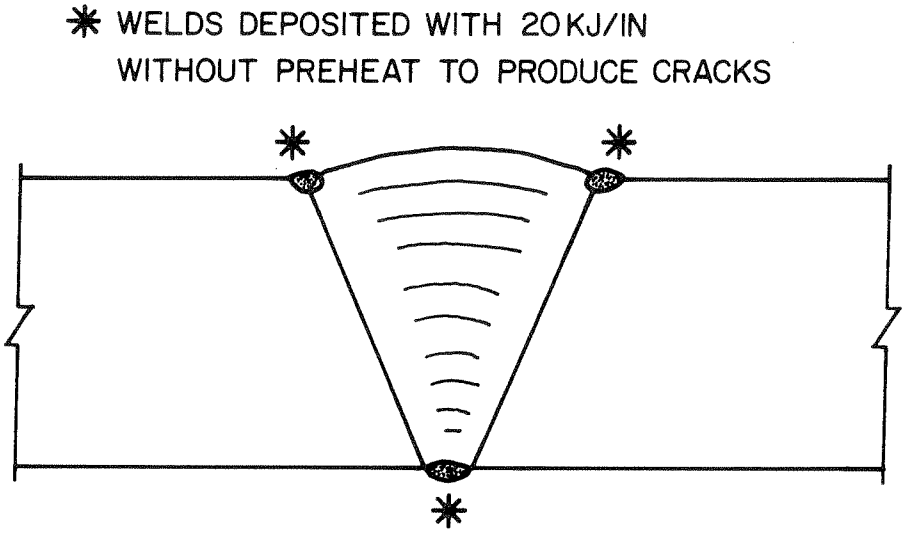

FIG. 60 DETAIL OF INTENTIONALLY INDUCED WELD DEFECTS IN CIRCUMFERENTIALLY WELDED PIPE SPECIMEN

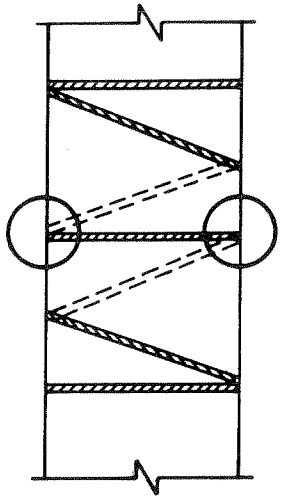

PIPE ELEVATION SHOWING
LOCATIONS OF WELD NOTCHES

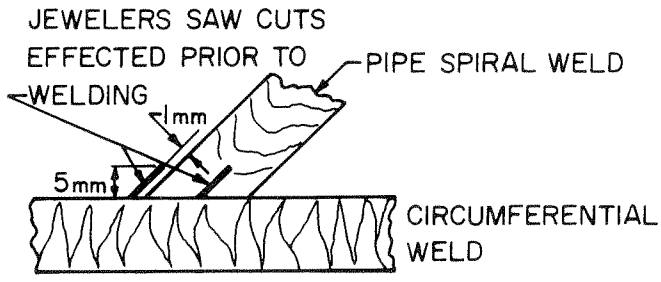

NOTCHES IN SPIRALLY WELDED PIPE

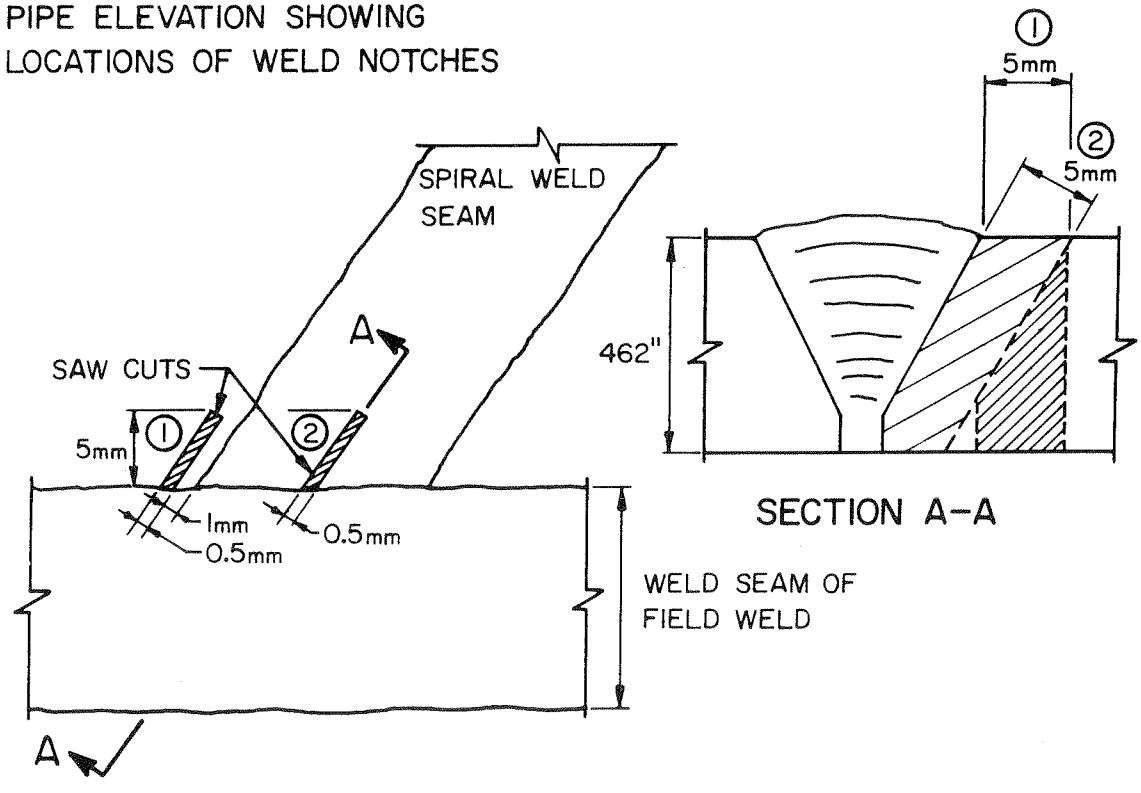

DETAIL OF WELD NOTCH LOCATIONS

FIG. 61 DETAIL OF NOTCHES IN SPIRALLY WELDED PIPE SPECIMEN

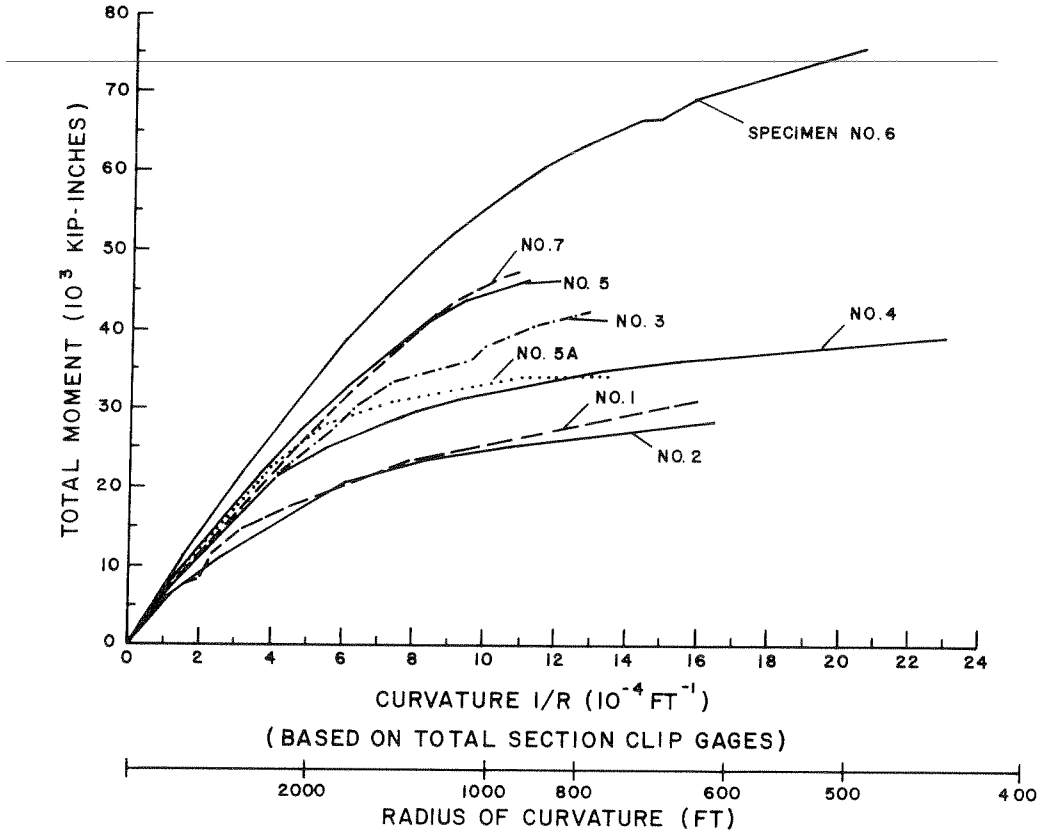

FIG. 62 MOMENT-CURVATURE RELATIONSHIP

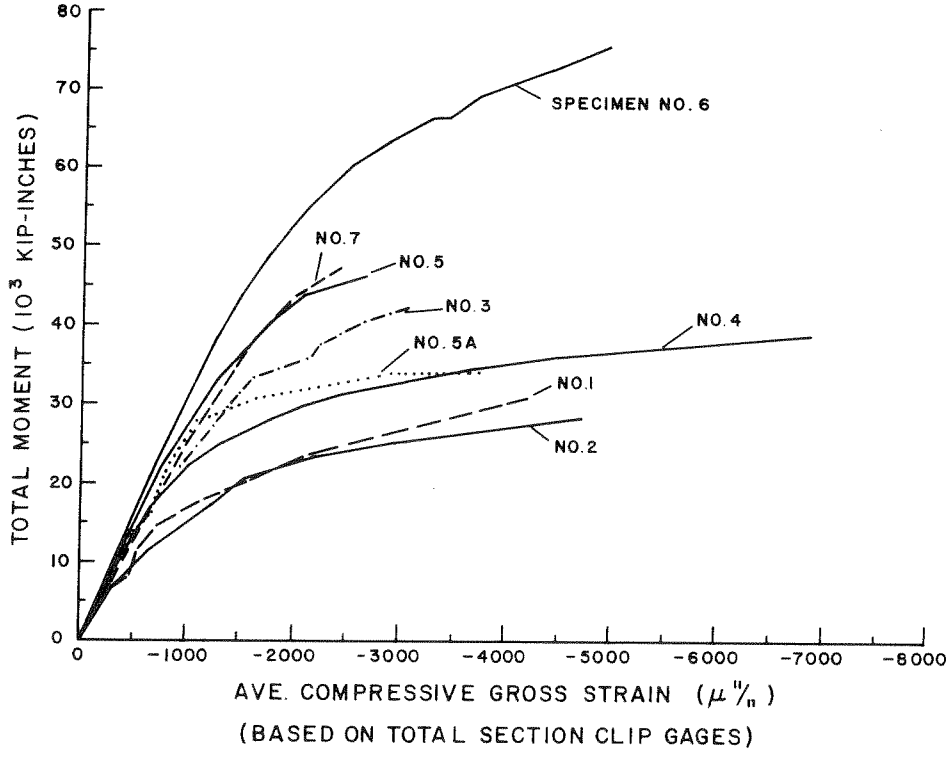

FIG. 63 MOMENT-GROSS STRAIN RELATIONSHIP

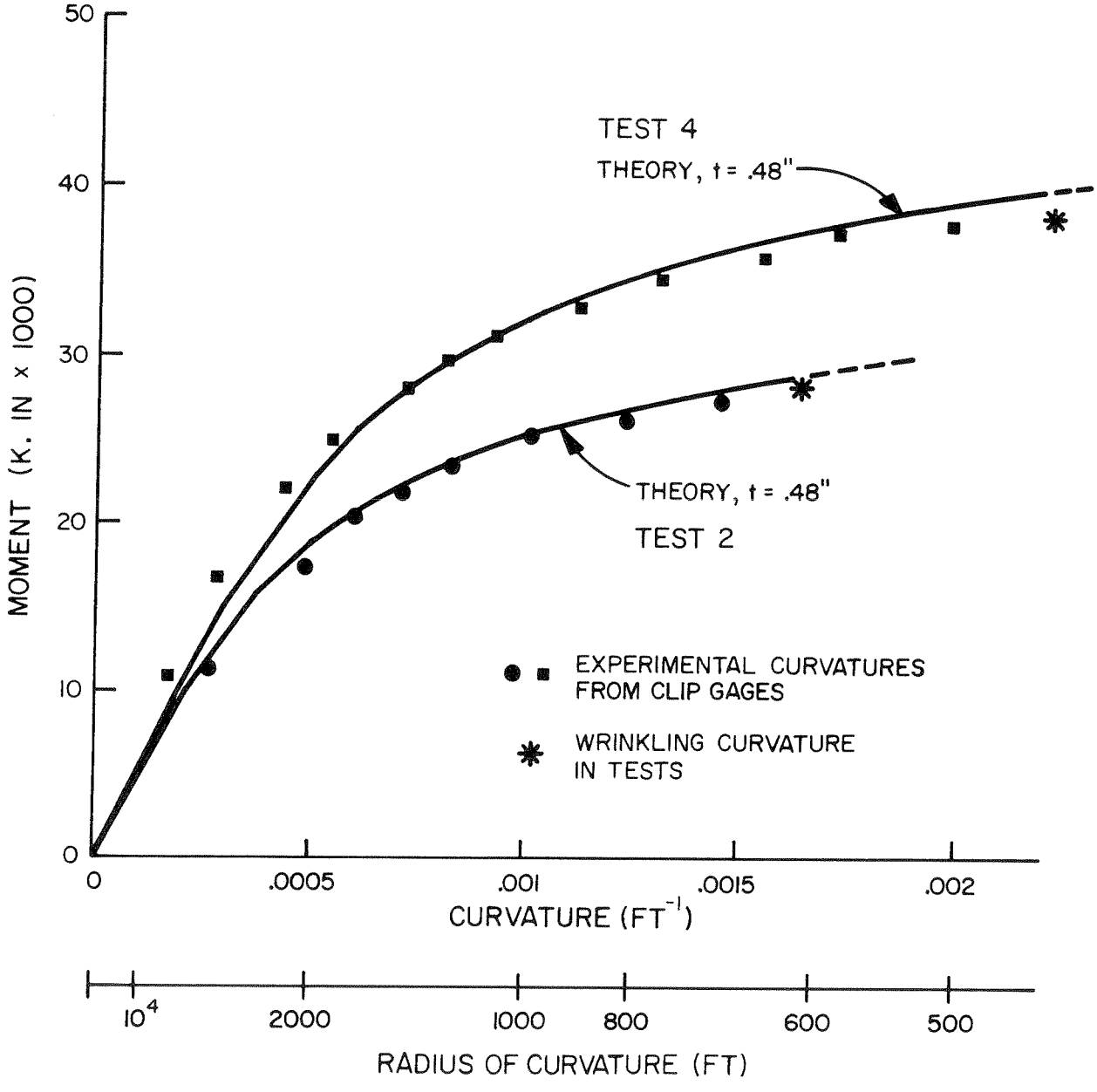

FIG. 64 THEORETICAL AND EXPERIMENTAL MOMENT–CURVATURE RELATIONSHIPS TEST NOS. 2 AND 4